The Hilbert Book Test Model

By J.A.J. van Leunen

Last modified: 5 april 2016

Abstract

The Hilbert book test model is a purely mathematical test model that starts from a solid foundation from which the whole model can be derived by using trustworthy mathematical methods. What is known about physical reality is used as a guidance, but the model is not claimed to be a proper reflection of physical reality. The mathematical toolkit still contains holes. These holes will be encountered during the development of the model and suggestions are made how those gaps can be filled. Some new insights are obtained and some new mathematical methods are introduced. The selected foundation is interpreted as part of a recipe for modular construction and that recipe is applied throughout the development of the model. This development is an ongoing project. The main law of physics appears to be a commandment: “Thou shalt construct in a modular way”.

Contents

1 Foreword of the author

The “Hilbert Book Model” is the name of my personal research project. My interest in the structure and phenomena of physical reality started in the third year of my physics study when I was first confronted with how quantum mechanics was configured. I was quite astonished by the fact that its methodology differed fundamentally from the way that classical mechanics was done. So I asked my very wise lecturer on what origin this difference is based. His answer was that this difference was caused by the superposition principle. I was not very happy with this answer, because the superposition principle was indeed part of the methodology of quantum mechanics, but in those days I did not comprehend how that could present the main cause of the difference between the two methodologies. I decided to dive into literature and after some search I encountered the booklet of Peter Mittelsteadt, “ Philosophische Probleme der Modernen Physik” (1963). This booklet contained a chapter about quantum logic and that appeared to me a more appropriate answer. Garret Birkhoff and John von Neumann published in 1936 a paper that published their discovery of what they called “quantum logic”. Quantum logic is since then in mathematical terminology known as an orthomodular lattice. The relational structure of this lattice is quite similar to the relational structure of classical logic. That is why the duo gave their discovery the name “quantum logic”. This was an unlucky choice, because no good reason exist to consider the orthomodular lattice as a system of logical propositions. In the same paper, the duo indicated that the set of closed subspaces of a separable Hilbert space has exactly the relational structure of an orthomodular lattice. That appears to be the reason why quantum physicists prefer Hilbert spaces as a realm in which they do their modeling of quantum physical systems. Another habit of quantum physicists also intrigued me. My lecturer thought me that all observable quantum physical quantities are eigenvalues of Hermitian operators. When I looked around I saw a world that had a structure that was configured from a three dimensional spatial domain and a one dimensional time domain. In the quantum physics of that time, no operator represents the time domain and no operator was used to deliver the spatial domain in a compact fashion. After some research I discovered a four dimensional number system that could provide an appropriate normal operator with an eigenspace that represented the full four dimensional representation of my living environment. At that moment I had not yet heard from quaternions, but an assistant professor quickly told me about the discovery of Rowan Hamilton that happened more than a century earlier. My university, the TUE, targeted applied physics and there was not much time nor support for diving deep into the fundamentals of quantum physics. After my study I started a career in high-tech industry where I joined the development of image intensifier devices. There followed my confrontation with optics and with the actual behavior of elementary particles. See: http://www.e-physics.eu/#_What_image_intensifiers reveal.

Only after my retirement I got sufficient time to dive deep into the foundations of physical reality. In 2009 I started my personal research project that in 2011 got its current name “The Hilbert Book Model”. The author takes the freedom to upgrade the papers in a steady rate.

I use vixra.org as my personal e-print archive: http://vixra.org/author/j_a_j_van_leunen . Vixra provides full two sided open access and has a flexible revision service, which I use extensively. I put preliminary papers on my website http://www.e-physics.eu . There my papers are available in .pdf and also in .docx format. I do not request copyright on these documents. I try to avoid the burden of peer review publishing. Instead I try to keep the quality of my papers at a high standard. The most recent versions of the author’s papers will appear on his website. Most of the older papers are superseded by newer ones that got different names. Older papers started with knowledge that was lectured in universities and or could be found in literature. Newer papers also contain corrections and discoveries that are made by the author.

2 Introduction

The Hilbert Book Test Model $\mathcal{M}$ is based on a foundation that has the relational structure of an orthomodular lattice [1] [2]. Nearly a century ago, the discovery of this lattice was published by the duo Garret Birkhoff and John von Neumann in a paper in which they also explained its relation to the notion of a ***separable Hilbert space*** [3] [4]. The orthonormal lattice does not contain the notion of number systems. Thus, this foundation cannot represent the concepts that define dynamic geometric data, such as time and location. These notions emerge by extending this foundation in the direction of the separable Hilbert space. By selecting this extension of the foundation, the freedom of the selection of the derived concepts is restricted. The separable Hilbert space provides operators that have countable eigenspaces that are filled with eigenvalues that must be members of division rings [5]. Only three suitable division rings exist. These are the real numbers, the complex numbers and the quaternions. The separable Hilbert space can only cope with the rational versions of these number systems. These restrictions appear very favorable for the pursued model building process. It strongly limits the range of choices. Still the resulting possibilities appear to be flexible enough to generate a powerful base model.

$\mathcal{M}$ interprets the orthomodular lattice as part of a recipe for modular construction. Modular construction represents a very beneficial strategy that strongly reduces relational complexity of the target system. For very complex systems the modular construction strategy is orders of magnitude more efficient than a monolithic approach. Reality offers huge resources in available time and in numbers of building components. In this way even stochastic design as is applied by nature can reach high levels of complexity. $\mathcal{M}$ applies modular construction as a general strategy.

In advance the model will apply a stochastic design an generation strategy. This will change when the model has achieved a level in which intelligent species appear. From that instant on the efficiency of the modular construction strategy will increase significantly. Intelligent design and construction will use far less design and generation time and other required resources. This will clearly affect the evolution of the model. Due to limited speed of information spread, these effects will appear at isolated locations.

$\mathcal{M}$ applies the fact that the set of closed subspaces of a separable Hilbert space has the relational structure of an orthomodular lattice. Not all closed subspaces of a separable Hilbert space represent modules or modular systems, thus the notion of a module must be further restricted.

$\mathcal{M}$ applies the fact that separable Hilbert spaces can only cope with number systems that are division rings. We use the most elaborate category of these division rings. That category is formed by the quaternionic number systems [6]. Quaternionic number systems exist in multiple versions, that differ in the way that they are ordered. This ordering may influence the arithmetic properties of the number system. For example right handed multiplying quaternions and left handed multiplying quaternions exist. Further, as will be shown in this paper, it appears that ordering influences the behavior of quaternionic functions under integration. This fact has astonishing consequences.

Another important fact is that every infinite dimensional separable Hilbert system owns a companion Gelfand triple, which is a ***non-separable Hilbert space*** [7]. $\mathcal{M}$ uses both kinds of Hilbert spaces as structured storage media, in which discrete quaternionic data and quaternionic manifolds can be archived. By applying Hilbert spaces $\mathcal{M}$ accepts that the model uses a storage medium in which all of its activities are precisely archived.

$\mathcal{M}$ uses a separable Hilbert space $\mathfrak{H}$ in order to archive countable sets of discrete quaternionic data and $\mathcal{M}$ uses the companion Gelfand triple $\mathcal{H}$ in order to archive continuous quaternionic

manifolds. $\mathcal{H}$ also contains an image of the content of $\mathfrak{H}$. $\boldsymbol{\mathcal{M}}$ Uses this fact in order to describe the embedding of the separable Hilbert space into its Gelfand companion. $\boldsymbol{\mathcal{M}}$ considers the embedding as an ongoing process. In taking this view $\boldsymbol{\mathcal{M}}$ selects between two possible views. The view taken classifies the model as a dynamic model. The alternative view accepts that besides the historic data the Hilbert spaces already contains the future data. In this alternative view a boundary splits the Hilbert space into three parts:

- The past history part of the model
- The current static status quo, which is represented by the boundary
- The future part of the model

This second view treats these three parts as sections of a model that is created as one whole system.

$\boldsymbol{\mathcal{M}}$ introduces ***the reverse bra-ket method*** and uses this method in order to relate operators and their eigenspaces to pairs of functions and their parameter spaces [8]. In this way, subspaces act as Hilbert space domains in relation to which manifolds are defined.

In the first view, the base version $\mathcal{M}$ of $\boldsymbol{\mathcal{M}}$ consists of the foundation, a quaternionic separable Hilbert space, its companion Gelfand triple and a set of mechanisms $\{\mathfrak{M}_n^x\}$ that control the dynamic split of this base version $\mathcal{M}$ in a historic part, a part that represents the present static status quo and a part that represents the future.

The first view shifts the equivalent of the mystery of the origin of the dynamics of physical reality to the mysteries of a set of mechanisms that control the coherence of the dynamics of the model.

$\boldsymbol{\mathcal{M}}$ applies an extended version of the generalized Stokes theorem in order to describe the split of the Hilbert space into these three parts [9] [10]. The generalized Stokes theorem enforces the encapsulation of artifacts that disrupt the continuity of the manifolds. This introduces an extra splitting of the base model in which elementary artifacts and domain cavities are set apart from the domains of the continuous parts of the manifolds.

Via the reverse bra-ket method smoothing operators are introduced that convolute the defining function of a primary operator with a blurring function. With an appropriate selection of the blurring function, the eigenspace of the smoothing operator will represent the “observable” version of the primary manifold. Here “observable” means the way that discrete objects sense the influence of the local disruptions of the continuity of the primary manifold that are caused by other discrete objects.

In this way $\boldsymbol{\mathcal{M}}$ introduces notions such as the wave function, the uncertainty principle and the equivalent of the gravitation potential.

The fact that $\boldsymbol{\mathcal{M}}$ steps with model wide steps in the separable Hilbert space $\mathfrak{H}$ and flows in the companion Gelfand triple $\mathcal{H}$ is the reason to use the name ***Hilbert Book Model*** for $\boldsymbol{\mathcal{M}}$. In order to warn that $\boldsymbol{\mathcal{M}}$ is not meant to be a physical model, but instead $\boldsymbol{\mathcal{M}}$ is a pure mathematical test model that is used to investigate the mathematical tools and methods that can be use in order to describe a physical model, the name of $\boldsymbol{\mathcal{M}}$ is extended to ***Hilbert Book Test Model***.

3 The orthomodular lattice

In this paper lattices are the most primitive structures that exist in the pursued model. Lattices are sets of relations and the lattice describes which kind of relations belong to the lattice and how they are mutually related. In short a lattice is a relational structure. The foundation of the model is an orthomodular lattice. This is a short name for a weak modular orthocomplemented lattice. Lattices are treated in detail in the appendix.

The orthocomplemented lattice was discovered by Garret Birkhoff and John von Neumann. Due to the strong similarity to the lattice that describes classical logic the duo gave it in their introductory paper the name “quantum logic”. This was the reason that since its introduction many scientists since this introduction have investigated the value of this structure as a logic system. For comprehensible reasons this was not very successful. In the same introductory paper the duo proved that the set of closed subspaces of a separable Hilbert space has exactly the relational structure of the orthocomplemented lattice. The closed subspaces have little in common with logical propositions. That is why this paper prefers a different interpretation of the orthomodular lattice. This paper sees the orthomodular lattice as part of a recipe for modular construction. In fact the relational structure stimulates modular construction of the systems that occur in the pursued model.

The effect of the orthomodular lattice can be expressed in the most basic and therefore most important law:

“Thou shalt construct in a modular way”.

This law is intentionally expressed in the form of a commandment. It is not possible to express this law in the form of a formula, such as $K = m\ a$ or $E\ =\ m\ c^2$. The impact of the commandment is far more influential, than the impact of these famous formulas.

The orthomodular lattice does not yet cover number systems. Thus this structure cannot implement notions such as space and time. These concepts emerge with the extension of this foundation to the separable Hilbert space. The separable Hilbert space can only cope with numbers that are elements of a division ring. Together with its stimulation of modular construction this restriction of the tolerable number systems has a healthy influence on the simplicity and the efficiency of model that will be designed.

4 Modular construction of dynamical systems

4.1 Modular construction

Modular construction is a very beneficial construction design method.

- It can reduce relational complexity with orders of magnitude.
  - It standardizes module access.
  - It standardizes information transfer between modules.
  - It encapsulates relations that are only used inside the module, such that they are not disturbing information exchange outside the module.
- It uses its resources in a very economical way.
  - It promotes reuse.
  - It uses standard module types.
- It makes system configuration very simple.

Most importantly, dynamic modular system construction enables ***stochastic modular system generation***. This is what drives model evolution in the first phase of the generation of modules and modular systems. In a later phase intelligent design and intelligent construction and configuration can take over at isolated regions.

4.2 Binding

Modules are bounded together in higher level modules.

- In loose binding each constituent module keeps its own encapsulation.
- In strong binding the modules join their encapsulations.
- Hybrid binding is a combination of loose and strong binding.

Elementary modules are not constructed from lower order modules.

4.3 Relation to a separable Hilbert space

The Hilbert space distinguishes modules in a restricted set of categories. Differentiation based on ordering of content is used to distinguish between elementary module types. Configuration of modular subsystems is used as another criterion for grouping into categories.

- Each closed subspace of the considered separable Hilbert space is a potential module or a potential modular system.
- The orthomodular lattice restricts the relational structure of the set of potential modules.
- Not every closed subspace of this Hilbert space is an actual module or an actual modular system.
- Actual modules are encapsulated and contain discrete content.

Hilbert spaces can house several parameter spaces that are represented by eigenspaces of normal operators and are spanned by a version of the quaternionic number system. Elementary modules feature their own private parameter space. Types of elementary modules correspond to types of parameter spaces. These private parameter spaces are categorized as ***symmetry centers***.

4.4 Dynamics

The modular systems are controlled by mechanisms that regulate information transfer such that no blockings, such as dead locks or race conditions obstruct the dynamic behavior of the modular system. This means that the model applies a stochastic real time operating system (RTOS) for controlling the activity of its lowest level modules.

4.5 Implementation

The describing data of both the discrete modules and the fields are stored in the Hilbert spaces. The modules are embedded in one or more basic fields. Basic fields are generated by the influences of mechanisms that are not part of the Hilbert spaces $\mathfrak{H}$ and $\mathcal{H}$. Other fields are derived from data that are already stored in the combined Hilbert spaces. Often fields are functional parts of other more basic fields. The Hilbert spaces own some model-wide basic fields. Part of this set represent parameter spaces. ***Symmetry centers*** are directly coupled to a set of basic fields that are private to corresponding modules.

Encapsulation is implemented by a closed skin that acts as a boundary, which corresponds to a form that can be described using a parameter space that has one dimension less than the space that it encapsulates. The skin has no fixed form or size. Its main characteristic is that it is defined in a region where the considered field is continuous. This enables the application of the ***generalized Stokes theorem***. This theorem defines integral balance equations. These integral balance equations correspond to differential continuity equations.

Two different views of the model are possible. The first view is a creation based view. In this view mechanisms create new data at the rim between history and future. This new data is then stored in the Hilbert spaces $\mathfrak{H}$ and $\mathcal{H}$. The second view is a panning view in which the splitting boundary is panning over existing data without changing these data. In this view the only dynamic object in the model is the panning boundary.

The model is not touched by these views. However, each of the views corresponds to a ***different interpretation*** of the model. We take the first view as the main description of the model, because it conforms better with the current physical models.

In the selected view, dynamics is implemented by a boundary that splits the Hilbert spaces into three parts:

- A fixed and precisely defined history that is archived in the eigenspaces of operators that reside in the involved Hilbert spaces.
- A present status quo whose description exist of the data that are delivered by controlling stochastic mechanisms and are archived in the eigenspaces that re archived in the eigenspaces of operators that reside in the separable Hilbert space.
    - This part represents the splitting boundary.
    - The mechanisms that provide new data have a stochastic nature and in that way they prevent blockings, such as dead locks and race conditions.
    - This stochastic nature also provides the stochastic nature of the RTOS that schedules the activity of the lower level modules.
- A future that is inaccessible to the objects that are archived in the previous parts.
    - No information leaks from the future part to the boundary or to the historic part.
    - However, when the boundary proceeds, information and objects may enter and pass through the boundary from the future part of the model to the historic part of the model. This restriction is in correspondence with the panning view.
- Creation and annihilation processes take place in the direct surround of the part that represents the static status quo. These processes take a standard number of progression steps. This assumption means that the panning boundary travels with constant or very slowly varying number of participating progression steps.

The creation based view involves stochastic mechanisms that provide new data. In the panning view the future part already contains these data but these data cannot be accessed until it is reached by the moving boundary. The model is not affected by these interpretations. However, the description of the model is certainly affected by the selected interpretation.

The combination of both views resolves Einstein's dilemma that it is unbelievable that the creator throws dices in order to generate his elementary modules. In the first view the creation is a stochastic process that occurs in in huge number of subsequent steps . In the second view the creation of the model took a single step, but still the modules are created in a stochastic way.

Information transfer occurs via ripples in the field that pass the panning boundary. Information carrying messengers transport information in the form of quantized packages of energy. These messengers are solutions of homogeneous second order differential equations. Thus information transfer is restricted by the properties and capabilities of the involved fields. The capabilities are described by the integral and differential field equations.

Observation by information receivers is blurred by the blurring, which is caused by the objects that emit and absorb the information messengers.

5 Quaternion geometry and arithmetic

Quaternions and quaternionic functions offer the advantage of a very compact notation of items that belong together [11].

Quaternions can be considered as the combination of a real scalar and a 3D vector that has real coefficients. The vector forms the imaginary part of the quaternion. Quaternionic number systems are division rings. Other division rings are real numbers and complex numbers. The separable Hilbert space only uses the rational subsets of these number systems.

Bi-quaternions exist whose parts exist of a complex scalar and a 3D vector that has complex coefficients. Octonions and bi-quaternions do not form division rings. This paper does not use them. However, one exception is tolerated, in considering the Dirac equation, bi-quaternionic functions and bi-quaternionic differential operators are used. The Dirac equation is treated in the appendix.

5.1 Notation

We indicate the real part of quaternion a by the suffix a_0.

We indicate the imaginary part of quaternion a by bold face $\boldsymbol{a}$.

$$a = a_0 + \boldsymbol{a} \tag{1}$$

We indicate the quaternionic conjugate by a superscript in the form of a star.

$$a^* = a_0 - \boldsymbol{a} \tag{2}$$

We introduce the ***complex base number*** $\mathbb{i}$ via

$$\mathbb{i} \cdot \mathbb{i} = -1 \tag{3}$$

$\mathbb{i}$ commutes with all quaternions.

$$\mathbb{i} \cdot a = a \cdot \mathbb{i} \tag{4}$$

However, the product is no longer a quaternion. Instead, it is a bi-quaternion. Bi-quaternions are indicated by a beret.

$$\breve{c} = a + \mathbb{i} \cdot b \tag{5}$$

Here a and b are both regular quaternions. Complex conjugation is acting as:

$$\mathbb{i}^{\bullet} = -\mathbb{i} \tag{6}$$

Complex conjugation is indicated with a superscript in the form of a filled circle.

$$\ddot{c}^{\bullet} = a - \mathbb{i} \cdot b \tag{7}$$

Here we see bi-quaternions as hyper-complex numbers with quaternionic coefficients. These numbers do not form a division ring. These numbers are not equivalent to octonions. This paper does not apply Clifford algebra, Jordan algebra or other than the pure division ring algebra's, because the author considers them to conceal more than they elucidate.

5.2 Quaternionic sum

$$c = c_0 + \boldsymbol{c} = a + b \tag{1}$$

$$c_0 = a_0 + b_0 \tag{2}$$

$$\boldsymbol{c} = \boldsymbol{a} + \boldsymbol{b} \tag{3}$$

5.3 Quaternionic product

$$f = f_0 + \boldsymbol{f} = d \cdot e \tag{1}$$

$$f_0 = d_0 \cdot e_0 - \langle \boldsymbol{d}, \boldsymbol{e} \rangle \tag{2}$$

$$\boldsymbol{f} = d_0 \cdot \boldsymbol{e} + e_0 \cdot \boldsymbol{d} \pm \boldsymbol{d} \times \boldsymbol{e} \tag{3}$$

Thus the product contains five parts. The $\pm$ sign indicates the influence of right or left handedness of the number system.

$\langle \boldsymbol{d}, \boldsymbol{e} \rangle$ is the inner product of $\boldsymbol{d}$ and $\boldsymbol{e}$.

$\boldsymbol{d} \times \boldsymbol{e}$ is the outer product of $\boldsymbol{d}$ and $\boldsymbol{e}$.

We usually omit the multiplication sign $\cdot$.

5.3.1 Handedness

We introduce by superscript $^{\emptyset}$ a switch in handedness of the quaternion. This does not touch the real part.

$$f^{\lozenge} = d^{\lozenge} \cdot e^{\lozenge} = d_0 \cdot e_0 - \langle \boldsymbol{d}^{\lozenge}, \boldsymbol{e}^{\lozenge} \rangle + d_0 \cdot \boldsymbol{e}^{\lozenge} + e_0 \cdot \boldsymbol{d}^{\lozenge} \mp \boldsymbol{d}^{\lozenge} \times \boldsymbol{e}^{\lozenge} \quad (1)$$

$$\boldsymbol{d}^{\lozenge} \times \boldsymbol{e}^{\lozenge} = -\boldsymbol{d} \times \boldsymbol{e} \quad (2)$$

$d \cdot e^{\lozenge}$ and $d^{\lozenge} \cdot e$ ***are undefined***!

Thus a right handed quaternion cannot be multiplied with a left handed quaternion. Quaternionic conjugation switches the handedness. In addition:

$$(a \cdot b)^* = b^* \cdot a^* \quad (3)$$

A continuous quaternionic function does not switch its handedness. Embedding a conflicting quaternion in the target space of a function produces a local artifact that produces a local discontinuity. This also holds for other aspects of the quaternion symmetries.

5.4 Norm

$$|a| = \sqrt{a_0 a_0 + \langle \boldsymbol{a}, \boldsymbol{a} \rangle} = \sqrt{a \cdot a^*} \quad (1)$$

5.5 Norm of quaternionic functions

Square-integrable functions are normalizable. The norm is defined by:

$$\|\psi\|^2 = \int_V |\psi|^2 \, dV \quad (1)$$

$$= \int_V \{|\psi_0|^2 + |\boldsymbol{\psi}|^2\} dV$$

$$= \|\psi_0\|^2 + \|\boldsymbol{\psi}\|^2$$

6 Quaternionic Hilbert spaces

Separable Hilbert spaces are linear vector spaces in which an inner product is defined. This inner product relates each pair of Hilbert vectors. The value of that inner product must be a member of a division ring [5]. Suitable division rings are real numbers, complex numbers and quaternions. Model $\mathcal{M}$ uses quaternionic Hilbert spaces.

Paul Dirac introduced the bra-ket notation that eases the formulation of Hilbert space habits [8].

$$\langle x|y\rangle = \langle y|x\rangle^* \tag{1}$$

$$\langle x+y|z\rangle = \langle x|z\rangle + \langle y|z\rangle \tag{2}$$

$$\langle \alpha x|y\rangle = \alpha\, \langle x|y\rangle \tag{3}$$

$$\langle x|\alpha y\rangle = \langle x|y\rangle\, \alpha^* \tag{4}$$

$\langle x|$ is a bra vector. $|y\rangle$ is a ket vector. α and $\langle x|y\rangle$ are quaternions.

This paper considers Hilbert spaces as no more and no less than ***structured storage media*** for dynamic geometrical data that have an Euclidean signature. Quaternions are ideally suited for the storage of such data. Quaternionic Hilbert spaces are more extensively described in "Quaternions and quaternionic Hilbert spaces" [11]. Of course, the quaternions may also have other meanings than the representation of geometric data. But representing geometric data will cover the majority of the application of the quaternionic data in model $\mathcal{M}$.

The operators of separable Hilbert spaces have countable eigenspaces. Each infinite dimensional separable Hilbert space owns a Gelfand triple. The Gelfand triple embeds this separable Hilbert space and offers as an extra service operators that feature continuums as eigenspaces. In the corresponding subspaces and child subspaces the ***definition of dimension loses its sense***.

6.1 Representing operators and their eigenspaces by continuous functions

Operators map Hilbert vectors onto other Hilbert vectors. For all Hilbert vectors $|y\rangle$ holds

$$\langle Tx|y\rangle = \langle z|y\rangle \Rightarrow \langle Tx| = \langle z| \tag{1}$$

Via the inner product, the operator T may be linked to an adjoint operator $T^\dagger$.

$$\langle Tx|y\rangle \stackrel{\text{def}}{=} \langle x|T^\dagger y\rangle \tag{2}$$

$$\langle Tx|y\rangle = \langle y|Tx\rangle^* = \langle T^\dagger y|x\rangle^* \tag{3}$$

A linear quaternionic operator T, which owns an adjoint operator $T^\dagger$ is normal when

$$T^\dagger T = T\, T^\dagger \tag{4}$$

If T is a normal operator, then $T_0 = (T + T^\dagger)/2$ is a self adjoint operator and $\boldsymbol{T} = (T - T^\dagger)/2$ is an imaginary normal operator. Self adjoint operators are also Hermitian operators. Imaginary normal operators are also anti-Hermitian operators.

By using what we will call ***reverse bra-ket notation***, special types of operators that reside in the Hilbert space and correspond to continuous functions, can easily be defined by starting from an orthonormal base of vectors. In this base the vectors are normalized and are mutually orthogonal. The vectors span a subspace of the Hilbert space. We will attach eigenvalues to these base vectors

via the ***reverse bra-ket notation***. In this way the base vectors become eigenvectors of the target operator. This works both in separable Hilbert spaces as well as in non-separable Hilbert spaces.

The reverse bracket method is discovered by the author. It appears to be a very powerful tool that couples a category of operators to corresponding defining functions and couples operators in the separable Hilbert space to corresponding operators in the non-separable Hilbert space.

We start with a very simple defining function $\mathcal{R}(q) = q$ and the corresponding operator $\mathcal{R}$.

Let $\{q_i\}$ be the set of ***rational*** quaternions in a selected quaternionic number system and let $\{|q_i\rangle\}$ be the set of corresponding base vectors. They are the eigenvectors of a normal operator $\mathcal{R}$. Here we enumerate the base vectors with index i.

$$\mathcal{R} \stackrel{\text{def}}{=} |q_i\rangle q_i \langle q_i| = |q_i\rangle \Re(q_i) \langle q_i| \tag{5}$$

$\mathcal{R}$ is the ***configuration parameter space operator***. $\Re(q)$ is a quaternionic function, whose target equals its parameter space. The definition (5) also covers the situation where the dimension of the (sub) space is infinite.

This ***reverse bra-ket notation*** must not be interpreted as a simple outer product between a ket vector $|q_i\rangle$, a quaternion q_i and a bra vector $\langle q_i|$. Actually, it involves a complete set of eigenvalues $\{q_i\}$ and a complete orthomodular set of Hilbert vectors $\{|q_i\rangle\}$. It implies a summation over these constituents, such that for all bra's $\langle x|$ and all ket's $|y\rangle$:

$$\langle x|\mathcal{R}\, y\rangle = \sum_i \langle x|q_i\rangle q_i \langle q_i|y\rangle \tag{6}$$

Thus formula (6) represents the full definition for the shorthand (5). $\Re$ is a special operator. It can be considered as a property of the combination of the separable Hilbert space $\mathfrak{H}$ and one of the existing versions of the quaternionic number system.

$\mathcal{R}_0 = (\mathcal{R} + \mathcal{R}^\dagger)/2$ is a self-adjoint operator. Its eigenvalues can be used to arrange the order of the eigenvectors by enumerating them with the real eigenvalues. The ordered eigenvalues can be interpreted as ***progression values***.

$\boldsymbol{\mathcal{R}} = (\mathcal{R} - \mathcal{R}^\dagger)/2$ is an imaginary operator. Its eigenvalues can also be used to order the eigenvectors. The eigenvalues can be interpreted as ***spatial values*** and can be ordered in several ways. For example eight independent ways exist to order the 3D spatial domain by using Cartesian coordinates.

Let $f(q)$ be a mostly continuous quaternionic function. Now the reverse bra-ket notation defines operator f as:

$$f \stackrel{\text{def}}{=} |q_i\rangle f(q_i) \langle q_i| \tag{7}$$

f defines a new operator that is based on function $f(q)$. Here we suppose that the target values of f belong to the same version of the quaternionic number system as its parameter space does.

Operator f has a countable set of discrete quaternionic eigenvalues.

For this operator the reverse bra-ket notation (7) is a shorthand for

$$\langle x|f\, y\rangle = \sum_i \langle x|q_i\rangle f(q_i) \langle q_i|y\rangle \tag{8}$$

Alternative formulations for the reverse bra-ket definition are:

$$f \stackrel{\text{def}}{=} |q_i\rangle f(q_i)\langle q_i| = |q_i\rangle\langle f(q_i)q_i| = |q_i\rangle\langle f q_i| = |f^*(q_i)q_i\rangle\langle q_i| = |f^\dagger q_i\rangle q_i\langle q_i| \qquad (9)$$

Here we used the same symbol for the operator f and the function $f(q_i)$. For this operator the eigenvalues of the Hermitian part $f_0 = (f + f^\dagger)/2$ are not interpreted as progression values. Often (not always!), these values can be interpreted as dynamic location density descriptors.

The left side of (8) only equals the right side when domain over which the summation is taken is restricted to the region of the parameter space $\mathcal{R}$ where $f(q)$ is sufficiently continuous.

6.2 Symmetry centers

We can define a category of anti-Hermitian operators $\{\mathfrak{S}_n^x\}$that have no Hermitian part and that are distinguished by the way that their eigenspace is ordered by applying a ***polar coordinate system***. We call them symmetry centers $\mathfrak{S}_n^x$. A polar ordering always start with a selected Cartesian ordering. The geometric center of the eigenspace of the symmetry center floats on a background parameter space of the normal reference operator $\mathcal{R}$, whose eigenspace defines a full quaternionic parameter space. The eigenspace of the symmetry center $\mathfrak{S}_n^x$ acts as a three dimensional spatial parameter space. The super script ^{x} refers to the symmetry flavor of $\mathfrak{S}_n^x$. The subscript $_n$enumerates the symmetry centers. Sometimes we omit the subscript.

$$\mathfrak{S}^x = |\mathfrak{s}_i^x\rangle\mathfrak{s}_i^x\langle\mathfrak{s}_i^x| \qquad (1)$$

$$\mathfrak{S}^{x\dagger} = -\mathfrak{S}^x \qquad (2)$$

It must be noticed that the eigenvalues of the symmetry center operator have no real part! However, when mapped to another parameter space, the center location of the symmetry center eigenvalues can be a function of progression.

6.3 Continuum eigenspaces

In a non-separable Hilbert space, such as the Gelfand triple, the continuous function $\mathcal{F}(q)$ can be used to define an operator, which features a continuum eigenspace. We start with defining a continuum parameter space.

$$\mathfrak{R} = |q\rangle q\langle q| = |q\rangle\mathfrak{R}(q)\langle q| \qquad (1)$$

The next definition relates the separable Hilbert space and its companion Gelfand triple.

$$\mathcal{F} = |q\rangle\mathcal{F}(q)\langle q| \qquad (2)$$

Via the continuous quaternionic function $\mathcal{F}(q)$, the operator $\mathcal{F}$ defines a curved continuum $\mathcal{F}$. This operator and the continuum reside in the Gelfand triple, which is a non-separable Hilbert space.

The function $\mathcal{F}(q)$ uses the eigenspace of the reference operator $\mathfrak{R}$ as a flat parameter space that is spanned by a quaternionic number system $\{q\}$. The continuum $\mathcal{F}$ represents the target space of function $\mathcal{F}(q)$.

Here we no longer enumerate the base vectors with index i. We just use the name of the parameter. If no conflict arises, then we will use the same symbol for the defining function, the defined operator and the continuum that is represented by the eigenspace.

For the shorthand of the reverse bra-ket notation of operator $\mathcal{F}$ the integral over q replaces the summation over q_i.

$$\langle x|\mathcal{F}\ y\rangle = \sum_{i=0}^{i=\infty} \langle x|q_i\rangle \mathcal{F}(q_i) \langle q_i|y\rangle \approx \int_q \langle x|q\rangle \mathcal{F}(q) \langle q|y\rangle\ dq \tag{3}$$

The integral only equals the sum sufficiently close when the function $\mathcal{F}(q)$ is sufficiently continuous in the domain over which the integration takes place. Otherwise the left side only equals the right side when domain is restricted to the region of the parameter space $\mathfrak{R}$ where $\mathcal{F}(q)$ is sufficiently continuous. The section that treats the generalized Stokes theorem explains the consequences of existing discontinuities. The parameter space operator $\mathfrak{R}$ does not encounter these discontinuities. The section that treats the generalized Stokes theorem also reveals the consequences of ordering of the used number systems.

An important fact is that $\mathfrak{R}$ can be split into a retarded (historic) part $\mathfrak{R}_-$ and an advanced (future) part $\mathfrak{R}_+$. The region between these two parts forms a boundary (rim) in which the parameter space(s) change the sign of their real parts. Domains that feature further differences in their parameter spaces must also be encapsulated and form floating islands. Within these islands integration makes no sense. Inside those regions only summation is acceptable. Elementary islands form modules that will be called symmetry centers. Symmetry centers have a fixed type of parameter space ordering. These symmetry centers will be later treated in more detail. An extended version of the Stokes theorem can properly describe the situation.

Smoothed versions of operators can use defining functions that are integrable over most regions where the original operator cannot be represented by the original defining function. The defining function of the smoothed operator equals the convolution of the original defining function and a suitable blurring function.

The blur is picked such that it represents the fundamental observation blur that is sensed by discrete objects.

Remember that quaternionic number systems exist in several versions, thus also the operators f and $\mathcal{F}$ exist in these versions. The same holds for the parameter space operators. When relevant, we will use superscripts in order to differentiate between these versions.

Thus, operator $f^x = |q_i^x\rangle f^x(q_i^x)\langle q_i^x|$ is a specific version of operator f. Function $f^x(q_i^x)$ uses parameter space $\mathcal{R}^x$.

Similarly, $\mathcal{F}^x = |q^x\rangle \mathcal{F}^x(q^x)\langle q^x|$ is a specific version of operator $\mathcal{F}$. Function $\mathcal{F}^x(q^x)$ and continuum $\mathcal{F}^x$ use parameter space $\mathfrak{R}^x$. If the operator $\mathcal{F}^x$ that resides in the Gelfand triple $\mathcal{H}$ uses the same

defining function as the operator $\mathcal{F}^x$ that resides in the separable Hilbert space, then both operators belong to the same quaternionic ordering version.

In general the dimension of a subspace loses its significance in the non-separable Hilbert space.

The continuums that appear as eigenspaces in the non-separable Hilbert space $\mathcal{H}$ can be considered as quaternionic functions that also have a representation in the corresponding infinite dimensional separable Hilbert space $\mathfrak{H}$. Both representations use a flat parameter space $\mathfrak{R}^x$ or $\mathcal{R}^x$ that is spanned by quaternions. $\mathcal{R}^x$ is spanned by rational quaternions.

The ***parameter space operators*** will be treated ***as reference operators***. The rational quaternionic eigenvalues $\{q_i^x\}$ that occur as eigenvalues of the reference operator $\mathcal{R}^x$ in the separable Hilbert space map onto the rational quaternionic eigenvalues $\{q_i^x\}$ that occur as subset of the quaternionic eigenvalues $\{q^x\}$ of the reference operator $\mathfrak{R}^x$ in the Gelfand triple. In this way the reference operator $\mathcal{R}^x$ in the infinite dimensional separable Hilbert space $\mathfrak{H}$ relates directly to the reference operator $\mathfrak{R}^x$, which resides in the Gelfand triple $\mathcal{H}$. This renders the reverse bra-ket method to an ideal tool in the coupling of the separable Hilbert space $\mathfrak{H}$ to its non-separable companion $\mathcal{H}$.

All operators that reside in the Gelfand triple and are defined via a mostly continuous quaternionic function have a representation in the separable Hilbert space.

In the sketched way the reverse bra-ket method and the extended generalized Stokes theorem complement each other in the description of the base model.

6.4 Types of operators

Only a special category of operators can directly be handled by the reverse bra-ket method. In that case the defining function must be available within the realm of the Hilbert space. All operators that are defined in the separable Hilbert space and that can be represented by a sufficiently continuous function, possess a smoothing companion in the non-separable Hilbert space. The integration process that is used by the reverse bra-ket method can handle point-like discontinuities and closed cavities in the parameter space of the defining function, where the defining function does not exist. These artifacts are handled by separating them from the ***validity domain***.

Other types of operators are:

- Stochastic operators
    - These operators get their eigenvalues via mechanisms that reside outside of the realm of the Hilbert space and use stochastic processes in order to generate the eigenvalues.
- Density operators
    - If a stochastic operator generates a ***coherent swarm*** of eigenvalues that can be characterized by a continuous location density distribution, then the reverse bra-ket method can be used to define the corresponding density operator.
- Function operators
    - Function operators act on functions and in that way they produce new functions that can be used as defining functions of the corresponding operator.
- Partial differential operators
    - These are special kinds of function operators.
    - The existence of partial differentials of quaternionic functions create the existence of partial differential operators that work in combination with the operators that define the function of the related operator.

- Smoothing operators
  - The existence of the convolution of a mostly continuous quaternionic function with a continuous blurring function can be used to define a smoothed version of the mostly continuous quaternionic function that is everywhere continuous or that at least has a far greater validity domain.
  - Smoothing operators do not extend the validity domain over space cavities.
  - Density operators are extreme cases of smoothing operators.
  - Smoothing operators are the reason of existence of the wave function and of the uncertainty principle.
  - ***Potentials*** are represented by smoothing operators.

In quaternionic differential calculus the differential operators work as multipliers.

If $\mathfrak{D}$ is a partial differential operator and $\mathcal{G} = \mathfrak{D}\mathcal{F}$ for a category of functions $\{\mathcal{F}\}$, where $\mathcal{G}$ is sufficiently continuous, then for all bra's $\langle x|$ and all ket's $|y\rangle$ hold:

$$\langle x|\mathcal{G}\ y\rangle = \langle x|\mathfrak{D}\mathcal{F}\ y\rangle \approx \int_q \langle x|q\rangle\mathfrak{D}\mathcal{F}(q)\langle q|y\rangle\ dq = \int_q \langle x|q\rangle\mathcal{G}(q)\langle q|y\rangle\ dq \qquad (1)$$

Differential operators work on the category of operators that can be represented by defining functions, which can be differentiated. Especially the Hermitian kind of these operators appear to be of interest for application in physical theories.

Some Hermitian partial differential operators do not mix scalar and vector parts of functions. These are:

$$\nabla_0$$

$$\nabla_0\nabla_0$$

$$\langle\boldsymbol{\nabla},\boldsymbol{\nabla}\rangle$$

These operators can be combined in additions as well as in products. Two particular operators are:

$$\nabla\nabla^* = \nabla^*\nabla = \nabla_0\nabla_0 + \langle\boldsymbol{\nabla},\boldsymbol{\nabla}\rangle$$

$$\mathfrak{O} = -\nabla_0\nabla_0 + \langle\boldsymbol{\nabla},\boldsymbol{\nabla}\rangle$$

The last one is the quaternionic version of d'Alembert's operator. The first one can be split into ∇ and ∇^*. The second one cannot be split into quaternionic first order partial differential operators. However, a biquaternionic split is possible. The biquaternionic differential operators will be treated in the appendix.

The field $\mathfrak{F}$ is considered to be regular in spatial regions where the defining function $\mathfrak{F}(q)$ obeys

$$\langle\boldsymbol{\nabla},\boldsymbol{\nabla}\rangle\mathfrak{F} = 0 \qquad (2)$$

Similar considerations hold for regions where:

$$\nabla\nabla^{*}\mathfrak{F} = (\nabla_0\nabla_0 + \langle\boldsymbol{\nabla},\boldsymbol{\nabla}\rangle)\mathfrak{F} = 0 \tag{3}$$

$$\mathfrak{D}\mathfrak{F} = (-\nabla_0\nabla_0 + \langle\boldsymbol{\nabla},\boldsymbol{\nabla}\rangle)\mathfrak{F} = 0 \tag{4}$$

The quaternionic differential operators will be treated in dedicated chapters.

Smoothing operators are defined by a convolution.

The defining function $\mathfrak{U}(q)$ of operator $\mathfrak{U}$ is defined by the convolution of blurring function $\mathfrak{X}\,(q)$ with function $\mathfrak{A}(q)$:

$$\mathfrak{U}(q) \;= \mathfrak{X}(q) \circ \mathfrak{A}(q) \tag{5}$$

In that way we can write for the corresponding operators:

$$\mathfrak{U} \;= \mathfrak{X} \circ \mathfrak{A} \tag{6}$$

It will be clear that equation (5) and thus equation (6) involves an integration operation.

6.5 Tensor products

The tensor product of two quaternionic Hilbert spaces is a real Hilbert space [5]. For that reason the quaternion based model cannot apply tensor products. As a consequence Fock spaces are not applied in this paper.

Instead the paper ***represents the whole model by a single infinite dimensional separable quaternionic Hilbert space and its companion Gelfand triple***. Elementary objects and their composites will be represented by subspaces of the separable Hilbert space. Their local living spaces coexist as eigenspaces of dedicated operators. These have been introduced as symmetry centers.

6.6 Change of base

In quaternionic Hilbert space a change of base can be achieved by:

$$\langle x|\tilde{\mathcal{F}}\,y\rangle = \int_{\tilde{q}} \langle x\,|\tilde{q}\rangle \left\{ \int_{q} \langle\tilde{q}|q\rangle\mathcal{F}(q)\langle q|\tilde{q}\rangle\, dq \right\} \langle\tilde{q}|y\rangle\, d\tilde{q} \tag{1}$$

$$= \int_{\tilde{q}} \langle x|\tilde{q}\rangle\tilde{\mathcal{F}}(\tilde{q})\langle\tilde{q}|y\rangle\; d\tilde{q}$$

$$\tilde{\mathcal{F}}(\tilde{q}) = \int_{q} \langle\tilde{q}|q\rangle\mathcal{F}(q)\langle q|\tilde{q}\rangle\; dq \tag{2}$$

$$\tilde{\mathfrak{R}}(\tilde{q}) = \int_{q} \langle\tilde{q}|q\rangle q\langle q|\tilde{q}\rangle\; dq \tag{3}$$

(4)

$$\langle x|\widetilde{\Re}\, y\rangle = \int_{\tilde{q}} \langle x|\tilde{q}\rangle \widetilde{\Re}(\tilde{q}) \langle \tilde{q}|y\rangle \; d\tilde{q}$$

$$\widetilde{\Re} = |\tilde{q}\rangle \tilde{q} \langle \tilde{q}| \tag{5}$$

However, as we see in the formulas this method merely achieves a rotation of parameter spaces and functions. In the complex number based Hilbert space it would achieve no change at all.

6.7 Fourier transform

A Fourier transform uses a different approach. It is not a direct transform between parameter spaces, but instead it is a transform between sets of mutually orthogonal functions, which are formed by inner products, which are related to different parameter spaces. In quaternionic space, the (quaternionic) Fourier transform exists in three versions. The first two versions have a reverse Fourier transform.

The ***left oriented Fourier transform*** is defined by:

$$\tilde{\mathcal{F}}_L(\tilde{q}_L) = \int_q \langle \tilde{q}_L|q\rangle \, \mathcal{F}(q) \; dq \tag{1}$$

Like the functions $\langle q|q'\rangle$ and $\langle \tilde{q}_L|\tilde{q}'_L\rangle$, the functions $\langle \tilde{q}_L|q\rangle$ and $\langle q|\tilde{q}_L\rangle$ form sets of mutually orthogonal functions, as will be clear from:

$$\langle q|q'\rangle = \delta(q - q') \tag{2}$$

$$\langle \tilde{q}_L|\tilde{q}'_L\rangle = \delta(\tilde{q}_L - \tilde{q}'_L) \tag{3}$$

$$\int_{\tilde{q}_L} \langle q'|\tilde{q}_L\rangle\langle \tilde{q}_L|q\rangle \; d\tilde{q}_L = \delta(q - q') \tag{4}$$

$$\int_q \langle \tilde{q}'_L|q\rangle\langle q|\tilde{q}_L\rangle \; dq = \delta(\tilde{q}_L - \tilde{q}'_L) \tag{5}$$

The reverse transform is:

$$\mathcal{F}(q) = \int_{\tilde{q}_L} \langle q|\tilde{q}_L\rangle \tilde{\mathcal{F}}_L(\tilde{q}_L)\, d\tilde{q}_L = \int_{\tilde{q}_L}\int_{q'} \langle q|\tilde{q}_L\rangle\langle \tilde{q}_L|q'\rangle \mathcal{F}(q')\, d\tilde{q}_L\, dq' \tag{6}$$

$$= \int_{q'} \left\{ \int_{\tilde{q}_L} \langle q|\tilde{q}_L\rangle\langle \tilde{q}_L|q'\rangle \, d\tilde{q}_L \right\} \mathcal{F}(q')\, dq' = \int_{q'} \delta(q - q')\mathcal{F}(q')\, dq'$$

The reverse bra-ket form of the operator $\tilde{\mathcal{F}}_L$ equals:

$$\tilde{\mathcal{F}}_L = |\tilde{q}_L\rangle \tilde{\mathcal{F}}_L(\tilde{q}_L) \langle \tilde{q}_L| \tag{7}$$

Operator $\widetilde{\Re}_L$ provides the parameter space for the left oriented Fourier transform $\tilde{\mathcal{F}}_L(\tilde{q}_L)$ of function $\mathcal{F}(q)$ in equations (1) and (6).

$$\widetilde{\Re}_L = |\tilde{q}_L\rangle \tilde{q}_L \langle \tilde{q}_L| \tag{8}$$

Similarly the ***right oriented Fourier transform*** can be defined.

$$\tilde{\mathcal{F}}_R(\tilde{q}) = \int_q \mathcal{F}(q')\langle q'|\tilde{q}\rangle \; dq' \tag{9}$$

The reverse transform is:

$$\mathcal{F}(q) = \int_{\tilde{q}_R} \tilde{\mathcal{F}}_R(\tilde{q}_R)\langle q|\tilde{q}_R\rangle \, d\tilde{q}_R = \int_{\tilde{q}_R}\int_{q'} \mathcal{F}(q')\langle q'|\tilde{q}_R\rangle\langle\tilde{q}_R|q\rangle \, dq' \, d\tilde{q}_R \tag{10}$$

$$= \int_{q'} \mathcal{F}(q')\left\{\int_{\tilde{q}_R} \langle q'|\tilde{q}_R\rangle\langle\tilde{q}_R|q\rangle \; d\tilde{q}_R\right\} dq' = \int_{q'} \mathcal{F}(q') \; \delta(q-q') \, dq'$$

Also here the functions $\langle q|q'\rangle$, $\langle\tilde{q}_R|\tilde{q}'_R\rangle$, $\langle\tilde{q}_R|q\rangle$ and $\langle q|\tilde{q}_R\rangle$ form sets of mutually orthogonal functions.

The reverse bra-ket form of the operator $\tilde{\mathcal{F}}_R$ equals:

$$\tilde{\mathcal{F}}_R = |\tilde{q}_R\rangle\tilde{\mathcal{F}}_R(\tilde{q}_R)\langle\tilde{q}_R| \tag{11}$$

Operator $\widetilde{\mathfrak{R}}_R$ provides the parameter space for the right oriented Fourier transform $\tilde{\mathcal{F}}_R(\tilde{q}_R)$ of function $\mathcal{F}(q)$ in equations (9) and (10).

$$\widetilde{\mathfrak{R}}_R = |\tilde{q}_R\rangle\tilde{q}_R\langle\tilde{q}_R| \tag{12}$$

The ***third version of the Fourier transform*** is:

$$\tilde{\mathcal{F}}(\tilde{q}_L, \tilde{q}_R) = \frac{\tilde{\mathcal{F}}_L(\tilde{q}_L) + \tilde{\mathcal{F}}_R(\tilde{q}_R)}{2} = ½ \int_q \{\langle\tilde{q}_L|q\rangle\mathcal{F}(q) + \mathcal{F}(q)\langle q|\tilde{q}_R\rangle\} \, dq \tag{13}$$

In contrast to the right and left version, the third version has no reverse.

7 Domains and parameter spaces

The quaternionic ***domain*** Ω is supposed to be defined as part of the ***domain*** $\mathfrak{R}$ of a ***reference operator*** $\mathfrak{R}$ that resides in the non-separable quaternionic Hilbert space $\mathcal{H}$. The reverse bra-ket method relates the eigenspace $\{q\}$ of reference operator $\mathfrak{R}$ to a flat quaternionic ***function*** $\mathfrak{R}(q)$. The target of function $\mathfrak{R}(q)$ is its own ***parameter space*** $\{q\}$. Here we explicitly use the same symbol $\mathfrak{R}$ for all directly related objects. In $\mathfrak{M}$, $\mathfrak{R}(q)$ is always and everywhere continuous.

$$\mathfrak{R} = |q\rangle\mathfrak{R}(q)\langle q| = |q\rangle q\langle q| \tag{1}$$

The domain $\mathfrak{R}$ is spanned by the eigenvectors $\{|q\rangle\}$ of operator $\mathfrak{R}$.

The reverse bra-ket method also relates the eigenspace $\mathfrak{R}$ to an equivalent eigenspace $\mathcal{R}$ of a reference operator $\mathcal{R}$, which resides in the infinite dimensional separable Hilbert space $\mathfrak{H}$. Both eigenspaces are related to the same version of the quaternionic number system. However, the second eigenspace $\mathcal{R}$ only uses rational quaternions q_i.

$$\mathcal{R} = |q_i\rangle\mathfrak{R}(q_i)\langle q_i| = |q_i\rangle q_i\langle q_i| \tag{2}$$

Quaternionic number systems can be ordered in several ways. Operator $\mathcal{R}$ corresponds with one of these orderings. $\mathcal{R}$ is supposed to be ***Cartesian-ordered***. $\mathcal{R}$ is a normal operator and its eigenspace is countable. Cartesian ordering means that the set of eigenvectors of $\mathcal{R}$ can be enumerated by the separate eigenvalues of $\mathcal{R}$. The eigenspace is the Cartesian product of four partially ordered sets in which the set, which represents the real part takes a special role. The eigenspace of the Hermitian part $\mathcal{R}_0 = ½\left(\mathcal{R} + \mathcal{R}^\dagger\right)$ of normal operator $\mathcal{R}$ can be used to enumerate a division of $\mathfrak{H}$ into a countable number of disjunctive subspaces, which are spanned by eigenvectors of $\mathcal{R}$. Cartesian ordering means partial ordering of the eigenvalues of $\mathcal{R}_0$ and additional ordering of the eigenvalues of the anti-Hermitian operator $\mathfrak{R} = ½\left(\mathfrak{R} - \mathfrak{R}^\dagger\right)$ by selecting a ***Cartesian coordinate system***. Eight mutually independent Cartesian coordinate systems exist. $\mathcal{R}_0 = \left(\mathcal{R} + \mathcal{R}^\dagger\right)/2$ is a self-adjoint operator. The ordered eigenvalues of $\mathcal{R}_0$ can be interpreted as ***progression values***. The eigenvalues of $\boldsymbol{\mathcal{R}}$ can be interpreted as ***spatial values.*** This differs from the physical notions of time and space. Here we are talking about a mathematical test model.

In this way, parameter spaces as well as domains correspond to closed subspaces of the Hilbert spaces. The domain subspaces are subspaces of the domains of the corresponding reference operators. The parameter spaces are ordered by a selected coordinate system. The Ω domain is represented by a part of the eigenspace of reference operator $\mathfrak{R}$. The flat quaternionic function $\mathfrak{R}(q)$ defines the parameter space $\mathfrak{R}$. It installs an ordering by selecting a Cartesian coordinate system for the eigenspace of its anti-Hermitian part $\mathfrak{R} = ½\left(\mathfrak{R} - \mathfrak{R}^\dagger\right)$. Several mutually independent selections are possible. The chosen selection attaches a corresponding symmetry flavor to this parameter space. In the mathematical test model, this symmetry flavor will become the reference symmetry flavor. Thus, the symmetry flavor of parameter space $\mathfrak{R}^{⓪}$ may be distinguished by its superscript ⓪.

The manifold ω is also defined as the continuum eigenspace of a dedicated normal operator ω which is related to domain Ω and to parameter space $\mathfrak{R}^{⓪}$ via function $\mathfrak{F}$. Within this parameter space $\mathfrak{F}$

may have discontinuities, but these must be excluded from the domain over which integration takes place. This exclusion will be treated below.

Symmetry centers are described by anti-Hermitian operators and their geometric center can float on another parameter space as a function of progression. At every progression step only one location of the symmetry center is used. In combination this produces a ***well ordered operator*** where a single progression value corresponds with a single spatial location. The spatial location is determined by a stochastic mechanism. This mechanism produces ***coherent location swarms***. The swarm can be described by a continuous location density distribution. Further, all swarm elements can be enumerated by a progression value and thus form ***a hopping path***.

8 Stokes theorem without discontinuities

The conventional generalized Stokes theorem is in fact a combination of two versions. One is the using the divergence part of the exterior derivative $d\omega$. It is also known as the generalized divergence theorem. The other version uses the curl part of the exterior derivative. For quaternionic manifolds the two versions can be combined in one formula. The domains typically cover a static status quo. The static status quo is characterized by three changes, a divergence, a gradient and a curl. The other two changes concern what disappears into history and what comes in from the future. These part concerns the change of the scalar and vector density distributions.

Without discontinuities in the manifold ω the conventional generalized Stokes theorem is represented by a simple formula [9].

$$\int_{\Omega} d\omega = \int_{\partial\Omega} \omega \left(= \oint_{\partial\Omega} \omega \right) \tag{1}$$

The theorem can be applied when everywhere in Ω the derivative dω exists and when everywhere in $\partial\Omega$ the manifold ω is continuous and integrable. The domain Ω is encapsulated by a boundary $\partial\Omega$.

$$\Omega \subset \partial\Omega \tag{2}$$

In this paper, the manifolds ω and $d\omega$ represent quaternionic fields $\mathfrak{F}$ and $d\mathfrak{F}$, while inside $\partial\Omega$ the manifold ω represents the quaternionic boundary of the quaternionic field $\mathfrak{F}$. These fields and manifolds correspond to defining functions $\mathfrak{F}(q)$ and $d\mathfrak{F}(q)$.

$d\omega$ is the exterior derivative of ω.

This view is focusing onto the spatial part $\mathfrak{R}$ of the quaternionic parameter space $\mathfrak{R}$. It uses only the spatial parts $\langle \boldsymbol{\nabla}, \boldsymbol{f} \rangle$ and $\boldsymbol{\nabla} \times \boldsymbol{f}$ of the first order differential equation.

$$\nabla f = \nabla_0 f_0 - \langle \boldsymbol{\nabla}, \boldsymbol{f} \rangle + \nabla_0 \boldsymbol{f} + \boldsymbol{\nabla} f_0 + \boldsymbol{\nabla} \times \boldsymbol{f} \tag{3}$$

Apparently in the conventional Stokes theorem the gradient $\boldsymbol{\nabla} f_0$ is neglected. In quaternionic space all five terms contribute to the balance and continuity equations. If both the historic and the future parts are taken into the view then a new extended Stokes theorem emerges.

In particular formula (1) does not pay any attention to the what exists outside of the splitting boundary. If the parameter space $\mathfrak{R}$ is an eigenspace of a reference operator in a quaternionic Hilbert space then the ignored region concerns the other part of the Hilbert space. A proper balance equation must consider all participating parts. ***We will extend the Stokes equation in that direction***.

8.1 Interpreting the exterior derivative

Via quaternionic defining functions, the reverse bra-ket method couples the separable Hilbert space to its non-separable companion.

The defining function $\mathcal{F}(\mathrm{q})$ links the integral over the full quaternionic q numbers to the summation over the rational $q_i$numbers.

$$\langle x|\mathcal{F}\ y\rangle = \sum_i \langle x|q_i\rangle \mathcal{F}(q_i)\langle q_i|y\rangle \approx \int_q \langle x|q\rangle \mathcal{F}(q)\langle q|y\rangle\ dq \tag{1}$$

This corresponds to:

$$\oint_{\partial\Omega} \mathcal{F} = \int_{\partial\Omega} \mathcal{F} \Leftrightarrow \sum_i \langle x|q_i\rangle \mathcal{F}(q_i)\langle q_i|y\rangle \tag{2}$$

$$\int_{\Omega} d\mathcal{F} \Leftrightarrow \int_q \langle x|q\rangle \mathcal{F}(q)\langle q|y\rangle\ dq \tag{3}$$

This divides the region over which the equation works into two parts. One in which summation equals integration and a region or a set of regions where integration does not work properly due to the existence of discontinuities of $\mathcal{F}(q)$ in those sub-regions. Exchanging $\mathcal{F}(q)$ against a smoothed version can completely or partly cure this problem.

Another possibility is the split of the parameter space $\mathfrak{R}$ of $\mathcal{F}(q)$ into the parts $\mathfrak{R}_-$ and $\mathfrak{R}_+$. This splits the parameter space in two parts that have different ordering of the real part of the parameter space. This split is treated later. If the two splits are combined, then the split between summation and integration can be interpreted as a leakage of the second split in which discrete objects pass though the sieve that splits $\mathfrak{R}_-$ and $\mathfrak{R}_+$. A similar interpretation can be given to larger regions in which $\mathcal{F}(q)$ is not defined.

Thus, the ***quaternionic extension of the Stokes theorem*** involves multiple splits:

- The split between $\mathfrak{R}_-$ and a history-side static status quo.
- The slit between the future-side static status quo and $\mathfrak{R}_+$.
- The split around point-like artifacts.
- The split around other regions where the defining function is not integrable.

The region between the two static status quos is not integrable. However, properly smoothed fields pass straight through this region.

The conventional generalized Stokes theorem exists in the form of a divergence based version and in the form of a curl based version [10]. However, for quaternionic manifolds the definition of the exterior derivative requests extra attention. In this section we assume that the quaternionic manifold ω is represented by the target of a quaternionic function $\mathfrak{F}(q)$. Function $\mathfrak{F}(q)$ has a flat parameter space $\mathfrak{R}$.

$\mathfrak{R}$ is a flat quaternionic manifold, which is represented by the target of function $\mathfrak{R}(q) \stackrel{\text{def}}{=} q$.

We presume that the exterior derivative $\mathrm{d}\mathfrak{F}$ of $\mathfrak{F}$ can be interpreted by the following equations:

$$\mathrm{d}\mathfrak{F} = \sum_{\mu=0}^{3} e^{\mu} \frac{\partial \mathfrak{F}}{\partial x_{\mu}} dx_{\mu} = \sum_{\mu=0}^{3} e^{\mu} dx_{\mu} \sum_{\nu=0}^{3} e^{\nu} \frac{\partial \mathfrak{F}_{\nu}}{\partial x_{\mu}} = e^{\mu\nu} D_{\mu} \mathfrak{F}_{\nu} \tag{4}$$

$$D_{\mu} \stackrel{\text{def}}{=} dx_{\mu} \frac{\partial}{\partial x_{\mu}} \tag{5}$$

Thus $\mathrm{d}\mathfrak{F}$ is represented by a tensor. This is not a very attractive presentation. It is more convenient to treat the change along the directions in which change takes place according to the first order partial differential equations.

The exterior derivative differs from the partial differentials that appear in partial differential equations.

$$\mathfrak{G} = \sum_{\varsigma=0}^{3} e^{\varsigma} \mathfrak{G}_{\varsigma} = e^{\varsigma} \mathfrak{G}_{\varsigma} \tag{3}$$

$$= \nabla\mathfrak{F} = \sum_{\mu=0}^{3} e^{\mu} \frac{\partial \mathfrak{F}}{\partial x_{\mu}} = \sum_{\mu=0}^{3} e^{\mu} \sum_{\nu=0}^{3} e^{\nu} \frac{\partial \mathfrak{F}_{\nu}}{\partial x_{\mu}} = e^{\mu} e^{\nu} \partial_{\mu} \mathfrak{F}_{\nu} = e^{\mu\nu} \partial_{\mu} \mathfrak{F}_{\nu}$$

In the right parts of the above formulas, the summation rules for subscripts and superscripts are applied.

We use the fact that quaternions can be considered as a combination of a real scalar and an imaginary vector. Further, we apply the fact that quaternionic partial differential operators act as multipliers.

$$\mathfrak{F} = \mathfrak{F}_0 + \boldsymbol{\mathfrak{F}} \tag{4}$$

$$\mathfrak{G} = \nabla\mathfrak{F} = \mathfrak{G}_0 + \boldsymbol{\mathfrak{G}} = (\nabla_0 + \boldsymbol{\nabla})(\mathfrak{F}_0 + \boldsymbol{\mathfrak{F}}) \tag{5}$$

$$\mathfrak{G}_0 = \nabla_0 \mathfrak{F}_0 - \langle \boldsymbol{\nabla}, \boldsymbol{\mathfrak{F}} \rangle \tag{6}$$

$$\boldsymbol{\mathfrak{G}} = \nabla_0 \boldsymbol{\mathfrak{F}} + \boldsymbol{\nabla}\mathfrak{F}_0 \pm \boldsymbol{\nabla} \times \boldsymbol{\mathfrak{F}} \tag{7}$$

For some fields, some parts of $\boldsymbol{\mathfrak{G}}$ may get special symbols. This is applied in Maxwell-like equations.

$$\mathfrak{E} = -\nabla_0 \mathfrak{F} - \boldsymbol{\nabla} \mathfrak{F}_0 \tag{8}$$

$$\mathfrak{B} = \boldsymbol{\nabla} \times \mathfrak{F} \tag{9}$$

Similar definitions are applied in Maxwell equations. However, despite these similarities, the derived fields $\mathfrak{E}$ and $\mathfrak{B}$ are not equivalent to the Maxwell fields **E** and **B**. The Maxwell equations are treated in the appendix.

In general, there is no guarantee that $\mathfrak{E}$ and $\mathfrak{B}$ are perpendicular. Thus in general:

$$\langle \mathfrak{E}, \mathfrak{B} \rangle \neq 0 \tag{10}$$

However, a third vector $\mathfrak{P}$ is perpendicular to both $\mathfrak{E}$ and $\mathfrak{B}$.

$$\mathfrak{P} = \mathfrak{E} \times \mathfrak{B} \tag{11}$$

Equation (6) is not part of the Maxwell set of partial differential equations. However, the terms $\nabla_0 \mathfrak{F}_0$ and $\langle \boldsymbol{\nabla}, \mathfrak{F} \rangle$ are used in gauge equations.

We may conclude that change covers five terms that do not represent four independent directions as is suggested by the conventional Maxwell differential equations.

Please note that

$$\nabla^* \mathfrak{F}^* = (\nabla_0 - \boldsymbol{\nabla})(\mathfrak{F}_0 - \mathfrak{F}) = \mathfrak{G}_0 - \nabla_0 \mathfrak{F} - \boldsymbol{\nabla} \mathfrak{F}_0 \pm \boldsymbol{\nabla} \times \mathfrak{F} \tag{12}$$

$$(\nabla \mathfrak{F})^* = \mathfrak{G}^* = \nabla^* \mathfrak{F}^* \mp 2 \boldsymbol{\nabla} \times \mathfrak{F} \tag{13}$$

Thus the partial differential of a ***curl free*** function connects to a Hermitian operator!

The $\pm$ sign indicates the fact that quaternionic parameter spaces and quaternionic functions exist in versions that differ in the handedness of their external vector product.

In the integrals below some terms of $\nabla \mathfrak{F}$ are combined.

$$\boldsymbol{\nabla} \mathfrak{F} = -\langle \boldsymbol{\nabla}, \mathfrak{F} \rangle \pm \boldsymbol{\nabla} \times \mathfrak{F} \tag{14}$$

$$\boldsymbol{\nabla}\mathfrak{F} = \boldsymbol{\nabla}\mathfrak{F}_0 - \langle \boldsymbol{\nabla}, \mathfrak{F} \rangle \pm \boldsymbol{\nabla} \times \mathfrak{F} \tag{15}$$

$$\nabla_0 \mathfrak{F} = \nabla_0 \mathfrak{F}_0 + \nabla_0 \mathfrak{F} \tag{16}$$

It must be noticed that

$$\mathrm{d}\mathfrak{F} \neq \sum_{\mu=0}^{3} e^{\mu} \mathfrak{G}_{\mu} dx_{\mu} \tag{17}$$

This is the reason that the generalized Stokes integral uses the wedge product $dx \wedge dy \wedge dz \wedge d\tau$. These wedge products are merely a warning that a tensor is active. In the quaternionic version of the Stokes theorem, it is not a clear exposure of the mechanism.

The Maxwell-like partial quaternionic differential equations differ from the Maxwell equations that are used in current physical theories. Thus, great care must be applied in comparing the two sets of partial differential equations. Especially equations (6) and (10) signal alarming differences.

8.2 A special domain split

In the special splitting case that is investigated here, the extended generalized Stokes theorem constructs a rim $\mathfrak{F}(\boldsymbol{x}, \tau)$ between the past history of the field $[\mathfrak{F}(\boldsymbol{x}, t)]_{t<\tau}$ and the future $[\mathfrak{F}(\boldsymbol{x}, t)]_{t>\tau}$ of that field. It means that the boundary $\mathfrak{F}(\boldsymbol{x}, \tau)$ of field $[\mathfrak{F}(\boldsymbol{x}, t)]_{t<\tau}$ represents a universe wide static status quo of that field.

More specifically, the form of the generalized Stokes theorem for the sketched situation runs as:

$$\int_{t=0}^{\tau} \iiint_{V} \mathrm{d}\mathfrak{F}\,(x) = \int_{t=0}^{\tau} \left(\iiint_{V} \nabla\mathfrak{F}(x)\, dx \wedge dy \wedge dz \right) \wedge d\tau = \left[\iiint_{V} \mathfrak{F}\,(\boldsymbol{x}) d\boldsymbol{x} \right]_{t=\tau} \tag{1}$$

$$x = \boldsymbol{x} + \tau \tag{2}$$

Here $[\mathfrak{F}(\boldsymbol{x}, t)]_{t=\tau}$ represents the static status quo of a quaternionic field at instance τ. V represents the spatial part of the quaternionic domain of $\mathfrak{F}$, but it may represent only a restricted part of that parameter space. This last situation corresponds to the usual form of the divergence theorem.

As mentioned above great care must be taken by interpreting the wedge product in

$$\mathrm{d}\mathfrak{F}(x) = \nabla\mathfrak{F}(x)\, dx \wedge dy \wedge dz \wedge d\tau. \tag{3}$$

Due to the danger of misinterpretation, we will avoid the wedge products that appear in the middle part of equation (1). In the right part of the equation only the divergence, the curl and a gradient play a role. The split that has been selected, sets a category of operators apart that are all Cartesian-ordered in the same way as operator $\mathcal{R}$ is. It enables a space-progression model in which progression steps in the separable Hilbert space $\mathfrak{H}$ and flows in its non-separable companion $\mathcal{H}$. Via the reverse bra-ket method the Cartesian-ordering of $\mathcal{R}$ can be transferred to $\mathfrak{R}$.

8.2.1 Interpretation of the selected encapsulation

The boundary $\partial\Omega$ is selected between the real part and the imaginary part of domain $\mathfrak{R}$. But it also excludes part of the real part. That part is the range of the real part from τ to infinity. τ is interpreted as the current progression value.

The boundary $\partial\Omega$ has one dimension less than the domain Ω. The failing dimension is taken by the form of the partition. In the special case the boundary is formed by most of the three dimensional spatial part of the parameter space. The theorem does not specify the form of the partition, but requires that the ***partition form*** does not traverse discontinuities or regions in which the defining function is not defined. Thus, if the partition wipes through the parameter space and encounters discontinuities or regions in which the defining function is not defined, then the partition must encapsulate these objects while it passes them. These encapsulating partitions become part of the boundary. In this way these objects stay outside of the boundary $\partial\Omega$. Symmetry centers and space cavities become objects that float as encapsulated modules over the domain Ω. If they enter the partition, then they can be considered to be created. If they keep floating with the partition, then these objects are alive. If they have completely passed the partition, then they can be considered to have been annihilated. A long lifetime will correspond to a tube-like history and a corresponding tube-like future.

The future $\mathfrak{R} - \Omega$ is kept on the outside of the boundary $\partial\Omega$. As a consequence, the mechanisms that generate new data, operate on the rim $\partial\Omega$ between past Ω and future $\mathfrak{R} - \Omega$. Two interpretations are possible. Either, the mechanisms generate data that was not yet present in the Hilbert spaces, or the mechanisms represent the data that are encountered during the passage of the partition. The observers cannot decide which of the two interpretations is correct. It is merely a question of what you want to belief. For $\mathfrak{M}$ this interpretation does not matter. This paper describes the model in accordance to the first interpretation. This avoids deliberation about why and how the creator of the model generated the data that are archived in $\mathfrak{M}$'s Hilbert spaces. In $\mathfrak{M}$ the relevant observers live inside the wiping boundary. In the selected interpretation the creator of the model is throwing dices!

The described split of quaternionic space results in a space-progression model that is to a significant extent similar to the way that physical theories describe their space time models. However, the physical theories apply a spacetime model that has a Minkowski signature. The quaternionic model, which is represented here, is strictly Euclidean.

The paper does not claim that this quaternionic space-progression model reflects the structure and the habits of physical reality. The quaternionic space-progression model is merely promoted as a mathematical test model.

What according to the selected interpretation happens in the mathematical test model can be seen as an ongoing process that embeds the subsequent static status quo's of the separable Hilbert space into the Gelfand triple.

Controlling mechanisms act as a function of progression τ in a stochastic and step-wise fashion in the realm of the separable Hilbert space. The results of their actions are stored in eigenspaces of

corresponding stochastic operators that reside in the separable Hilbert space. These stochastic operators differ from the kind of operators that are handled by the reverse bra-ket method. However, if the stochastic operators produce coherent swarms that feature a continuous density distribution, then that distribution corresponds with an operator that is defined by this distribution.

The controlling mechanisms have no notion of the fields. They only work with discrete objects that appear in swarms.

At the same instance this part of the separable Hilbert space is embedded into its companion Gelfand triple. The controlling mechanisms will provide all generated data with a ***progression stamp*** τ. This progression stamp reflects the state of a model wide clock tick. The whole model, including its "physical" fields will proceed with these progression steps. However, in the Gelfand triple this progression can be considered to flow.

At the defined rim, any forecasting will be considered as mathematical cheating. Thus, at the rim, the uncertainty principle does not work for the progression part of the parameter spaces. Differential equations that offer advanced as well as retarded solutions must reinterpret the advanced solutions and turn them in retarded solutions, which in that case represent another kind of object. If the original object represents a particle, then the reversed particle is the anti-particle. Thus the tubes that represent elementary modules will appear to reflect on the boundary in one interpretation and will just pass the boundary in the other interpretation. In the panning view the tube just passes undisturbed through the boundary.

As a consequence of the construct, the history, which is stored-free from any uncertainty-in the already processed part of the eigenspaces of the physical operators, is no longer touched. Future is unknown or at least it is inaccessible for observation.

8.2.2 Integrals over regular spatial domains

If in a spatial domain, function $\mathfrak{F}$ obeys the homogeneous equation

$$\boldsymbol{\nabla}\boldsymbol{\nabla}\mathfrak{F} = 0 \tag{1}$$

then the function $\mathfrak{F}$ and the corresponding field $\mathfrak{F}$ is considered to be regular in that domain. For functions $\mathfrak{F}$ that are this kind of regular in spatial domain V hold:

$$\iiint_V \boldsymbol{\nabla}\mathfrak{F} = \oiint_S \boldsymbol{n}\mathfrak{F} \tag{2}$$

$$\iiint_V \boldsymbol{\nabla}\mathfrak{F}_0 = \oiint_S \boldsymbol{n}\mathfrak{F}_0 \tag{3}$$

$$\iiint_V \langle \boldsymbol{\nabla}, \mathfrak{F} \rangle = \oiint_S \langle \boldsymbol{n}, \mathfrak{F} \rangle \tag{4}$$

$$\iiint_V \boldsymbol{\nabla} \times \mathfrak{F} = \oiint_S \boldsymbol{n} \times \mathfrak{F} \tag{5}$$

8.2.3 Integrating irregular functions

We can use the gradient of the inverse of the spatial distance $|\boldsymbol{q} - \boldsymbol{c}|$.

$$\boldsymbol{\nabla} \frac{1}{|\boldsymbol{q} - \boldsymbol{c}|} = -\frac{\boldsymbol{q} - \boldsymbol{c}}{|\boldsymbol{q} - \boldsymbol{c}|^{\boldsymbol{3}}} \tag{1}$$

The divergence of this gradient is a Dirac delta function.

$$\delta(\boldsymbol{q} - \boldsymbol{c}) = -\frac{1}{4\pi} \langle \boldsymbol{\nabla}, \boldsymbol{\nabla} \frac{1}{|\boldsymbol{q} - \boldsymbol{c}|} \rangle = -\frac{1}{4\pi} \langle \boldsymbol{\nabla}, \boldsymbol{\nabla} \rangle \frac{1}{|\boldsymbol{q} - \boldsymbol{c}|} \tag{2}$$

This means that:

$$\phi(\boldsymbol{c}) = \iiint_V \phi(\boldsymbol{q}) \delta(\boldsymbol{q} - \boldsymbol{c}) = -\frac{1}{4\pi} \iiint_V \phi(\boldsymbol{q}) \langle \boldsymbol{\nabla}, \boldsymbol{\nabla} \rangle \frac{1}{|\boldsymbol{q} - \boldsymbol{c}|} \tag{3}$$

As alternative, we can also use the Green's function $G(\boldsymbol{q})$ of the partial differential equation.

$$\phi(\boldsymbol{c}) = \iiint_V \phi(\boldsymbol{q}) G(\boldsymbol{q} - \boldsymbol{c}) \tag{4}$$

For the Laplacian $\langle \boldsymbol{\nabla}, \boldsymbol{\nabla} \rangle$ this obviously means:

$$\langle \boldsymbol{\nabla}, \boldsymbol{\nabla} \rangle \mathfrak{F} = \phi(\boldsymbol{q}) \tag{5}$$

$$G(\boldsymbol{q} - \boldsymbol{c}) = \frac{1}{|\boldsymbol{q} - \boldsymbol{c}|} \tag{6}$$

However, when added to the Green's function, every solution f of the homogeneous equation

$$\langle \boldsymbol{\nabla}, \boldsymbol{\nabla} \rangle f = 0 \tag{7}$$

is also a solution of the Laplace equation.

$$\phi(\boldsymbol{c}) = \iiint_V \frac{\phi(\boldsymbol{q})}{|\boldsymbol{q} - \boldsymbol{c}|} \tag{8}$$

Function $\phi(\boldsymbol{c})$ can be interpreted as the potential that is raised by charge distribution $\phi(\boldsymbol{q})$.

In pure spherical conditions the Laplacian reduces to:

$$\langle \boldsymbol{\nabla}, \boldsymbol{\nabla} \rangle \mathfrak{F}(r) = \frac{1}{r^2} \frac{\partial}{\partial r} \left(r^2 \frac{\partial \mathfrak{F}(r)}{\partial r} \right) \tag{9}$$

For the following ***test function*** $\mathfrak{T}(r)$ this means [12]:

$$\mathfrak{T}(r) = \frac{Q}{4\pi} \frac{ERF\left({}^{r}/_{\sigma\sqrt{2}}\right)}{r} \tag{10}$$

$$\rho(r) = \langle \boldsymbol{\nabla}, \boldsymbol{\nabla} \rangle \mathfrak{F}(r) = \frac{Q}{\left(\sigma\sqrt{2\pi}\right)^3} \exp\left(- \frac{r^2}{2\sigma^2} \right) \tag{11}$$

Thus, for a ***Gaussian location distribution*** $\rho(r)$ of point-like artifacts the corresponding contribution to field $\mathfrak{T}(r)$ equals an error function divided by its argument. At first sight this may look in contradiction with equations (4) − (8), but here the distribution of artifacts extends over the boundary of domain V.

$$\frac{1}{r^2} \frac{\partial}{\partial r} \left(r^2 \frac{\partial}{\partial r} \frac{ERF(r)}{r} \right) = \frac{1}{r^2} \frac{\partial}{\partial r} \left(- ERF(r) + r \frac{2}{\sqrt{\pi}} \exp(-r^2) \right)$$

$$= \frac{1}{r^2} \left(- \frac{2}{\sqrt{\pi}} \exp(-r^2) + \frac{2}{\sqrt{\pi}} \exp(-r^2) - 2r \frac{2}{\sqrt{\pi}} \exp(-r^2) \right) = \frac{4}{\sqrt{\pi}} \exp(-r^2)$$

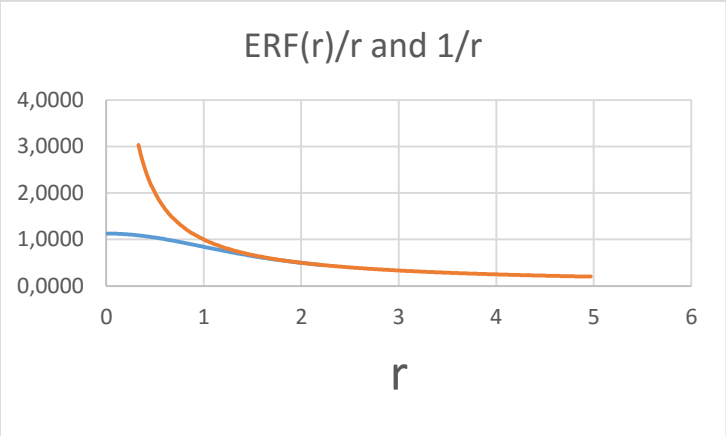

Figure 1. Close to the geometric center the singularities are converted in a smooth function. Further from the center the form of the Green's function (1/r) is retained.

9 The detailed generalized Stokes theorem

We separate all point-like discontinuities from the domain Ω by encapsulating them in an extra boundary. Symmetry centers represent spherically ordered parameter spaces in regions H_n^x that float on a background parameter space $\mathfrak{R}$. The boundaries $\partial\mathrm{H}_n^x$ separate the regions H_n^x from the domain Ω. The regions H_n^x are platforms for local discontinuities in basic fields [2]. These fields are continuous in domain $\Omega - \mathrm{H}$.

$$H = \bigcup_n \mathrm{H}_n^x \tag{1}$$

The symmetry centers $\mathfrak{S}_n^x$ are encapsulated in regions H_n^x and the encapsulating boundary $\partial\mathrm{H}_n^x$ is not part of the disconnected boundary which encapsulates all continuous parts of the quaternionic manifold ω that exist in the quaternionic model.

$$\int_{\Omega-\mathrm{H}} d\omega = \int_{\partial\Omega\cup\partial\mathrm{H}} \omega = \int_{\partial\Omega} \omega - \sum_n \int_{\partial\mathrm{H}_n^x} \omega \tag{2}$$

If we take the unit normal to point outward on all of the boundary, this reverses the direction of the normal on $\partial\mathrm{H}_n^x$, which negates the integral. ***Thus, in this formula, the contributions of boundaries*** $\{\partial\mathrm{H}_n^x\}$ ***are subtracted from the contributions of boundary*** $\partial\Omega$. This means that $\partial\Omega$ also surrounds the regions $\{\mathrm{H}_n^x\}$. This fact renders the integration sensitive to the ordering of the participating domains.

Domain Ω corresponds to part of the reference parameter space $\mathfrak{R}^{⓪}$. As mentioned before the symmetry centers $\{\mathfrak{S}_n^x\}$ represent encapsulated regions $\{\mathrm{H}_n^x\}$ that float on parameter space $\mathfrak{R}^{⓪}$.

The geometric center of symmetry center $\mathfrak{S}_n^x$ is represented by a floating location on parameter space $\mathfrak{R}^{⓪}$.

The relation between the ***subspace*** S_Ω that corresponds to the domain Ω and the ***subspace*** $S_\mathfrak{R}$ that corresponds to the parameter space $\mathfrak{R}^{⓪}$ is given by:

$$\underbrace{\Omega}_{S_\Omega} \subset \underbrace{\mathfrak{R}^{⓪}}_{S_\mathfrak{R}} \tag{3}$$

Similarly:

(4)

$$\underbrace{\mathrm{H}_n^x}_{S_{\mathrm{H}_n^x}} \subset \underbrace{\mathfrak{S}_n^x}_{S_{\mathfrak{S}_n^x}}$$

10 Symmetry flavors

10.1 Ordering

Quaternionic number systems exist in many versions that differ in the way that these number systems are ordered. For example it is possible to order the real parts of the quaternions up or down. A Cartesian coordinate system can be used to order the imaginary parts of the quaternions. If the orientation of the coordinate axes is kept fixed, then this Cartesian ordering can be done in eight mutually independent ways. It is also possible to apply spherical symmetric ordering by using a polar coordinate system. This can be done by starting with the azimuth and order it up or down and then order the polar angle and order it up or down. It is also possible to start with the polar angle. A spherical coordinate system starts from a selected Cartesian coordinate system.

The reverse bra-ket method enables the attachment of these different symmetry flavors of the quaternionic number system to dedicated operators that reside in an infinite dimensional separable quaternionic Hilbert space. Separable Hilbert spaces can only handle countable eigenspaces. Thus the reverse bracket method can only use the rational subsets of the quaternionic number systems.

Each infinite dimensional separable Hilbert space owns a companion Gelfand triple, which is a non-separable Hilbert space and which also supports operators that feature continuums as their eigenspaces. The reverse bra-ket method relates operators in the separable Hilbert space o operators in the Gelfand triple.

These representations of quaternionic number systems can act as parameter spaces of quaternionic functions that can also be represented by operators and their eigenspaces. The reverse bra-ket method establishes this link.

Together, this means that the two companion quaternionic Hilbert spaces can represent ordered discrete sets and ordered fields via the eigenspaces of some of their operators and that these sets and fields can also be represented by pairs of quaternionic functions and their parameter spaces.

The selection of a preferred Cartesian coordinate system sins against the cosmological principle. Thus, ***with respect to the definition of symmetry flavors, $\mathfrak{M}$ is in conflict with the cosmological principle***.

10.2 Defining symmetry flavors

Quaternions can be mapped to Cartesian coordinates along the orthonormal base vectors 1, $\boldsymbol{i}$, $\boldsymbol{j}$ and $\boldsymbol{k}$; with $\boldsymbol{ij} = \boldsymbol{k}$

Due to the four dimensions of quaternions, quaternionic number systems exist in 16 well-ordered versions $\{q^x\}$ that differ only in their discrete Cartesian symmetry set. The quaternionic number systems $\{q^x\}$ correspond to 16 versions $\{q_i^x\}$ of rational quaternions.

Half of these versions are right handed and the other half are left handed. Thus the handedness is influenced by the symmetry flavor.

The superscript ^{x} can be ⓪, ①, ②, ③, ④, ⑤, ⑥, ⑦, ⑧, ⑨, ⑩, ⑪, ⑫, ⑬, ⑭, or ⑮.

This superscript represents the ***symmetry flavor*** of the superscripted subject. For the reference operator we neglect the superscript ⓪.

The reference operator $\mathcal{R} = |q_i\rangle q_i \langle q_i|$ in separable Hilbert space $\mathfrak{H}$ maps into the reference operator $\mathfrak{R} = |q\rangle q \langle q|$ in Gelfand triple $\mathcal{H}$.

The symmetry flavor of the symmetry center $\mathfrak{S}^x$, which is maintained by operator $\mathfrak{S}^x = |\mathfrak{s}_i^x\rangle\mathfrak{s}_i^x\langle\mathfrak{s}_i^x|$ is determined by its Cartesian ordering and then compared with the reference symmetry flavor, which is the symmetry flavor of the reference operator $\mathcal{R}$.

Now the symmetry related charge follows in three steps.

1. Count the difference of the spatial part of the symmetry flavor of symmetry center $\mathfrak{S}^x$ with the spatial part of the symmetry flavor of reference operator $\mathcal{R}$.
2. If the handedness changes from **R** to **L**, then switch the sign of the count.
3. Switch the sign of the result for anti-particles.

We use the names of the corresponding particles that appear in the standard model in order to distinguish the different symmetry flavor combinations. Elementary fermions relate to solutions of a corresponding second order partial differential equation that describes the embedding of these particles. Elementary bosons relate to solutions of a different second order partial differential equation.

In a suggestive way, we use the names of the elementary fermions that appear in the standard model in order to distinguish the possible combinations of symmetry flavors.

Fermion symmetry flavor					
Ordering x y z τ	Super script	Handedness Right/Left	Color charge	Electric charge * 3	Symmetry center type. Names are taken from the standard model
	⓪	**R**	N	+0	neutrino
	①	**L**	R	−1	down quark
	②	**L**	G	−1	down quark
	③	**L**	B	−1	down quark
	④	**R**	B	+2	up quark
	⑤	**R**	G	+2	up quark
	⑥	**R**	R	+2	up quark
	⑦	**L**	N	−3	electron
	⑧	**R**	N	+3	positron
	⑨	**L**	R	−2	anti-up quark
	⑩	**L**	G	−2	anti-up quark
	⑪	**L**	B	−2	anti-up quark
	⑫	**R**	B	+1	anti-down quark
	⑬	**R**	R	+1	anti-down quark
	⑭	**R**	G	+1	anti-down quark
	⑮	**L**	N	−0	anti-neutrino

Elementary fermions switch their handedness when the sign of the real part is switched. Spherical ordering can be done by first starting with the azimuth and next proceeding by the polar angle. Both can be done up or down. Fermions and bosons appear to differ in this choice.

Also continuous functions and continuums feature a symmetry flavor. Continuous quaternionic functions $\psi^x(q^x)$ and corresponding continuums do not switch to other symmetry flavors ^{y}.

The reference symmetry flavor $\psi^y(q^y)$ of a continuous function $\psi^x(q^y)$ is the symmetry flavor of the parameter space $\{q^y\}$.

If the continuous quaternionic function describes the density distribution of a set $\{a_i^x\}$ of discrete objects a_i^x, then this set must be attributed with the same symmetry flavor ^{x}. The real part describes the location density distribution and the imaginary part describes the displacement density distribution.

This section shows that ordering of an embedded (parameter) space can represent specific properties of that space that distinguishes this embedded space from differently ordered embedded (parameter) spaces. This also hold for embedding fields. The consequences comes to the front in situations where differences in ordering play an essential role. We will encounter that situation where different parameter spaces are used in the integration procedure as occurs in the extended Stokes theorem. This is treated in chapter 13. First we take a look at modules and especially the elementary modules will be investigated. Elementary modules appear to possess their own private parameter space.

11 Modules

Modules are represented by closed subspaces of the separable Hilbert space, but not every closed subspace represents a module or modular system. In fact only a small minority of the closed subspaces will act as actual modules. So, what renders a closed subspace into a module and what combines modules into subsystems or systems? The answers to these questions can only be found by investigating the contents of the closed subspaces.

A special category of modules are ***elementary modules***. Elementary modules are not constituted of other modules. They are the atoms of the orthomodular lattice, which describes the relations between modules and modular systems. This indicates that at every progression instant the elementary module is represented by a single Hilbert vector.

A single Hilbert vector spans the smallest possible type of subspace. Thus it is the proper candidate for representing an elementary module, which forms an atom of the orthomodular lattice. This subspace cannot be split into smaller subspaces. As eigenvector of a corresponding normal operator σ the vector can only accept a single quaternionic eigenvalue. If the real value of that eigenvalue represents progression, then the Hilbert vector can only represent a single instant of the 'life' of the elementary module. The imaginary part of the eigenvalue then represents the spatial location of the elementary module at that instant. It is a precise (not blurred!) location. Each elementary particle owns a normal operator σ whose eigenvalues describe the 'life' of the elementary module. The operator σ is a private descriptor of the elementary module.

At other instances another Hilbert vector represents the elementary module.

The eigenvectors of a normal operator are all mutually orthogonal. Within a set of mutually orthogonal Hilbert vectors exists no notion of closest member. Only the corresponding eigenvalues may provide a notion of neighborhood. The normal operator that represents the elementary module has no means for controlling the nearness of the subsequent eigenvalues. The normal operator only acts as a descriptor. It does not act as a controller of the nearness of the eigenvalues!

Thus, the elementary module hops along a series of eigenvectors of which the real values can be ordered with respect to increasing ***progression***. Each of these values represent a location in an harmonica of sheets, that each represent a progression instant. Each elementary module takes only one spatial location in such a sheet. The sheets form subspaces of the separable Hilbert space that represent a static status quo. In that subspace the eigenvalues of the considered operators all feature the same real part. In this view the model steps with model-wide steps through the full separable Hilbert space.

The quaternionic values that represent a single elementary module, all belong to Hilbert vectors that together span a subspace of the Hilbert space that corresponds to a ***symmetry center***. We will indicate the operator that describes the symmetry center with symbol $\mathfrak{S}$.

A symmetry center is described by an anti-Hermitian operator. This anti-Hermitian operator $\mathfrak{S}$ has only imaginary and thus spatial eigenvalues. The eigenvalues of the operator that describes the symmetry center are ordered by a Cartesian coordinate system. This means that in contrast to the operator σ, which describes the 'life' of the elementary module, this symmetry center operator $\mathfrak{S}$ controls the nearness of its eigenvalues.

For the operator that describes via its eigenvalues the 'life' of the elementary module, each subsequent real progression value is accompanied by an imaginary part and together these parts form the eigenvalue that belongs to the Hilbert vector, which at this progression instant represents the elementary module. This single value has not much to say about the owner of this eigenvalue. Only a series of subsequent eigenvalues can do that job. A large series of these numbers can tell the types of elementary modules apart. These subsequent quaternionic numbers form a ***dynamic location swarm***. At the same time these numbers form a ***hopping path***. The spatial parts of these numbers are taken from the eigenspace of the anti-Hermitian operator $\mathfrak{S}$ that due to its role determines part of the properties of the elementary module. This operator defines a symmetry center. Thus, all elementary modules reside on a their own individual symmetry center. The symmetry center covers a closed subspace and the module covers a subspace of that subspace. The private symmetry center floats over a background space and its center location is a function of

progression. In each sheet that belongs to a progression value the symmetry center can be considered as an ordered region that acts as a “life space” for the elementary module.

The location of the geometric center of the floating symmetry center is not part of the eigenspace of the anti-Hermitian operator $\mathfrak{S}$, which describes the symmetry center. This floating location is a property of the elementary module and is formulated in terms of a value of another parameter space. This parameter space is eigenspace of another reference operator $\mathfrak{R}$. This second reference operator is a normal operator and provides full quaternionic eigenvalues that can represent progression values as well as spatial locations.

Thus, symmetry centers represent regional platforms that possess an ordered pure spatial parameter space. We consider such operators as “physically relevant” when their eigenspaces are Cartesian-ordered. Thus, closed subspaces of the Hilbert space can represent modules when they correspond to eigenspaces of which the spatial part is ordered by a Cartesian coordinate system. This is a narrower specification than the earlier specification that modules are represented by closed subspaces of a separable Hilbert space.

11.1 Module content

In free translation, the spectral theorem for normal operators that reside in a separable Hilbert space states: “If a normal operator maps a closed subspace onto itself, then the subspace is spanned by an orthonormal base consisting of eigenvectors of the operator.” The corresponding eigenvalues characterize this closed subspace.

Thus, it is possible to select a quaternionic normal operator $\mathscr{o}$ for which a subset of the eigenvectors span the closed subspace and the corresponding eigenvalues describe the dynamic geometric data of this module. By ordering the real values of these eigenvalues, the geometric data become functions of what we already have called ***progression***. The selected operator describes the module content.

This operator only acts as a descriptor. The operator does not generate eigenvalues. It has eigenvalues that are generated by a mechanism $\mathfrak{M}$, which is not part of the Hilbert space.

A companion ***reference operator*** $\mathfrak{T}$ provides a Cartesian coordinate base for this subspace. Its eigenspace corresponds to a subspace that encapsulates the eigenspace of the first operator. This second operator corresponds to the symmetry center $\mathfrak{S}$. On the other hand it also covers the progression window of the first operator. The symmetry center corresponds to an anti-Hermitian operator. The second operator $\mathfrak{T}$ is a normal operator. It can be considered as the ***capsule*** or the encapsulating operator of the elementary module. Its eigenspace can be viewed as a ***tube*** in which the elementary module travels.

The operator $\mathfrak{S}$ that describes the symmetry center is only a descriptor. This also holds for the operator $\mathscr{o}$ that describes the content of the corresponding elementary module. The real actor is the controlling mechanism $\mathfrak{M}$, which is responsible for establishing the characteristics that are typical for the elementary module. These characteristics are the statistical characteristics and the symmetry of the swarm and the dynamic characteristics of the corresponding hopping path. The mechanism $\mathfrak{M}$ takes care of the fact that the swarm is a ***coherent swarm*** and stays that way.

11.1.1 Progression window

Stochastic processes that are controlled by dedicated mechanisms provide the elementary modules with dynamic geometric data. Here we only consider elementary modules for which the content is ***well-ordered***. This means that in the eigenspace of the selected operator every progression value is ***only used once***.

For the most primitive modules the closed subspace may be reduced until it covers a ***generation cycle*** in which the statistically averaged characteristics of the module mature to fixed values. The resulting closed subspace acts as a ***sliding progression window***. The sliding window covers a (large) series of sheets.

The sliding window separates a deterministic history from a partly uncertain future. Inside the sliding window ***a dedicated mechanism*** $\mathfrak{M}_n$ ***fills the eigenspace*** of stochastic operator $\mathcal{O} = |a_j\rangle a_j \langle a_j|$. The mechanism is a function of progression. If it is a cyclic function of progression, then the module is recurrently regenerated by its private mechanism.

The phrase "recurrently regenerated" is related to the interpretation of the model where mechanisms generate new eigenvalues in contrast to the alternative interpretation where the boundary is passing over data that already exist as eigenvalues in the Hilbert space. The model itself is not influenced by these interpretations. For describing the model, the paper follows the first interpretation. However, it is also good to keep the second interpretation in mind. It throws a slightly different light upon the model.

11.2 Symmetry center as platform

All elementary modules are supposed to reside in an individual symmetry center. However, at every progression instant the elementary module occupies only one location of the symmetry center. During the regeneration cycle of the module the occupied locations form a coherent location swarm and at the same time the locations form a hopping path. In the model the hopping path is represented by a hopping string that stays within its private tube. The hopping string passes through the boundary that splits the model in past part and a future part. The view of the hopping path is restricted to the spatial part of the corresponding eigenspace and uses a sliding window. The view of the hopping string uses the full quaternionic eigenspace. The view of the swarm integrates over the regeneration cycle. The swarm represents the projection of the hopping path onto the symmetry center.

Symmetry centers float on a supporting medium. That supporting medium corresponds to a Cartesian-ordered normal reference operator $\mathcal{R}^{⓪}$, whose eigenvectors span the whole infinite dimensional separable Hilbert space.

11.3 Map into a continuum

By imaging the discrete eigenvalues into a reference space, the discrete eigenvalues form a ***swarm*** $\{a_j^x\}$, which is a subset of the rational quaternions $\{\mathfrak{s}_i^x\}$ that form the symmetry center on which the module resides. At the same time the discrete eigenvalues form a ***hopping path***. With other words the swarm forms a spatial map of the dynamic hopping of the point-like object. The swarm and the hopping path conform to a stochastic operator $\mathcal{O}^x$ that is well ordered with respect to its progression values, but is not ordered in spatial sense like reference operators $\mathcal{R}$ or $\mathfrak{S}_n^x$.

$$\mathcal{O}^x = |a_j^x\rangle a_j^x \langle a_j^x|$$

This temporal ordering is installed via the quaternionic version of the screened Poisson equation. That equation involves a symmetry center wide clock that can synchronize the location generation process with the model wide progression steps that are oppressed by reference operator $\mathcal{R}^{⓪}$. This will be explained later.

Our plan is to construct a map of the elements $\{a_j^x\}$ of the swarm onto the deformable continuum $\mathfrak{C}$.

The continuum $\mathfrak{C}$ deforms because this continuum is the result of a smoothing operation that is installed by a mathematical convolution with blurring functions. That convolution involves integration and this integration appears to be sensitive to the ordering of the involved integration domains. The tiniest blurring function is the Green's function of the field $\mathfrak{C}$. This corresponds to a single point-like disruption, which is due to the fact that the ordering of the parameter space of the disruption differs from the ordering of the surrounding integration domains. A coherent swarm of point-like disruptions will correspond to a much broader blurring function. The test function that was treated earlier is an example of broader blurring

function. Thus, the deformation of $\mathfrak{C}$ is due to the participation of non-conformant integration domains. For that reason we will mark the parameter spaces that act as integration domains with a superscript ^{x} that identifies the type of ordering of the parameter space. The parameter spaces are not deformed. Only the smoothed fields get deformed by the disruptive embedding of artifacts. These artifacts represent local exceptions in an otherwise rather evenly distributed set of rational quaternions that is described by the smoothed field.

We perform the construction of the map in a sequence of *virtual* steps. The first virtual step maps the location a_j^x in the symmetry center $\mathfrak{S}_n^x$ onto a virtual location b_j^x in the reference parameter space $\mathcal{R}^x$. The following step maps the location b_j^x onto a virtual location c_j^x in the continuum parameter space $\mathfrak{R}^x$. There it represents a rational number with corresponding symmetry flavor ^{x}. The last step maps c_j^x to an actual location d_j^x in the deformable continuum $\mathfrak{C}$. Since the symmetry flavor ^{x} of d_j^x conflicts with the reference symmetry flavor ^{⓪} of $\mathfrak{C}$, the embedding process causes a reaction of the embedding field $\mathfrak{C}$. In chapter 13 we will explain the reason of this conflict in more detail. None of the eigenspaces of the parameter space operators are influenced by the mapping process. Only this last step causes space curvature in the deformable target field. During this map the swarm $\{a_j^x\}$ gets spatially reordered into the swarm $\{e_j^{⓪}\}$. The embedding of each of the elements last only a short instant and is immediately released. What results is the impact on the smoothed field $\mathfrak{C}$. Thus, field is not only smoothed in spatial sense. It is also averaged over the progression window.

11.4 Coherent elementary modules

Coherent elementary modules are characterized by a coherent location swarm. The coherent elementary modules are directly related to an individual symmetry center. The elements of the coherent location swarm that characterizes the coherent elementary module are taken from this symmetry center. These elements are ordered with respect to progression, but spatially they are selected in a stochastic fashion. This selection is described by operator σ^x. In the map onto the reference continuum, coherent elementary modules feature a hopping path. Inside the symmetry center the hopping path is closed. Further, for coherent elementary modules, the map of the location swarm into the reference continuum corresponds to a density operator ρ that is defined by a ***continuous function***. That continuous function is a ***normalized location density distribution*** and it has a ***Fourier transform***. As a consequence the swarm owns a ***displacement generator*** and as a further consequence in first approximation the swarm will ***move as one unit***.

The operator that conforms to the continuous location density distribution has a different ordering with respect to its spatial values. That new operator ρ has $\mathcal{R}$ and thus $\mathfrak{R}$ as its parameter space. It tends to describe the swarm as a whole unit. It no longer describes the hopping path. The operator ρ is no more than a special descriptor. It does not affect the distribution of the density of the locations that is described by this operator and its defining function.

The coherence is ensured by the private mechanism $\mathfrak{M}_n$ that selects the eigenvalues such that a coherent swarm is generated.

This paper gives no explanation for this special habit of the mechanism. However, this habit is essential for the coherence of the whole model.

Some guesses about the way that mechanism $\mathfrak{M}_n$ works are possible. A combination of a Poisson process and a binomial process that is implemented by a spatial spread function can establish a location density distribution, which approaches the Gaussian distribution, which underlies the described test function. This might provide a partial indication of how the mechanism works. A Poisson process that is combined with an attenuating binomial process can again be considered as a Poisson process that has a lower efficiency. Thus, in this interpretation, the spread function defines the spatial spread of the efficiency of the local Poisson processes.

The notion of ***coherent swarm*** will later be defined in more detail. Coherent elementary modules are also characterized by the symmetry flavor of their symmetry center $\mathfrak{S}_n^x$. When mapped into a reference continuum that is eigenspace of reference operator $\mathfrak{R}^{⓪} = |q^{⓪}\rangle q^{⓪}\langle q^{⓪}|$ the module is characterized by a ***symmetry related charge***, which is *located at the center of symmetry*. The symmetry related charge is a property of the local ***symmetry center*** $\mathfrak{S}_n^x$.

The size and the sign of the symmetry related charge depends on the difference of the symmetry flavor of the local symmetry center with respect to the symmetry flavor of the surrounding reference continuum $\mathcal{R}^{⓪}$. The coherent swarm $\{a_j^x\}$ inherits the symmetry flavor of the local symmetry center $\mathfrak{S}_n^x$. However, the controlling mechanism $\mathfrak{M}_n$ picks the elements of this set in a spatially stochastic way instead of in a spatially ordered fashion. Thus the stochastic operator σ^xthat reflects the stochastic selection by $\mathfrak{M}_n$, corresponds with another operator, this time a density operator ρ^x that reflects the spatial ordering and characterizes the coherent stochastic mechanism $\mathfrak{M}_n$ with respect to its achievement to establish spatial coherence.

Symmetry related charges are the reason of existence of a symmetry related field $\mathfrak{A}$. This field will be treated later.

11.5 The function of coherence

Embedding of point-like objects into the affected embedding continuum spreads the reach of the separate embedding locations and offers the possibility to bind modules. The spread of the embedded point-like object is defined by the Green's function of the non-homogeneous second order partial differential equation. However, spurious embedding locations have not enough strength and not enough reach to implement an efficient binding effect. In contrast, coherent location swarms offer enough locality, enough spread and enough embedding strength in order to bind two coherent swarms that are sufficiently close.

For example, a Gaussian distribution of the location swarm would turn the very peaky Green's functions into a rather broad spherical painting brush that can be described by the potential:

$$\varphi(r) = \frac{ERF(r)}{r} \tag{1}$$

This is a smooth function without a trace of a singularity. Thus the coherent swarm bends the embedding field in a smooth fashion!. We will give this particular function a name and call it ***test function***. At the center location, the amplitude of the test function equals about 1,128379. The test function has a standard spread. The standard deviation is about 0,598758. A graph of function $\varphi(r)$ was shown in figure 1.

The actual location density distribution may differ from the Gaussian distribution. The amplitude of the resulting function will depend on the form of the density distribution will depend on the number of participating point-like obstructions. For large numbers of participating point-like obstructions, the coherence of the swarm ensures that the smoothed embedding field stays integrable, while each of the elements of the swarm would separately cause a singularity. The actual smoothness of the affected field will depend on the number of participating obstructions. This plays a greater role in the outskirts of the distribution. In that region the signal to noise ratio is much lower than in the center. This results in a larger local relative variance. We assumed that all obstructions have similar impact on the affected field. However, the process that governs the generation of the obstructions has a stochastic nature. The characteristics of this process depends on the properties of the controlling mechanism. The number of elements in the coherent swarms that corresponds to actual elementary modules depends on the type of the module. For most types this number is huge. If the generator of the obstructions is a Poisson

process in combination with a binomial process that is implemented by a spatial spread function, then the local signal to noise ratio can be calculated at any location where the number of participating obstructions is still large enough. This is due to the fact that a Poisson process in combination with a binomial process is again a Poisson process with an attenuated efficiency. An object that will approach these outskirts will sense the local relative variance of the field and may act accordingly. As a consequence its behavior in response to the local field value may appear to show some turbulence. Closer to the center of the swarm the signal to noise is much larger and the behavior of the respondent will become more consistent.

If for some reason the generation process is halted, then the controlling mechanism changes to another control mode and because of that the discrete nature of the swarm will becomes noticeable. In this case the last location in the location swarm indicates the exact location where the generation process was disrupted. After this instance the location density distribution has lost its validity and collapses. In physics the group of physicists that support the Copenhagen interpretation named this phenomenon “the collapse of the wave function”.

Imaging of the location swarm onto the reference continuum is only used to define coherence and it is used to indicate the influence of the symmetry related charges. The embedding onto the affected continuum $\mathfrak{C}$ is used to exploit the corresponding potential binding effect of the swarm. The stochastic process that implements the stochastic location distribution under control of mechanism $\mathfrak{M}_n$ is the de facto actuator in establishing the coherent swarm. The embedding field $\mathfrak{C}$ is not affected by symmetry differences. In contrast the symmetry related field $\mathfrak{A}$ is caused by these differences. Thus $\mathfrak{C}$ and $\mathfrak{A}$ differ fundamentally! For the elementary module the symmetry center couples the two fields.

11.6 The effect of the blur

The coherent swarm represents an effective blur of every observation of the spatial location of the corresponding object. ***All information about the swarm will be transmitted via the fields*** that are influenced by the presence of the swarm. ***The model does not support other information carriers***.

In this aspect the model differs from theories that postulate the existence of force carriers. This model does not support force carriers. Nor does it support the corresponding force fields. However, the basic fields can cause acceleration of the discrete objects that reside on symmetry centers.

It means that every object that must be informed about the properties of the observed object will perceive this observed object with a blur that is defined by the actual location density distribution. This is not the smooth density distribution ρ. However, for coherent swarms the actual location density distribution will closely approach the smooth location density distribution ρ.

Due to the blur, no observer will directly perceive the difference between an object that is constructed as a swarm of discrete elements and an object that has a more compact structure such as a sphere. This fact is increased if the observer itself has a similar structure. The swarm contains a huge number of elements. Only in this way the signal to noise ratio of the transferred information is large enough in order to tolerate reliable reactions of the observer on the signal that it receives via the surrounding fields.

Thus, every interaction is afflicted with a certain signal to noise ratio.

12 The dynamic orthomodular base model

We have achieved a level in which the major chain of mathematical structures does no longer offer an inescapable self-evident extension. The model uses separable and non-separable Hilbert spaces in order to store numeric data that can describe a series of discrete objects that are embedded in a continuum. The real parts of the parameters can be used to order the parameters and the target values of functions. If properly ordered these descriptions can represent a sequence of static status quos. However, without controlling mechanisms this model features no dynamics and contains no means to establish the ***coherence*** between the subsequent members of the sequence. This reflects our earlier decision to pick the interpretation that new data are generated by these controlling mechanisms. According to the other interpretation a virtual boundary travels over existing data and represents a static status quo that is defined by a single and increasing progression value. In both cases the boundary divides the model into a historic part and a future part. In both views the reason of the existence of the coherence of swarms is not (yet) explained. In this paper that explanation is not achieved. We just make use of the coherence that the mechanisms appear to establish. Thus, ***according to the view that is selected by this paper, the origin of the dynamics of the model is located in the mechanisms that generate the coherent swarms.***

12.1 The model

In the selected view, the model describes the evolution of the embedding of a quaternionic infinite dimensional separable Hilbert space into its companion Gelfand triple. This is achieved by applying an extended version of the generalized Stokes theorem to an eigenspace of a normal operator in a non-separable quaternionic Hilbert space that embeds a separable Hilbert space. On the rim between the history and the future operate controlling mechanisms that fill eigenspaces of operators, which reside in the separable Hilbert space with new data, that subsequently will be embedded into a deformable eigenspace of an operator that resides in the Gelfand triple. The history is no longer touched and stays stored in eigenspaces of operators that reside in the separable Hilbert space. That storage is no longer afflicted by noise. All dynamic data are precisely known and stored as quaternionic values. In contrast, the future is not yet known and will be generated by the stochastic processes, which are owned/controlled by dedicated mechanisms that act as functions of progression. ***This description uses one of the possible interpretations of the base model.***

We will call this stage of the model development "***The dynamic orthomodular base model***". Any further development of the model would involve the investigation of the mechanisms that ensure the coherence between the subsequent members of the sequence of static status quos. This paper will not perform that investigation. Instead, we use a detailed definition of what we mean by a coherent swarm of point-like obstructions of the embedding field $\mathfrak{C}$.

The orthomodular base model describes the relational structure of modular systems. Via the management mechanisms it can add characteristics to the modules. These characteristics are based on eigenvalues of normal operators that reside in the separable Hilbert space and have eigenvectors in the closed subspace that represents the module.

The elementary modules are based on a huge number of rational quaternionic numbers. This number is about 2^{37}. It corresponds to a 37 dimensional binary valued space. The module does not use this huge amount of degrees of freedom. Instead it is characterized by a few statistical and symmetry characteristics.

The Hilbert spaces only supports storage and description. Further, the Hilbert spaces restrict the type of the data that can be stored. The management mechanisms represent the actual drivers of the model. However, the Hilbert spaces pose restrictions on what the mechanisms can do.

The numeric data that occur in the orthonormal base model must be taken from division rings. The most elaborate choice for these data are quaternions.

Quaternions and Hilbert spaces can represent a wider usage than just the storage of dynamic geometric data. Quaternions can implement rotations. In this way they can shift properties between dimensions. This is shown the appendix; Tri-state spaces. (still to-do)

The peculiarities of these quaternions influence the features and the behavior of the discrete objects and the fields that occur in the orthonormal model. Many of these peculiarities are hardly known by scientists. As far as they apply to this paper these subjects are treated in the related sections.

Concepts such as symmetry centers and coherent location swarms are not part of the orthonormal base model, but these features make use of the structure and the properties of the orthonormal base model. The same holds for the symmetry related field $\mathfrak{A}$ and the embedding continuum $\mathfrak{C}$. However, the reference operators that can be applied as parameter spaces can be considered as standard properties of quaternionic Hilbert spaces. They can be considered to belong to the household of the orthomodular base model.

12.2 The rim

The past part of the model is fixed and is stored in exact values in the Hilbert spaces. The future part is inaccessible by the past part and does not yet influence the current static status quo. In the selected view of the model, all dynamics occurs in the direct vicinity of the splitting boundary. For that reason, the rim is the most interesting part of the model. It is a region in the direct vicinity of the splitting boundary and includes this boundary. The boundary itself concerns a static status quo of the model. The rim is constituted of a harmonica of such static status quos. Each of the sheets of this harmonica is represented by a Hilbert space in which the progression value is fixed. In fact these Hilbert spaces are subspaces of the encapsulating separable Hilbert space. The harmonica covers the regeneration cycle of the elementary modules. Within the harmonica each elementary module is represented by a tube and a hopping string that stays inside this encapsulating tube. Inside each of the sheets of the harmonica, each of the elementary modules has a different location. That location is determined by a corresponding management mechanism that works in a stochastic fashion, such that the subsequent locations form a coherent swarm. This means that the location swarm can be described by a continuous location density distribution, which on its turn possesses a Fourier transform. These conditions ensure that the swarm possesses a private displacement generator and it also means that at first approximation, the swarm can be considered as to move as one unit. As a consequence the module can be treated as an individual object that has its own kinematics. Despite the fact that at each harmonica sheet the elementary module has only one (exact!) position, the module can be characterized by its short term dynamic behavior. That behavior is obviously related to the ordering inside the symmetry center on which the elementary module resides.

In comparison to string theory, which uses elastic strings, this model uses stochastic tubes that house hopping paths that proceed in the direction from past to future. In projection onto a static status quo boundary the hopping path forms a coherent swarm.

The fact that for every individual module each sheet of the harmonica contains only one location, corresponds to the fact that all symmetry centers are enumerated with the separate progression values of the sheets and at every progression instance one location on each symmetry center represents only one location of the corresponding elementary module. The eigenspace of the operator that describes these locations is ***well ordered*** with respect to progression and is stochastic in the spatial domain.

It is interesting to try to estimate the number of sheets in the harmonica. This number is related to the inverse of Planck's constant. With other words, it is a huge number. We already estimated it as 2^{37}. Reality appears to be wastefully with its progression ticks!

Apart from the obstructions, the rim also contains continuums. These continuums spread over the spatial parts of the domains. In these regions differentiation and integration makes sense. In these conditions the more conventional form of the Stokes theorem and the divergence theorem become applicable.

Symmetry centers are defined by anti-Hermitian operators. This means that they fit inside the sheets of the harmonica. In that sheet each symmetry center carries only one location of the represented elementary module. That location does not coincide with the location of the geometric center of the symmetry center.

13 Symmetry centers as floating parameter spaces

If we tolerate discontinuities inside quaternionic manifolds, then these artifacts must be encapsulated by boundaries $\partial \mathrm{H}_n^x$ and in that way they are separated from the main domain Ω.

In this case the model may apply different parameter spaces, which have their own private way of ordering. A separable quaternionic Hilbert space can cope with series of coexisting parameter spaces and these parameter spaces are served by dedicated operators. The reverse bra-ket method relates the parameter space to a corresponding reference operator. Symmetry centers are examples of such parameter spaces. Symmetry centers use a version of the quaternionic number system in order to represent the ordering of the parameter space. This results in a parameter space that features a Cartesian coordinate system. In addition the parameter space is ordered by a polarnate system. The symmetry center uses only the rational quaternions. In this way the parameter space stays countable.

13.1 Symmetry flavor and the origin of the symmetry related charge

The symmetry center $\mathfrak{S}_n^x$ is characterized by a private symmetry flavor. That symmetry flavor relates to the Cartesian ordering of this parameter space. When the orientation of the coordinate axes is fixed, then eight independent Cartesian orderings are possible. We use the Cartesian ordering of $\mathfrak{R}^{⓪}$ as the reference for the orientation of the axes. $\mathfrak{R}^{⓪}$ has the same Cartesian ordering as $\mathcal{R}^{⓪}$ has.

$$\int_{\Omega-\mathrm{H}} d\omega = \int_{\partial\Omega} \omega - \sum_n \int_{\partial \mathrm{H}_n^x} \omega \tag{1}$$

In this formula the boundaries $\partial\Omega$ and $\partial \mathrm{H}_n^x$ are subtracted from each other. This subtraction is controlled by the difference in ordering of the domains Ω and H_n^x.

Due to the smoothness of the embedding field, we have some freedom with the spatial placement of the encapsulating boundaries. We exploit that freedom by selecting a cubic, rather than a spherical encapsulation of the point-like discontinuities. This enables us to correctly determine the influence of the differences in ordering along the coordinate axes.

The consequence of the differences of the symmetry flavor on the subtraction can best be comprehended when the encapsulation $\partial \mathrm{H}_n^x$ is performed by a ***cubic space form*** that is aligned along the Cartesian axes. Now the six sides of the cube contribute different to the effects of the encapsulation when the ordering differs from the Cartesian ordering of the reference parameter space $\mathfrak{R}^{⓪}$. Each discrepant axis ordering corresponds to one third of the surface of the cube. This effect is represented by the ***symmetry related charge*** and the ***color charge*** of the symmetry center. It is easily related to the algorithm which is introduced for the computation of the symmetry related charge. Also the relation to the color charge will be clear. ***Thus, this effect couples the ordering of the local parameter spaces to the symmetry related charge of the encapsulated elementary object.*** The differences with the ordering of the surrounding space determines the value of the symmetry related charge of the object that resides inside the encapsulation!

The symmetry related charge and the color charge of symmetry center $\mathfrak{S}_n^x$ are supposed to be located at the geometric center of the symmetry center. A Green's function together with these charges can represent the local defining function $\varphi^x(q)$ of the contribution φ^x to the ***symmetry related field*** $\mathfrak{A}^x$ within and beyond the realm of the floating region H_n^x.

Nothing else than the discrepancy of the ordering of symmetry center $\mathfrak{S}_n^x$ with respect to the ordering of the parameter spaces $\mathcal{R}^{⓪}$and $\mathfrak{R}^{⓪}$ causes the existence of the symmetry related charge, which is related to the symmetry center. Anything that resides on this symmetry center will ***inherit*** that symmetry related charge.

13.2 Spin

The extra spherical coordinate system is defined relative to the axes of the Cartesian coordinate system. This extra ordering introduces extra symmetry characteristics that become important when spherical integration is applied. These influence are related to the spin characteristics of the elementary module.

13.3 Single symmetry center

H_n^x is a spatial domain. The regions H_n^x that are combined in H are excluded from domain Ω. The Stokes theorem does not hold for the separate regions H_n^x. Instead, the difference between the integrals defines a potential. In case of isotropic symmetry flavor of the symmetry center $\mathfrak{S}_n^x$ holds:

$$Q_n^x = |\boldsymbol{q} - \boldsymbol{c}_n^x| \left\{ \int_{\mathrm{H}_n^x} d\omega - \int_{\partial \mathrm{H}_n^x} \omega \right\} \tag{1}$$

$\boldsymbol{c}_n^x$ is the geometric center of symmetry center $\mathfrak{S}_n^x$. Q_n^x is the symmetry related charge. This corresponds to the symmetry related potential $\varphi_n^x(q)$ that exists at the outskirts of the encapsulation.

$$\varphi_n^x(\boldsymbol{q}) = \frac{Q_n^x}{|\boldsymbol{q} - \boldsymbol{c}_n^x|} = \int_{\mathrm{H}_n^x} d\omega - \int_{\partial \mathrm{H}_n^x} \omega \tag{2}$$

The potential $\varphi_n^x(\boldsymbol{q} - \mathbf{c}_n^x)$ contributes to the symmetry related field $\mathfrak{U}^x$.

13.4 Bounded center

A locally a spatially connected union $H_⊎$ of encapsulations H_n^x is defined by:

$$H_⊎ = \bigcup_{n=1}^{N^x} \mathrm{H}_n^x \tag{1}$$

$H_⊎$ encapsulates multiple symmetry centers. In case that $H_⊎$ exists, we consider the objects that reside within that encapsulation $\partial H_⊎$ as bounded by the symmetry related charges.

$$\phi^x(\boldsymbol{q}) = \sum_{n=1}^{N^x} \frac{Q_n^x}{|\boldsymbol{q} - \boldsymbol{c}_n^x|} \tag{2}$$

At large enough distance from this bounded center, all charges can be considered to be merged in a single charge with symmetry related potential function $\phi(q)$:

$$\phi(q) = \frac{\sum_{n=1}^{N} Q_n^x}{|\boldsymbol{q} - \boldsymbol{r}|} \tag{3}$$

$$\boldsymbol{r} = \frac{1}{N}\sum_{n=1}^{N} \boldsymbol{c}_n \tag{4}$$

13.5 Discrepant regions

The symmetry centers correspond to point-like discontinuities. However, also large connected regions of $\Re^{⓪}$ may exist that disrupt the continuity of the manifold. For example a region that is surrounded by a boundary where the deformation is so strong that information contained in ω cannot pass the boundary of this region. These regions must also be separated from domain Ω. In this way these regions will correspond to ***cavities*** in the domain Ω. ***The information contained in the manifold cannot pass the surface of the cavity.*** The cavities act as information holes. Within the cavity the manifold can be considered to be non-existent. Within that region it has no defining function.

Current mathematical integration technology appears to lack proper solutions for this situation.

Discrepant regions cannot be hidden by applying a smoothing operator to the underlying field.

The discrepant regions are the “black holes” of the model.

14 Fields

14.1 Fields in contrast to sets of discrete objects

Coherent sets of discrete quaternions have much in common with continuums that describe the density of these location swarms. The set of rational quaternions is densely embedded in the continuum of the corresponding quaternions. A continuous function can relate the coherent set that corresponds to the target of the rational quaternionic function and the corresponding smooth continuum. If you want to estimate the impact of point-like disruptions of the continuity, it makes more sense to investigate the set of rational target values of the relating function, than to try investigate the disrupted continuum. Putting the point-like disruptions in capsules will partly solve integration and differentiation problems. In this way smoothed versions of the fields can be derived that circumvent the problems that integration has with the existence of point-like disruptions.

14.2 Differentiable and integrable basic fields

By applying the reverse bra-ket method, a category of operators can represent quaternionic functions. This is applicable both in the separable Hilbert space and in the Gelfand triple.

In this paper, fields are continuums that are target spaces of quaternionic functions that define eigenspaces of operators, which reside in the Gelfand triple.

Quaternionic functions and their differentials can be split in real scalar functions and imaginary vector functions. Here we will only consider the not too violent disruptions of the continuity of the fields. We also restrict the validity range of the equations. With these restrictions the ***quaternionic nabla*** can be applied and the discontinuities restrict to point-like artifacts. The quaternionic nabla has the advantage that it works as a multiplying operator. It obeys quaternionic multiplication rules.

Quaternionic functions can represent fields and continuums, but they can also represent density distributions of discrete dynamic locations. A point-like disruption then corresponds to a single exception in a large assembly of nearly equal values. The vector field that goes together with the scalar field may then represent the displacements of the discrete objects. Quaternionic differentiation of such fields is treated in the next chapter.

Double differentiation of a basic field leads to a non-homogeneous second order partial differential equation that relates the basic field to the corresponding density distributions of discrete dynamic locations of the artifacts that cause the local discontinuities of the basic field. For quaternionic functions two different second order partial differential equations exist. They offer different views of the dynamic behavior of the same basic field and the two second order partial differential equations can offer views on different behavior of the investigated field.

The symmetry related field $\mathfrak{A}$ and the embedding continuum $\mathfrak{C}$ are basic fields. This paper only investigates these two basic fields. In this paper, all other fields are derived from these two basic fields.

The symmetry related field $\mathfrak{A}$ is based on the existence of symmetry centers. These symmetry centers float over a reference parameter space that acts as a background in the whole model.

The embedding continuum $\mathfrak{C}$ is based on the existence of a dynamic deformable function $\mathfrak{C}$ that describes the embedding of discrete artifacts, which reside on symmetry centers and are mapped onto $\mathfrak{C}$. The artifacts are selected by mechanisms $\mathfrak{M}_n$ that are dedicated to the symmetry center $\mathfrak{S}_n^x$. The results of the activity of these mechanisms can be described by a corresponding stochastic operator $\mathscr{o}$. All stochastic operators have countable eigenspaces and can be considered to reside in the separable Hilbert space.

14.3 Subspace maps

The orthomodular base model consist of two related Hilbert spaces.

- A separable Hilbert space $\mathfrak{H}$ that acts as a descriptor of the properties of all discrete objects.
- A non-separable Hilbert space $\mathcal{H}$ that acts as a descriptor of the properties of all continuums.

An ongoing process which is governed by dedicated mechanisms embeds a part of the separable Hilbert space $\mathfrak{H}$ into its non-separable companion Hilbert space $\mathcal{H}$. This ongoing process corresponds to a partition that moves through the reference parameter spaces $\mathcal{R}^{⓪}$ and $\mathfrak{R}^{⓪}$ and splits them into three parts: history, present static status quo and future. We already introduced the harmonica that splits the vicinity of the boundary in a series of sheets. The middle sheet is the actual boundary. Thus. in the neighborhood of the boundary we treat progression as a discrete parameter. Further away, progression may be considered to flow. The mechanism $\mathfrak{M}$ that governs the embedding of an elementary module is active in the splitting boundary, but its control is influenced by historic and future sheets that belong to the harmonica, which covers the regeneration cycle that produces the coherent location swarm, which is characteristic for the elementary module. The behavior of the mechanism is stochastic and only determined by statistical and symmetry related characteristics. Nothing, not even the creator of the model, has deterministic insight in the decisions of the mechanism.

This view corresponds to the interpretation of the model in which mechanisms generate new spatial data as a function of the progression value. An alternative interpretation suspects that the future data are already present in the Hilbert space and are encountered by the moving boundary. In that case the mechanisms must have been active as generators at the instance of the formation of the whole Hilbert space. Also in that case the activity of the mechanisms is stochastic and is not governed and deterministically determined by the creator of the model. The model itself is not affected by these different interpretations.

The two Hilbert spaces are coupled by the Cartesian-ordered reference operator $\mathcal{R}^{⓪}$ and the corresponding reference operator $\mathfrak{R}^{⓪}$. Both are defined by the quaternionic function $\mathfrak{R}(q) \stackrel{\text{def}}{=} q$.

On the rim between history and future will controlling mechanisms $\{\mathfrak{M}_n\}$ fill the module related subspaces of separable Hilbert space $\mathfrak{H}$ with data and the new contents of these subspaces are subsequently embedded into the non-separable Hilbert space $\mathcal{H}$. The history stays untouched. The fill of subspaces with data is described by dedicated stochastic operators. The mechanisms $\{\mathfrak{M}_n\}$ use stochastic processes in order to generate these data.

A closed subspace in $\mathfrak{H}$ maps into a subspace of $\mathcal{H}$. Only the countable subspaces of $\mathcal{H}$ have a sensible dimension. By applying the reverse bra-ket method, defining functions can map countable eigenspaces of operators that reside in the separable Hilbert space into continuum eigenspaces in the Gelfand triple. Mapping does not influence the flat reference fields that are in use as parameter spaces. However, the embedding process affects the deformable field $\mathfrak{C}$. Indirectly, the embedding process affects the symmetry related field $\mathfrak{A}$. In fact both fields interact by affecting the location of the geometric center of the symmetry centers that correspond to elementary modules.

14.4 Parameter spaces

The reference operator $\mathfrak{R}^{⓪}$ that resides in the Gelfand triple delivers a simple field that can act as a flat parameter space. This field is not affected by the embedding map. Via its defining function $\mathfrak{R}^{⓪}\left(q^{⓪}\right) \stackrel{\text{def}}{=} q^{⓪}$, it is a direct map of parameter space $\mathcal{R}^{⓪}$.

Symmetry centers are spanned by the eigenvectors $\{|\mathfrak{s}_i^x\rangle\}$ of a compact symmetry center reference operator $\mathfrak{S}_n^x$. The superscript ^{x} distinguishes between properties such as symmetry flavors and spin.

Symmetry centers are special forms of parameter spaces that reside in the separable Hilbert space $\mathfrak{H}$. They also have a representation in the Gelfand triple. In the separable Hilbert space $\mathfrak{H}$ they have a fixed finite dimension, which is supposed to be the same for all symmetry centers. Or the dimension is the same for all elementary modules that belong to the same type. Reference operator $\mathfrak{R}^{⓪}$ acts as the playground of maps of symmetry centers that define local symmetry related charges. Symmetry centers float over this background space. The reason for fixing the finite size of the dimension of the symmetry centers will be explained later.

14.5 Embedding field

The elements of the eigenspace of the stochastic operator $\mathcal{O}$, which is used by a controlling mechanism $\mathfrak{M}_n$ will be embedded in the eigenspace of operator $\mathfrak{C}$. A more smoothed version $\mathfrak{U}$ of this operator exists that mimics the view that observers get from the field $\mathfrak{C}$. For example $\mathfrak{C}$ is smoothed by its Green's function and $\mathfrak{U}$ is smoothed by a blur that approaches the blur of the test function. Observers are the receivers of information that is transported by messengers or by other vibrations or deformations of the embedding field. The messengers are objects that use the embedding field as their transport medium. Smoothing blurs the perception of the observer. The smoothing implemented by $\mathfrak{U}$ represents the minimal observation blur for elementary modules.

With this interpretation the embedding process can be seen as the pursuit by the embedding field to follow the density distribution of a set of rational and thus discrete quaternionic target values as close as it tolerated by a selected blurring function. This process involves a convolution and this convolution involves an integration. The target values are the targets of the defining function for a selected set of parameter values. $\mathfrak{C}$ uses a narrower blurring function than $\mathfrak{U}$ does. $\mathfrak{C}$ is interpreted as a field, while $\mathfrak{U}$ is interpreted as a potential.

Operator $\mathfrak{C}$ can be described by a quaternionic function $\mathfrak{C}(q^{⓪})$ that has a parameter space $\mathfrak{R}^{⓪}$, which is generated by the eigenspace of reference operator $\mathfrak{R}^{⓪}$. When applicable, we use the same symbol for the parameter space, the defining function and the operator. With the installed restrictions, the dynamics of the embedding process can be described by quaternionic differential calculus.

If the discontinuities that are generated by local discontinuities are not too violent , then the non-homogeneous second order partial differential equation will elucidate the embedding process. This will be treated in detail in the next chapter.

In $\mathcal{H}$ the operator $\mathfrak{C} \stackrel{\text{def}}{=} |q^{⓪}\rangle\mathfrak{C}(q^{⓪})\langle q^{⓪}|$ is defined by function $\mathfrak{C}(q^{⓪})$ and represents an embedding continuum $\mathfrak{C}$. This continuum gets affected by the embedding process and thus deforms dynamically.

We will show that two different non-homogeneous second order partial differential equations exist that offer different views on the embedding process. The equation that is based upon the double quaternionic nabla $\nabla\nabla^*$ cannot show wave behavior. However, the equation that is based on d'Alembert's operator $\mathfrak{D}$ acts as a wave equation, which offers waves as part of its set of solutions.

$$\nabla\nabla^* = \nabla_0\nabla_0 + \langle \boldsymbol{\nabla}, \boldsymbol{\nabla} \rangle \tag{1}$$

$$\mathfrak{D} \stackrel{\text{def}}{=} -\nabla_0\nabla_0 + \langle \boldsymbol{\nabla}, \boldsymbol{\nabla} \rangle \tag{2}$$

The embedding continuum $\mathfrak{C}$ ***is always and (nearly) everywhere present.*** The space cavities form an exception to this rule. $\mathfrak{C}$ is deformed and vibrated by discrete artifacts that are embedded in this field. In the considered domain, $\mathfrak{C}$ may contain point-like artifacts and connected regions where $\mathfrak{C}(q)$ is not defined.

In $\mathcal{H}$, the representations of symmetry centers float over the natural parameter space $\mathfrak{R}^{\textcircled{0}}$ of the embedding continuum. The symmetry related charges of the symmetry centers generate local contributions φ to the symmetry related field $\mathfrak{A}$. The location of the center of the symmetry center $\mathfrak{S}_n^x$ within parameter space $\mathfrak{R}^{\textcircled{0}}$ is affected by the symmetry related field $\mathfrak{A}$. The symmetry related field $\mathfrak{A} \stackrel{\text{def}}{=} |q^{\textcircled{0}}\rangle\mathfrak{A}(q^{\textcircled{0}})\langle q^{\textcircled{0}}|$ uses the same natural parameter space $\mathfrak{R}^{\textcircled{0}}$ as the embedding field $\mathfrak{C}$ does. This indicates that the fields $\mathfrak{A}$ and $\mathfrak{C}$ influence each other in an indirect way via the symmetry centers.

The mechanism $\mathfrak{M}_n$ that controls stochastic operator $\mathscr{o}$ picks members of a symmetry center $\mathfrak{S}_n^x$ and stores them in the eigenvalues of that operator. These eigenvalues are mapped to parameter space $\mathcal{R}^{\textcircled{0}}$ and in that way they become eigenvalues of a new operator $\mathscr{b}$. This map involves relocation and re-ordering. This fact couples the location of the symmetry related charge of this symmetry center with the locations that get embedded in the eigenspace of operator $\mathfrak{C}$. However, the parameter location of the symmetry related charge does not coincide with the parameter location of the eigenvalue of operator $\mathscr{b}$,that will be embedded in the eigenspace of operator $\mathfrak{C}$. This embedding involves a map that is described by function $\mathfrak{C}(\mathrm{q})$. The eigenvalues of operator $\mathscr{b}$ will form a mapped swarm whose center will coincide with the mapped parameter location of the symmetry related charge. That location also coincides with the location of the mapped geometric center of the symmetry center. The images of eigenvalues of $\mathscr{b}$ onto $\mathfrak{C}$ correspond to point-like artifacts. However, the images of these eigenvalues on the smoothed version $\mathfrak{U}$ of $\mathfrak{C}$ correspond with proper locations in $\mathfrak{U}$.

$\mathfrak{C}$ and $\mathfrak{U}$ lay like snow blankets over the set of discrete rational quaternions. $\mathfrak{U}$ represents a thicker and thus smoother snow blanket than $\mathfrak{C}$.

14.6 Symmetry related fields

Due to their four dimensions, quaternionic number systems exist in sixteen versions that only differ in their symmetry flavor. The elements of coherent sets of quaternions belong to the same symmetry flavor. This is the symmetry flavor of the symmetry center $\mathfrak{S}_n^x$ that supports the original location swarm. Differences between symmetry flavors of a symmetry center $\mathfrak{S}_n^x$ and the symmetry flavor of the eigenspace of the surrounding reference operator $\mathcal{R}^{\textcircled{0}}$ cause the presence of a symmetry related charge at the center location of that symmetry center. The countable reference parameter space $\mathcal{R}^{\textcircled{0}}$ in the separable Hilbert space $\mathfrak{H}$ maps onto the continuum parameter space $\mathfrak{R}^{\textcircled{0}}$, which resides in the Gelfand triple $\mathcal{H}$.

Symmetry related charges are point-like objects. These charges ***generate a field*** $\mathfrak{A}$ that fundamentally differs from the embedding continuum. This symmetry related field also plays a role in the binding of modules, but that role differs significantly from the role of the embedding continuum $\mathfrak{C}$. The defining function $\mathfrak{A}(q)$ of field $\mathfrak{A}$ and the defining function $\mathfrak{C}(\mathrm{q})$ of field $\mathfrak{C}$ use the same parameter space $\mathfrak{R}^{\textcircled{0}}$.

Symmetry related charges are located at the geometric centers of local symmetry centers. The size and the sign of the symmetry related charge depends on the difference of the symmetry flavor of the symmetry center with respect to the symmetry flavor of the embedding continuum. Symmetry centers that belong to different symmetry related charges appear to react on the symmetry

differences. Equally signed charges repel and differently signed charges attract. The attached coherent location sets that are attached to the symmetry centers will be affected by these effects.

The symmetry related charges do not directly affect the embedding continuum $\mathfrak{C}$. Their effects are confined to the map of the symmetry center $\mathfrak{S}_n^x$ to the parameter space $\mathfrak{R}^{⓪}$. However, with their action the symmetry related charges ***relocate*** the centers of the corresponding coherent swarms. The elements of the swarms deform the embedding continuum.

The symmetry related charges are point charges. As a consequence the range of the field that is generated by a single charge is rather limited. The corresponding Green's function diminishes as 1/r with distance r from the charge $\mathfrak{C}$.

Fields of point charges superpose. A wide spread uniform distribution of symmetry related point charges can generate a corresponding wide spread symmetry related field $\mathfrak{A}$. This works well if a majority of the charges have the same sign. Still, relevant values of the symmetry related field $\mathfrak{A}$ depend on the nearby existence of symmetry related charges.

Coherent swarms are recurrently regenerated on their symmetry centers. The symmetry centers are not recurrently generated, but instead their geometric center can get relocated. Together with these symmetry centers, the corresponding symmetry related charges and the residing swarms get relocated.

The relative short range of relevant field values makes the symmetry related field a bad candidate for the medium on which long range messengers can travel. For that purpose the embedding field $\mathfrak{C}$ is a much better candidate.

14.7 Free space

In the separable Hilbert space, the eigenvectors of the Cartesian-ordered reference operator $\mathcal{R}^{⓪}$ that do not belong to a module subspace together span free space. The elementary modules reside on symmetry centers whose center locations float on the eigenspace of $\mathcal{R}^{⓪}$.

At every progression instant only one element of the swarm $\{a_j^x\}$ is used. Thus "free space" surrounds all elements of the swarm. It forms most of the continuum $\mathfrak{C}$, which is deformed by the embedding of the currently selected swarm element.

15 Field dynamics

With respect to quaternionic differential calculus the basic fields behave in a similar way. Thus we will use a more general symbol for the investigated field in order to analyze behavior of the fields under differentiation and integration. In the appendix we will describe the difference between quaternionic differential calculus and Maxwell based differential calculus. In order to support that comparison we will define the derived subfields $\mathfrak{E}$ and $\mathfrak{B}$. Thus both $\mathfrak{C}$ and $\mathfrak{A}$ have such subfields!

15.1 Differentiation

In the model that we selected, the dynamics of the fields can be described by quaternionic differential calculus. Apart from the eigenspaces of reference operators and the symmetry centers we encountered two basic fields that are defined by quaternionic functions and corresponding operators. One is the symmetry related field $\mathfrak{A}$ and the other is the embedding field $\mathfrak{C}$.

$\mathfrak{A}$ determines the dynamics of the symmetry centers. $\mathfrak{C}$ gets deformed and vibrated by the recurrent embedding of point-like elementary particles that each reside on an individual symmetry center.

Apart from the way that they are affected by point-like artifacts that disrupt the continuity of the field, both fields obey, under not too violent conditions and over not too large ranges, the same differential calculus.

Two quite similar, but still significantly different kinds of dynamic geometric differential calculus exist. One kind is the genuine quaternionic differential calculus. The other kind is known as Maxwell based differential calculus. These two kinds will appear to represent different views onto the basic fields. In order to perform the comparison we must extend the set of Maxwell equations. In principle this means that the Maxwell based set of differential equations is incomplete. However, in practice and in order to achieve certain goals the set of Maxwell equations is extended with gauge equations. In this chapter only the quaternionic differential calculus will be treated. The Maxwell based differential equations and the comparison of the two kinds are treated in the appendix.

15.2 Quaternionic differential calculus.

First we will investigate the validity range of our pack of pure quaternionic differential equations.

Under rather general conditions the change of a quaternionic function $f(q)$ can be described by:

$$df(q) \approx \sum_{\mu=0\ldots3} \left\{ \frac{\partial f}{\partial q_\mu} + \sum_{\mu=0\ldots3} \frac{\partial}{\partial \nu} \frac{\partial f}{\partial q_\mu} dq^\nu \right\} dq^\mu = c_\mu(q) dq^\mu + c_{\mu\nu}(q) dq^\mu dq^\nu \tag{1}$$

Here the coefficients $c^\mu(q)$ and $c_{\mu\nu}(q)$ are full quaternionic functions. dq^μ are real numbers. e^ν are quaternionic base vectors.

The conditions that are accepted by equation (1) do not require more than second order differentiation. Thus, these conditions cannot be considered to be general conditions!

Under more moderate and sufficiently short range conditions the differential function is supposed to behave more linearly.

(2)

$$df(q) \approx \sum_{\mu=0\ldots3} \frac{\partial f}{\partial q_\mu} dq^\mu = c_\mu(q) dq^\mu$$

Under even stricter conditions the partial differential functions become real functions $c_0^\mu(q)$ that are attached to quaternionic base vectors:

$$df(q) = c_0^\tau \, dq_\tau + c_0^x \, \boldsymbol{i} \, dq_x + c_0^y \, \boldsymbol{j} \, dq_y + c_0^z \, \boldsymbol{k} \, dq_z = c_0^\mu(q) \, e_\mu \, dq_\mu \tag{3}$$

$$= \sum_{\mu=0}^{3} \left(\sum_{\varsigma=0}^{3} \frac{\partial f^\varsigma}{\partial q_\mu} e_\varsigma \right) e_\mu dq^\mu = \sum_{\mu=0\ldots3}^{3} \Phi_\mu e_\mu dq^\mu$$

$$\Phi_\mu = c_0^\mu = \sum_{\varsigma=0}^{3} \frac{\partial f^\varsigma}{\partial q_\mu} e_\varsigma = \frac{\partial f^\varsigma}{\partial q_\mu} e_\varsigma = \frac{\partial f}{\partial q_\mu} \tag{4}$$

Thus, in a rather flat continuum we can use the quaternionic nabla ∇. This is the situation that we want to explore with our set of pure quaternionic equations. ***The resulting conditions are very restrictive!*** These conditions are far from general conditions. However, these restrictions tolerate point-like disturbances of the continuity of the original function f.

$$\nabla = \left\{ \frac{\partial}{\partial \tau}, \frac{\partial}{\partial x}, \frac{\partial}{\partial y}, \frac{\partial}{\partial z} \right\} = \frac{\partial}{\partial \tau} + \boldsymbol{i} \frac{\partial}{\partial x} + \boldsymbol{j} \frac{\partial}{\partial y} + \boldsymbol{k} \frac{\partial}{\partial z} = \nabla_0 + \boldsymbol{\nabla} \tag{5}$$

$$\nabla f = \sum_{\mu=0}^{3} \frac{\partial f}{\partial q_\mu} e_\mu \tag{6}$$

This form of the partial differential equation highlights the fact that in first order and second order partial differential equations ***the nabla operator can be applied as a multiplier***. This means that we can apply the quaternionic multiplication rule.

$$\Phi_0 = \nabla_0 \psi_0 - \langle \boldsymbol{\nabla}, \boldsymbol{\psi} \rangle \tag{7}$$

$$\boldsymbol{\Phi} = \nabla_0 \boldsymbol{\psi} + \boldsymbol{\nabla} \psi_0 \pm \boldsymbol{\nabla} \times \boldsymbol{\psi} \tag{8}$$

The $\pm$ sign indicates that the nabla operator is also afflicted by symmetry properties of the applied quaternionic number system. The above equations represent only low order partial differential equations. In this form the equations can still describe point-like disruptions of the continuity of the field. We can take the conjugate:

$$\Phi^* = (\nabla\psi)^* = \nabla^*\psi^* - 2\,\boldsymbol{\nabla} \times \boldsymbol{\psi} \tag{9}$$

$$\nabla^*(\nabla^*\psi^*)^* = \nabla^*\Phi = \nabla^*\nabla\psi \tag{10}$$

15.2.1 The second order quaternionic partial differential equation

This kind of double partial differentiation will then result in the following quaternionic ***non-homogeneous second order partial differentiation equation***:

$$\xi = \xi_0 + \boldsymbol{\xi} = \nabla^*\nabla\psi = (\nabla_0 - \boldsymbol{\nabla})(\nabla_0 + \boldsymbol{\nabla})(\psi_0 + \boldsymbol{\psi}) \tag{1}$$

$$= \{\nabla_0\nabla_0 + \langle\boldsymbol{\nabla},\boldsymbol{\nabla}\rangle\}\psi = \frac{\partial^2\psi}{\partial\tau^2} + \frac{\partial^2\psi}{\partial x^2} + \frac{\partial^2\psi}{\partial y^2} + \frac{\partial^2\psi}{\partial z^2}$$

We can split the above equation in a real (scalar) part and an imaginary (vector) part.

Investigation of the details shows that the $\nabla^*\nabla$ operator has a rather simple consequence that is shown in formula (1)

$$\zeta_0 = \nabla_0\phi_0 + \langle\boldsymbol{\nabla},\boldsymbol{\phi}\rangle \tag{2}$$
$$= \nabla_0\nabla_0\varphi_0 - \nabla_0\langle\boldsymbol{\nabla},\boldsymbol{\varphi}\rangle + \langle\boldsymbol{\nabla},\boldsymbol{\nabla}\rangle\varphi_0 + \nabla_0\langle\boldsymbol{\nabla},\boldsymbol{\varphi}\rangle \pm \langle\boldsymbol{\nabla},\boldsymbol{\nabla}\times\boldsymbol{\varphi}\rangle$$
$$= (\nabla_0\nabla_0 + \langle\boldsymbol{\nabla},\boldsymbol{\nabla}\rangle)\varphi_0$$

$$\boldsymbol{\zeta} = -\boldsymbol{\nabla}\phi_0 + \nabla_0\boldsymbol{\phi} \mp \boldsymbol{\nabla}\times\boldsymbol{\phi} \tag{3}$$
$$= -\boldsymbol{\nabla}\nabla_0\varphi_0 + \boldsymbol{\nabla}\langle\boldsymbol{\nabla},\boldsymbol{\varphi}\rangle + \nabla_0\boldsymbol{\nabla}\varphi_0 + \nabla_0\nabla_0\boldsymbol{\varphi} \pm \nabla_0\boldsymbol{\nabla}\times\boldsymbol{\varphi}$$
$$\mp\boldsymbol{\nabla}\times\boldsymbol{\nabla}\varphi_0 \mp \boldsymbol{\nabla}\times\nabla_0\boldsymbol{\varphi} - \boldsymbol{\nabla}\times\boldsymbol{\nabla}\times\boldsymbol{\varphi}$$
$$= -\boldsymbol{\nabla}\nabla_0\varphi_0 + \boldsymbol{\nabla}\times\boldsymbol{\nabla}\times\boldsymbol{\varphi} + \langle\boldsymbol{\nabla},\boldsymbol{\nabla}\rangle\boldsymbol{\varphi} + \nabla_0\boldsymbol{\nabla}\varphi_0 + \nabla_0\nabla_0\boldsymbol{\varphi} \pm \nabla_0\boldsymbol{\nabla}\times\boldsymbol{\varphi}$$
$$\mp\boldsymbol{\nabla}\times\boldsymbol{\nabla}\varphi_0 \mp \boldsymbol{\nabla}\times\nabla_0\boldsymbol{\varphi} - \boldsymbol{\nabla}\times\boldsymbol{\nabla}\times\boldsymbol{\varphi}$$
$$= (\nabla_0\nabla_0 + \langle\boldsymbol{\nabla},\boldsymbol{\nabla}\rangle)\boldsymbol{\varphi}$$

Here ξ is a quaternionic function that for a part ρ describes the density distribution of a set of point-like artifacts that disrupt the continuity of function $\psi(q)$.

$$\rho = \rho_0 + \boldsymbol{\rho} = \langle \boldsymbol{\nabla}, \boldsymbol{\nabla} \rangle \psi = \frac{\partial^2 \psi}{\partial x^2} + \frac{\partial^2 \psi}{\partial y^2} + \frac{\partial^2 \psi}{\partial z^2} \tag{4}$$

$$\xi - \rho = \nabla_0 \nabla_0 \psi \tag{5}$$

In case of a single static point-like artifact, the solution ψ will describe the corresponding Green's function. Its actual form depends on the boundary conditions.

Function $\psi(q)$ describes the mostly continuous field ψ.

The second order partial differential equation that is based on the double quaternionic nabla can be split into two continuity equations, which are quaternionic first order partial differential equations:

$$\Phi = \nabla \psi \tag{6}$$

$$\rho = \nabla^* \Phi \tag{7}$$

If ψ and Φ are normalizable functions and $\|\psi\| = 1$, then with real m and $\|\zeta\| = 1$ follows:

$$\nabla \psi = m\, \zeta \tag{9}$$

15.2.2 The other second order partial differential equation

We will encounter another quaternionic second order partial differential equation, but that one cannot be split into two first order quaternionic partial differential equations. It is based on d'Alembert's operator $\mathfrak{D}=(-\nabla_0 \nabla_0 + \langle \boldsymbol{\nabla}, \boldsymbol{\nabla} \rangle)$.

$$\zeta = \zeta_0 + \boldsymbol{\zeta} = \mathfrak{D}\varphi = \mathfrak{D}(\varphi_0 + \boldsymbol{\varphi}) = \{-\nabla_0 \nabla_0 + \langle \boldsymbol{\nabla}, \boldsymbol{\nabla} \rangle\} \varphi \tag{1}$$

Dirac has shown that it can be split into two biquaternionic partial differential equations. This fact is treated in the appendix.

In contrast to the first kind of second order quaternionic partial differential equation, the second kind accepts waves as solutions of the homogeneous version of the equation. The waves are ***eigenfunctions*** of differential operator $\mathfrak{D}$. All superpositions of such eigenfunctions are again solutions of the homogeneous equation and can be added to the solutions of the inhomogeneous

equation. These superpositions form so called ***wave packages***. When they move, wave packages tend to disperse.

$$\nabla_0 \nabla_0 f = \langle \nabla, \nabla \rangle f = -\omega^2 f \tag{2}$$

$$f(t,x) = a \exp\big(i\omega(ct - |\boldsymbol{x} - \boldsymbol{x}'|)\big)\,; c = \pm 1 \tag{3}$$

This leads to a category of solutions that are known as solutions of the Helmholtz equation.

15.3 Fourier equivalents

In this quaternionic differential calculus, differentiation is implemented as multiplication.

This is revealed by the Fourier equivalents of the equations (4) through (10) in the previous paragraph:

$$\widetilde{\Phi} = \widetilde{\Phi}_0 + \widetilde{\boldsymbol{\Phi}} = p\,\tilde{\psi} = (p_0 + \boldsymbol{p})(\tilde{\psi}_0 + \widetilde{\boldsymbol{\psi}}) \tag{1}$$

The nabla ∇ is replaced by operator p. $\widetilde{\Phi}$ is the Fourier transform of Φ.

$$\widetilde{\Phi}_0 = p_0 \tilde{\psi}_0 - \langle \boldsymbol{p}, \widetilde{\boldsymbol{\psi}} \rangle \tag{2}$$

$$\widetilde{\boldsymbol{\Phi}} = p_0 \widetilde{\boldsymbol{\psi}} + \boldsymbol{p}\tilde{\psi}_0 \pm \boldsymbol{p} \times \widetilde{\boldsymbol{\psi}} \tag{3}$$

The equivalent of the quaternionic second order partial differential equation is:

$$\tilde{\xi} = \tilde{\xi}_0 + \tilde{\boldsymbol{\xi}} = p^* p\,\tilde{\psi} = \{p_0 p_0 + \langle \boldsymbol{p}, \boldsymbol{p} \rangle\}\tilde{\psi} \tag{4}$$

$$\tilde{\rho} = \tilde{\rho}_0 + \tilde{\boldsymbol{\rho}} = \langle \boldsymbol{p}, \boldsymbol{p} \rangle \tilde{\psi} \tag{5}$$

The continuity equations result in:

$$\widetilde{\Phi} = p\tilde{\psi} \tag{6}$$

$$\tilde{\rho} = p^* \widetilde{\Phi} \tag{7}$$

15.4 Poisson equations

The ***screened Poisson equation*** is a special condition of the non-homogeneous second order partial differential equation in which some terms are zero or have a special value.

$$\nabla^*\nabla\psi = \nabla_0\nabla_0\psi + \langle\boldsymbol{\nabla},\boldsymbol{\nabla}\rangle\psi = \xi \tag{1}$$

$$\nabla_0\nabla_0\psi = -\lambda^2\,\psi \tag{2}$$

$$\langle\boldsymbol{\nabla},\boldsymbol{\nabla}\rangle\psi - \lambda^2\psi = \xi \tag{3}$$

The 3D solution of this equation is determined by the screened Green's function $G(r)$.

Green functions represent solutions for point sources. In spherical symmetric boundary conditions the Green's function becomes:

$$G(r) = \frac{\exp(-\lambda\, r)}{r} \tag{4}$$

$$\psi = \iiint G(\boldsymbol{r}-\boldsymbol{r}')\,\rho(\boldsymbol{r}')\,d^3\boldsymbol{r}\,' \tag{5}$$

G(r) has the shape of the Yukawa potential [12]

In case of $\lambda = 0$ it resembles the Coulomb or gravitation potential of a point source.

If $\lambda \neq 0$, then a solution of equation (3) is:

$$\psi = a(\boldsymbol{x})\,\exp(\pm\, i\,\omega\,\tau);\, \lambda = \pm\, i\,\omega \tag{6}$$

These solutions concern a screened Poisson equation that is based on the first version of the second order partial differential equation. The equation that is based on d'Alembert's operator delivers:

$$\mathfrak{D}\varphi = \mathfrak{D}(\varphi_0 + \boldsymbol{\varphi}) = \{-\nabla_0\nabla_0 + \langle\boldsymbol{\nabla},\boldsymbol{\nabla}\rangle\}\varphi = \zeta \tag{7}$$

$$\nabla_0\nabla_0\varphi = \frac{\partial^2\varphi}{\partial\tau^2} = \lambda^2\,\varphi$$

$$(\langle \boldsymbol{\nabla}, \boldsymbol{\nabla} \rangle - \lambda^2)\varphi = \frac{\partial^2 \varphi}{\partial x^2} + \frac{\partial^2 \varphi}{\partial y^2} + \frac{\partial^2 \varphi}{\partial z^2} - \lambda\varphi = \zeta \tag{8}$$

$$\varphi = a(\boldsymbol{x}) \exp(\pm\lambda\tau) \tag{9}$$

The Green's function is the same, but solution (9) differs significantly from solution (6). The difference only concerns the temporal behavior of the field.

15.5 Special solutions of the homogeneous partial differential equations

Here we focus on special solutions of the quaternionic homogeneous second order partial differential equations. These solutions are of special interest because for odd numbers of participating dimensions these equations have solutions in the form of ***shape keeping fronts***.

The homogeneous equations run as:

$$\frac{\partial^2 \psi}{\partial x^2} + \frac{\partial^2 \psi}{\partial y^2} + \frac{\partial^2 \psi}{\partial z^2} \pm \frac{\partial^2 \psi}{\partial \tau^2} = \frac{1}{r^2}\frac{\partial}{\partial r}\left(r^2 \frac{\partial \psi}{\partial r}\right) \pm \frac{\partial^2 \psi}{\partial \tau^2} = 0 \tag{1}$$

Here we treat the two kinds of homogeneous equations together.

First we focus on the solutions that vary in one dimension. Thus:

$$\frac{\partial^2 \psi}{\partial z^2} \pm \frac{\partial^2 \psi}{\partial \tau^2} = 0 \tag{2}$$

We try a solution in the form $\varphi = f(\alpha z + \beta\tau)$:

$$\frac{\partial f}{\partial z} = \alpha f'; \frac{\partial^2 f}{\partial z} = \alpha \frac{\partial f'}{\partial z} = \alpha^2 f'' \tag{3}$$

$$\frac{\partial f}{\partial \tau} = \beta f'; \frac{\partial^2 f}{\partial \tau^2} = \beta \frac{\partial f'}{\partial \tau} = \beta^2 f'' \tag{4}$$

$$\alpha^2 f'' \pm \beta^2 f'' = 0 \tag{5}$$

This is solved when $\alpha^2 = \mp\beta^2$.

For the first kind of the second order partial differential equation this means: $\beta = \pm\alpha\, \boldsymbol{i}$, where $\boldsymbol{i}$ is a normalized imaginary quaternion. With $g(z) = f(\beta\, z)$ follows:

$$\varphi = g(z\, \boldsymbol{i} \pm \tau) \tag{6}$$

The function g represents a shape keeping front. It is not a wave.

The imaginary $\boldsymbol{i}$ represents the base vector in the x, y plane. Its orientation θ may be a function of z.

That orientation determines the polarization of the one-dimensional shape keeping front. The ***messengers*** that are mentioned earlier are constituted of strings of these one-dimensional shape keeping fronts.

For the second kind of the second order partial differential equation this means: $\beta = \pm\alpha$. With $g(z) = f(\beta\, z)$ follows:

$$\varphi = g(z \pm \tau) \tag{7}$$

Next we focus on the three dimensional spherical symmetric condition. In that case the equations can be separated by writing $\psi = r\, \varphi(r, \tau)$

$$\frac{\partial^2 \varphi}{\partial r^2} + \frac{2}{r}\frac{\partial \varphi}{\partial r} \pm \frac{\partial^2 \varphi}{\partial \tau^2} = 0 \Longrightarrow \frac{\partial^2 \psi}{\partial r^2} \pm \frac{\partial^2 \psi}{\partial \tau^2} = 0 \tag{8}$$

With other words ψ fulfills the conditions of the one-dimensional case. Thus solutions in the form $\varphi = f(\alpha r + \beta\tau)/r$ will fit.

For the first kind of the second order partial differential equation this means: $\beta = \pm\alpha\, \boldsymbol{i}$, where $\boldsymbol{i}$ is a normalized imaginary quaternion. With $g(x) = f(\beta\, x)$ follows:

$$\varphi = g(r\, \boldsymbol{i} \pm \tau)/r \tag{9}$$

$\boldsymbol{i}$ represents a base vector in radial direction.

For the second kind of the second order partial differential equation this means: $\beta = \pm\alpha$. With $g(x) = f(\beta\, x)$ follows:

$$\varphi = g(x \pm \tau)/r \tag{10}$$

The imaginary $\boldsymbol{i}$ represents the base vector in the x, y plane. Its orientation θ may be a function of z.

That orientation determines the polarization of the one-dimensional shape keeping front. The ***messengers*** that are mentioned earlier are constituted of strings of these one-dimensional shape keeping fronts.

The shape keeping fronts are not waves and do not form wave packages. Instead the shape keeping fronts occur in strings and do not disperse.

15.6 Special formulas

We list a series of interesting formulas that hold generally for the nabla operator $\boldsymbol{\nabla}$.

$$\boldsymbol{\nabla}\langle \boldsymbol{k}, \boldsymbol{x}\rangle = \boldsymbol{k} \tag{1}$$

$\boldsymbol{k}$ is constant.

$$\langle \boldsymbol{\nabla}, \mathbf{x}\rangle = \mathbf{3} \tag{2}$$

$$\boldsymbol{\nabla} \times \mathbf{x} = \mathbf{0} \tag{3}$$

$$\boldsymbol{\nabla}|\mathbf{x}| = \frac{\mathbf{x}}{|\mathbf{x}|} \tag{4}$$

$$\boldsymbol{\nabla}\frac{1}{|\mathbf{x}-\mathbf{x}'|} = -\frac{\mathbf{x}-\mathbf{x}'}{|\mathbf{x}-\mathbf{x}'|^3} \tag{5}$$

$$\langle \boldsymbol{\nabla}, \frac{\mathbf{x}-\mathbf{x}'}{|\mathbf{x}-\mathbf{x}'|^3}\rangle = \langle \boldsymbol{\nabla}, \boldsymbol{\nabla}\rangle \frac{1}{|\mathbf{x}-\mathbf{x}'|} = \langle \boldsymbol{\nabla}, \boldsymbol{\nabla}\frac{1}{|\mathbf{x}-\mathbf{x}'|}\rangle = 4\pi\, \delta(\mathbf{x}-\mathbf{x}') \tag{6}$$

Similar formulas apply to the quaternionic nabla and parameter values.

$$\nabla x = 1 - 3\,;\ \nabla^* x = 1 + 3;\ \nabla x^* = 1 + 3 \tag{7}$$

$$\nabla(x^* x) = x \tag{8}$$

$$\nabla|x| = \nabla\sqrt{(x^* x)} = \frac{x}{|x|} \tag{9}$$

$$\nabla \frac{1}{|x-x'|} = -\frac{x-x'}{|x-x'|^3} \tag{10}$$

$$\nabla^* \frac{x-x'}{|x-x'|^3} = \nabla\, \nabla^* \frac{1}{|x-x'|} = \left(\frac{\partial}{\partial\tau}\frac{\partial}{\partial\tau} + \langle \boldsymbol{\nabla}, \boldsymbol{\nabla}\rangle\right)\frac{1}{|x-x'|} \neq 4\pi\, \delta(x-x') \tag{11}$$

Instead:

$$(\nabla_0\nabla_0 + \langle \boldsymbol{\nabla}, \boldsymbol{\nabla}\rangle)\frac{1}{|x|} = \frac{3\tau^2}{|x|^5} - \frac{1}{|x|^3} + \frac{3\tau^2}{|x|^5} = \frac{6\tau^2 - |x|^2}{|x|^5} = \frac{5\tau^2 - |\boldsymbol{x}|^2}{|x|^5} \tag{12}$$

$$(\nabla_0\nabla_0 - \langle \boldsymbol{\nabla}, \boldsymbol{\nabla}\rangle)\frac{1}{|x|} = -\frac{1}{|x|^3} \tag{13}$$

$$\langle \boldsymbol{\nabla}, \boldsymbol{\nabla}\rangle \frac{1}{|\boldsymbol{x}|} = 4\pi\, \delta(\boldsymbol{x}) \tag{14}$$

Thus, with spherical boundary conditions, $\frac{1}{4\pi\,|\boldsymbol{x}-\boldsymbol{x'}|}$ is suitable as the Green's function for the Poisson equation, but $\frac{1}{4\pi\,|x-x'|}$ does not represent a Green's function for the quaternionic operator $(\nabla_0\nabla_0 + \langle \boldsymbol{\nabla}, \boldsymbol{\nabla}\rangle)$!

For a homogeneous second order partial differential equation a Green's function is not required. Thus, the deficit of a green's function does not forbid the existence of a quaternionic homogeneous second order partial differential equation. Still equation (6) forms the base of the Poisson equation.

15.7 Differential field equations

By introducing new symbols $\mathfrak{E}$ and $\mathfrak{B}$ we will keep the quaternionic differential equations closer to the Maxwell differential equations. Still essential differences exist between these two sets of differential equations. This will be elucidated in detail in the appendix.

Like the quaternions themselves the quaternionic nabla can be split in a scalar part and a vector part. The quaternionic nabla acts as a multiplying operator and this means that the first order partial differential equation splits in five terms. Part of these terms are scalars. The other terms are vectors.

The following formulas are not Maxwell equations. At the utmost the formulas are Maxwell-like.

$$\begin{aligned}\phi = \nabla\,\varphi &= (\nabla_0 + \boldsymbol{\nabla})\,(\varphi_0 + \boldsymbol{\varphi}) = \nabla_0\varphi_0 - \langle \boldsymbol{\nabla}, \boldsymbol{\varphi}\rangle + \nabla_0\boldsymbol{\varphi} + \boldsymbol{\nabla}\varphi_0 \pm \boldsymbol{\nabla}\times\boldsymbol{\varphi} \\ &= \nabla_0\varphi_0 - \langle \boldsymbol{\nabla}, \boldsymbol{\varphi}\rangle - \mathfrak{E} \pm \mathfrak{B}\end{aligned} \tag{1}$$

$$\mathfrak{E} \stackrel{\text{def}}{=} -\nabla_0 \boldsymbol{\varphi} - \boldsymbol{\nabla}\varphi_0 \tag{2}$$

$$\nabla_0 \mathfrak{E} = -\nabla_0 \nabla_0 \, \boldsymbol{\varphi} - \nabla_0 \boldsymbol{\nabla}\varphi_0 \tag{3}$$

$$\langle \boldsymbol{\nabla}, \mathfrak{E} \rangle = -\nabla_0 \langle \boldsymbol{\nabla}, \boldsymbol{\varphi} \rangle - \langle \boldsymbol{\nabla}, \boldsymbol{\nabla} \rangle \varphi_0 \tag{4}$$

$$\mathfrak{B} \stackrel{\text{def}}{=} \boldsymbol{\nabla} \times \boldsymbol{\varphi} \tag{5}$$

These definitions imply:

$$\langle \mathfrak{E}, \mathfrak{B} \rangle = 0 \tag{6}$$

$$\nabla_0 \mathfrak{B} = -\boldsymbol{\nabla} \times \mathfrak{E} \tag{7}$$

$$\langle \boldsymbol{\nabla}, \mathfrak{B} \rangle = 0 \tag{8}$$

$$\boldsymbol{\nabla} \times \mathfrak{B} = \boldsymbol{\nabla} \langle \boldsymbol{\nabla}, \boldsymbol{\varphi} \rangle - \langle \boldsymbol{\nabla}, \boldsymbol{\nabla} \rangle \boldsymbol{\varphi} \tag{9}$$

The Maxwell equations ignore the real part of ϕ.

$$\phi_0 = \nabla_0 \phi_0 = \nabla_0 \nabla_0 \, \varphi_0 - \nabla_0 \langle \boldsymbol{\nabla}, \boldsymbol{\varphi} \rangle \tag{10}$$

$$\boldsymbol{\nabla}\phi_0 = \nabla_0 \, \boldsymbol{\nabla}\varphi_0 - \, \boldsymbol{\nabla}\langle \boldsymbol{\nabla}, \boldsymbol{\varphi} \rangle = \nabla_0 \, \boldsymbol{\nabla}\varphi_0 - \boldsymbol{\nabla} \times \boldsymbol{\nabla} \times \, \boldsymbol{\varphi} - \, \langle \boldsymbol{\nabla}, \boldsymbol{\nabla} \rangle \, \boldsymbol{\varphi} \tag{11}$$

$$\zeta = \zeta_0 + \boldsymbol{\zeta} = (\nabla_0 + \langle \boldsymbol{\nabla}, \boldsymbol{\nabla} \rangle)\varphi \tag{12}$$

$$\zeta_0 = (\nabla_0 \nabla_0 + \langle \boldsymbol{\nabla}, \boldsymbol{\nabla} \rangle)\varphi_0 = \nabla_0 \, \phi_0 - \langle \boldsymbol{\nabla}, \mathfrak{E} \rangle \tag{13}$$

$$\boldsymbol{\zeta} = (\nabla_0 \nabla_0 + \langle \boldsymbol{\nabla}, \boldsymbol{\nabla} \rangle)\boldsymbol{\varphi} = -\boldsymbol{\nabla}\phi_0 - \nabla_0 \mathfrak{E} - \boldsymbol{\nabla} \times \boldsymbol{\mathcal{B}} \tag{14}$$

More in detail the equations mean:

$$\zeta_0 = \nabla_0\phi_0 + \langle \boldsymbol{\nabla}, \boldsymbol{\phi} \rangle \tag{15}$$
$$= \{\nabla_0\nabla_0\varphi_0 - \nabla_0\langle \boldsymbol{\nabla}, \boldsymbol{\varphi} \rangle\} + \{\langle \boldsymbol{\nabla}, \boldsymbol{\nabla} \rangle\varphi_0 + \nabla_0\langle \boldsymbol{\nabla}, \boldsymbol{\varphi} \rangle \pm \langle \boldsymbol{\nabla}, \boldsymbol{\nabla} \times \boldsymbol{\varphi} \rangle\}$$
$$= (\nabla_0\nabla_0 + \langle \boldsymbol{\nabla}, \boldsymbol{\nabla} \rangle)\varphi_0$$

$$\boldsymbol{\zeta} = -\boldsymbol{\nabla}\phi_0 + \nabla_0\boldsymbol{\phi} \mp \boldsymbol{\nabla} \times \boldsymbol{\phi} \tag{16}$$
$$= \{-\boldsymbol{\nabla}\nabla_0\varphi_0 + \boldsymbol{\nabla} \times \boldsymbol{\nabla} \times \boldsymbol{\varphi} + \langle \boldsymbol{\nabla}, \boldsymbol{\nabla} \rangle\boldsymbol{\varphi}\} + \{\nabla_0\boldsymbol{\nabla}\varphi_0 + \nabla_0\nabla_0\boldsymbol{\varphi} \pm \nabla_0\boldsymbol{\nabla} \times \boldsymbol{\varphi}\}$$
$$\{\mp\boldsymbol{\nabla} \times \boldsymbol{\nabla}\varphi_0 \mp \boldsymbol{\nabla} \times \nabla_0\boldsymbol{\varphi} - \boldsymbol{\nabla} \times \boldsymbol{\nabla} \times \boldsymbol{\varphi}\}$$
$$= (\nabla_0\nabla_0 + \langle \boldsymbol{\nabla}, \boldsymbol{\nabla} \rangle)\boldsymbol{\varphi} + \boldsymbol{\nabla} \times \boldsymbol{\nabla} \times \boldsymbol{\varphi} - \boldsymbol{\nabla} \times \boldsymbol{\nabla} \times \boldsymbol{\varphi}$$

$$\rho_0 = \langle \boldsymbol{\nabla}, \boldsymbol{\nabla} \rangle\varphi_0 = \zeta_0 - \nabla_0\nabla_0\varphi_0 \tag{17}$$
$$\boldsymbol{\rho} = \langle \boldsymbol{\nabla}, \boldsymbol{\nabla} \rangle\boldsymbol{\varphi} = \boldsymbol{\zeta} - \nabla_0\boldsymbol{\nabla_0}\boldsymbol{\varphi} \tag{18}$$

15.8 Quaternionic differential operators

When applied to quaternionic functions, quaternionic differential operators result in another quaternionic function that uses the same parameter space.

The operators $\nabla_0, \boldsymbol{\nabla}, \nabla = \nabla_0 + \boldsymbol{\nabla}, \nabla^* = \nabla_0 - \boldsymbol{\nabla}, \langle \boldsymbol{\nabla}, \boldsymbol{\nabla} \rangle, \nabla\nabla^* = \nabla^*\nabla = \nabla_0\nabla_0 + \langle \boldsymbol{\nabla}, \boldsymbol{\nabla} \rangle$ and

$\mathfrak{O} = -\nabla_0\nabla_0 + \langle \boldsymbol{\nabla}, \boldsymbol{\nabla} \rangle$ are all quaternionic differential operators.

∇ is the quaternionic nabla operator.

∇^* is its quaternionic conjugate.

The Dirac nabla operators $\mathcal{D} = \mathbb{i}\,\nabla_0 + \boldsymbol{\nabla}$ and $\mathcal{D}^* = \mathbb{i}\,\nabla_0 - \nabla$ convert quaternionic functions into biquaternionic functions. The equation

$$\mathcal{D}\mathcal{D}^* f = \mathfrak{O} f = -\nabla_0\nabla_0 + \langle \boldsymbol{\nabla}, \boldsymbol{\nabla} \rangle f = g \tag{19}$$

represents a wave equation and is a pure quaternionic equation! The Dirac operator and the Dirac equation are treated in detail in the appendix.

15.9 Poynting vector

The definitions of $\boldsymbol{\mathfrak{E}}$ and $\boldsymbol{\mathcal{B}}$ invite the definition of the Poynting vector $\boldsymbol{S}$:

$$\boldsymbol{S} = \boldsymbol{\mathfrak{E}} \times \boldsymbol{\mathcal{B}} \tag{1}$$
$$u = \tfrac{1}{2}(\langle \boldsymbol{\mathfrak{E}}, \boldsymbol{\mathfrak{E}} \rangle + \langle \boldsymbol{\mathcal{B}}, \boldsymbol{\mathcal{B}} \rangle) \tag{2}$$
(3)

$$\frac{\partial u}{\partial \tau} = \langle \boldsymbol{\nabla}, \boldsymbol{S} \rangle + \langle \boldsymbol{J}, \mathfrak{E} \rangle$$

Where ρ represents the presence of charges will $\boldsymbol{J}$ represent the flow of charges.

16 Double differentiation

16.1 Right and left sided nabla

The quaternionic nabla can be split into a right sided version and a left sided version. Without further indication we consider the right version as the current version. The version is determined by the imaginary part and is linked with the handedness of the product rule.

$$\nabla_r f = e^\mu \frac{\partial f}{\partial x_\mu} = e^\mu e^\nu \frac{\partial f_\nu}{\partial x_\mu} = e^\mu e^\nu \nabla_\mu f_\nu = \nabla f$$

$$\nabla_l f = \frac{\partial f}{\partial x_\mu} e^\mu = e^\nu e^\mu \frac{\partial f_\nu}{\partial x_\mu} = e^\nu e^\mu \nabla_\mu f_\nu = (e^\mu e^\nu)^* \nabla_\mu f_\nu = (\nabla_r f)^* = (\nabla f)^* = \nabla f - 2\boldsymbol{\nabla} \times \boldsymbol{f}$$

$$\nabla_r(\nabla_l f) = e^\rho e^\nu e^\mu \nabla_\rho \nabla_\mu f_\nu$$

16.2 Double partial differentiation

The partial differential equations hide that they are part of a differential equation.

$$\nabla' \nabla f = \xi = \sum_{\nu=0}^{3} e'_\nu \frac{\partial}{\partial q'_\nu} \left(\sum_{\mu=0}^{3} e_\mu \frac{\partial f}{\partial q_\mu} \right) = \left(e'_\nu e_\mu \frac{\partial^2}{\partial q_\mu \partial q'_\nu} \right) f \tag{1}$$

16.3 Single difference

Single difference is defined by

$$df(q) = \sum_{\mu=0}^{3} \sum_{\varsigma=0}^{3} \frac{\partial f^\varsigma}{\partial q_\mu} e_\mu e_\varsigma \, dq^\mu = \sum_{\nu=0}^{3} \phi_\nu e_\nu dq^\nu \tag{2}$$

$$\frac{\partial f^\varsigma}{\partial q_\mu} e_\mu e_\varsigma = \begin{bmatrix} \frac{\partial f^0}{\partial q_0} & \frac{\partial f^1}{\partial q_0}\boldsymbol{i} & \frac{\partial f^2}{\partial q_0}\boldsymbol{j} & \frac{\partial f^3}{\partial q_0}\boldsymbol{k} \\ \frac{\partial f^0}{\partial q_1}\boldsymbol{i} & \frac{\partial f^1}{\partial q_1} & \frac{\partial f^2}{\partial q_1}\boldsymbol{k} & -\frac{\partial f^3}{\partial q_1}\boldsymbol{j} \\ \frac{\partial f^0}{\partial q_2}\boldsymbol{j} & -\frac{\partial f^1}{\partial q_2}\boldsymbol{k} & \frac{\partial f^2}{\partial q_2} & \frac{\partial f^3}{\partial q_2}\boldsymbol{i} \\ \frac{\partial f^0}{\partial q_3}\boldsymbol{k} & \frac{\partial f^1}{\partial q_3}\boldsymbol{j} & -\frac{\partial f^2}{\partial q_3}\boldsymbol{i} & \frac{\partial f^3}{\partial q_3} \end{bmatrix} \tag{3}$$

$$= \begin{bmatrix} \dfrac{\partial f^0}{\partial q_0} & -\mathcal{E}_x \boldsymbol{i} & -\mathcal{E}_y \boldsymbol{j} & -\mathcal{E}_z \boldsymbol{k} \\ \mathcal{E}_x \boldsymbol{i} & \dfrac{\partial f^1}{\partial q_1} & -\mathcal{B}_{z1} \boldsymbol{k} & -\mathcal{B}_{y2} \boldsymbol{j} \\ \mathcal{E}_y \boldsymbol{j} & -\mathcal{B}_{z2} \boldsymbol{k} & \dfrac{\partial f^2}{\partial q_2} & -\mathcal{B}_{x1} \boldsymbol{i} \\ \mathcal{E}_z \boldsymbol{k} & -\mathcal{B}_{y1} \boldsymbol{j} & -\mathcal{B}_{x2} \boldsymbol{i} & \dfrac{\partial f^3}{\partial q_3} \end{bmatrix}$$

Here

$$\mathcal{B}_x = \mathcal{B}_{x1} - \mathcal{B}_{x2};\ \mathcal{B}_y = \mathcal{B}_{y1} - \mathcal{B}_{y2};\ \mathcal{B}_z = \mathcal{B}_{z1} - \mathcal{B}_{z2} \tag{4}$$

$$\dot{f} = \frac{df}{d\lambda} = \sum_{\mu=0}^{3} \phi_\mu e_\mu \frac{dq^\mu}{d\lambda} = \sum_{\mu=0}^{3} \phi_\mu e_\mu \dot{q}^\mu \tag{5}$$

The scalar λ is can be a linear function of τ or a scalar function of q.

$$\dot{q} \stackrel{\text{def}}{\equiv} \frac{dq}{d\lambda} = e_\mu \frac{dq^\mu}{d\lambda} = e_\mu \dot{q}^\mu \tag{6}$$

Double difference is defined by:

$$d^2 f(q) = \sum_{\nu=0}^{3} e'_\nu \left(\sum_{\mu=0}^{3} \frac{\partial^2 f^\varsigma}{\partial q_\mu \partial q'_\nu} e_\mu dq^\mu \right) e_\varsigma dq'^\nu \tag{7}$$

$$\ddot{f} \stackrel{\text{def}}{\equiv} \frac{d^2 f(q)}{d\lambda^2} = e_\varrho \ddot{f}^\varrho = \sum_{\nu=0}^{3} e'_\nu \left(\sum_{\mu=0}^{3} \frac{\partial^2 f^\varsigma}{\partial q_\mu \partial q'_\nu} e_\mu \frac{dq^\mu}{d\lambda} \right) e_\varsigma \frac{dq'^\nu}{d\lambda} \tag{8}$$

$$= \sum_{\nu=0}^{3} e'_\nu \left(\sum_{\mu=0}^{3} \frac{\partial^2 f^\varsigma}{\partial q_\mu \partial q'_\nu} e_\mu \dot{q}^\mu \right) e_\varsigma \dot{q}'^\nu = \left(\dot{q}^\mu \dot{q}'^\nu \frac{\partial^2}{\partial q_\mu \partial q'_\nu} e'_\nu e_\mu \right) f = \zeta_{\nu\mu}\, f$$

$$\zeta_{\nu\mu} = e'_\nu e_\mu\, \dot{q}'^\nu\, \dot{q}^\mu \frac{\partial^2}{\partial q_\mu \partial q'_\nu} = e'_\nu e_\mu \Upsilon_{\nu\mu} \tag{9}$$

(10)

$$\Upsilon_{\nu\mu} = \dot{q}'^{\nu}\,\dot{q}^{\mu}\frac{\partial^2}{\partial q_\mu \partial q'_\nu}$$

If we apply $\phi = \nabla f$ as the first differential operation and $\xi = \nabla^* \phi$ as the second differential operation, then $e = \{1, +\boldsymbol{i}, +\boldsymbol{j}, +\boldsymbol{k}\}$ and $e' = \{1 - \boldsymbol{i}, -\boldsymbol{j}, -\boldsymbol{k}\}$ and

$$\Upsilon_{\nu\mu} = \begin{bmatrix} +\Upsilon_{00} & +\Upsilon_{01}\boldsymbol{i} & +\Upsilon_{02}\boldsymbol{j} & +\Upsilon_{03}\boldsymbol{k} \\ -\Upsilon_{10}\boldsymbol{i} & \circledast\,\Upsilon_{11} & +\Upsilon_{12}\boldsymbol{k} & +\Upsilon_{13}\boldsymbol{j} \\ -\Upsilon_{20}\boldsymbol{j} & -\Upsilon_{21}\boldsymbol{k} & \circledast\,\Upsilon_{22} & -\Upsilon_{23}\boldsymbol{i} \\ -\Upsilon_{30}\boldsymbol{k} & -\Upsilon_{31}\boldsymbol{j} & +\Upsilon_{32}\boldsymbol{i} & \circledast\,\Upsilon_{33} \end{bmatrix} \tag{11}$$

Here the switch $\circledast$ distinguishes between quaternionic differential calculus and Maxwell based differential calculus. See the appendix.

16.4 Deformed space

If the investigated field represents deformed space $\mathfrak{C}$, then the field $\mathfrak{R}$, which represents the parameter space of function $\mathfrak{C}(q)$ represents the virgin state of that deformed space.

Further, the equation $\frac{d^2\mathfrak{C}(q)}{d\lambda^2} = 0$ represents a local condition in which $\mathfrak{C}$ is not affected by external influences. Here λ can be any linear combination of progression τ or it can represent the equivalent of local quaternionic distance:

$$\lambda = a\,q_0 + b$$

or

$$\lambda = |q|$$

17 Actions of the fields

Apart from the symmetry related fields $\mathfrak{A}^x$ that are raised by the charges of the symmetry centers, at least one other fields exists. That field is the embedding field $\mathfrak{C}$.

The origins of the two fields differ fundamentally. The embedding field smoothly follows a distribution of discrete quaternionic values, which are eigenvalues of a series of operators. Some of these values do not fit properly in the set of values that surrounds them. In the special condition that these disparities appear in coherent swarms, we have indicated the swarm as the representative of an elementary particle. The disparities are due to difference in the symmetries of the underlying domains. These symmetries determine how the values cooperate in convolutions. If the disparities were not present, then the embedding field would be equal to the parameter space $\mathcal{R}$ and that continuum would follow parameter space $\mathfrak{R}$.

The embedding field is not directly affected by the symmetry related charges of the symmetry centers. It is indirectly affected, because the symmetry related fields affect the location of the symmetry centers that house the objects that can deform the embedding field. In principle each disruption of the continuity of the field, thus each element of the swarm that represents an elementary particle affects the embedding field $\mathfrak{C}$. The smoothed version $\mathfrak{U}$ of the embedding field is far less vigilant. Also the symmetry related field $\mathfrak{A}$,which is coupled to the geometric center of the symmetry center reacts much less vigilant.

In this view, fields are more or less blurred representations of discrete distributions, where the elements of the distribution are target values of a function that has rational quaternions as its parameter space. In some cases the discrete distribution represents a dynamic location density distribution.

The embedding field $\mathfrak{C}$ is affected by the embedding of artifacts that are picked by a dedicated controlling mechanism that uses a symmetry center $\mathfrak{S}_n^x$. as a resource. After selection of the location of the artifact, the controlling mechanism embeds this artifact into the embedding continuum $\mathfrak{C}$. This continuum is represented by the continuum eigenspace of operator $\mathfrak{C}$.

Each of these mechanisms operates in a cyclic and stochastic fashion. The embedding events occur in the direct neighborhood of the geometric center of the corresponding symmetry center. The result is a recurrently regenerated coherent location swarm that also represent a stochastic hopping path. The swarm is centered around the geometric center of the symmetry center. Hopping means that the controlling mechanism generates at the utmost one embedding location per progression step. This means that the hopping object can be considered as a point-like artifact. At the embedding instant the artifact actually resides at the location that is represented by an element of the location swarm. Thus, the swarm represents the spatial map of a set of potential detection locations. The swarm is generated within the symmetry center $\mathfrak{S}_n^x$ and is encapsulated by $\partial \mathrm{H}_n^x$. The actions of the mechanisms deform the field $\mathfrak{C}$ inside the floating regions H_n^x. The deformation of $\mathfrak{C}$ reaches beyond the region H_n^x.

In this way, the mechanism creates an elementary object, which is able to deform the embedding field $\mathfrak{C}$ and inherits the symmetry related charge from the symmetry center. The deformation represents the local contribution to the embedding field by the elementary object that owns the swarm.

On the other hand the geometric center of the symmetry center houses the electric charge that influences field $\mathfrak{A}$. This view can be reversed. It is possible to consider the path that the geometric center of the symmetry center takes under the influence of both fields. This view requires an estimate of the results of the actions of these fields. This will be achieved via the ***path***

integral. First we will investigate the influence of the embedding field $\mathfrak{C}$. In a later phase we will add the results of the much less vigilant actions of the symmetry related field $\mathfrak{A}$.

17.1 Path of the symmetry center

The symmetry center $\mathfrak{S}_n^x$ that conforms to encapsulated region H_n^x, keeps its private symmetry flavor. At the passage through the boundary the symmetry flavor of the background parameter space $\mathfrak{R}^{⓪}$ flips from history to future. As a consequence the symmetry related charge of the symmetry center will flip.

However, the passage of the symmetry center through the rim may also be interpreted as the annihilation of the historic symmetry center and the creation of a new symmetry center with a reverse symmetry flavor that will extend its live in the future.

The passage of the symmetry centers through the rim goes together with annihilation and creation phenomena for the objects that reside on these platforms. Thus, this passage is related to the annihilation and creation of elementary objects. However, most of these occurrences do not lead to the complete conversion of the concerned object into another behavior mode. These exceptional occurrences are known as pair production and pair annihilation. Thus, in most cases the behavior mode of the module persists.

In the quaternionic space-progression model the existence of symmetry centers is independent of progression. With other words the number of symmetry centers is a model constant. The passage through the rim does not influence this number. Only the characteristics of the combination of the symmetry center and the background parameter space are affected by the passage.

17.2 Path integral

In this primary investigation we ignore the actions of the symmetry related potential. They are far less vigilant than the direct results of the embedding of individual locations.

Elementary objects reside on an individual symmetry center. A dedicated mechanism controls its recurrent generation and embeds the object into the embedding field. The path of the symmetry center is the averaged path of the embedded object. The embedded object is hopping along the elements of the generated location swarm. The landing locations of the hops are generated by the controlling mechanism in a stochastic fashion, but such that at first approximation the swarm as a whole can be considered to be moving as one unit. This is possible when the swarm is characterized by a continuous location density distribution, which owns a displacement generator. That is the case when the location density distribution owns a Fourier transform. This fact enables the description of the path of the swarm by a “path integral”. The hopping of the embedded object can be described by a sequence of factors that after multiplication represent the whole path. Each factor represents three sub-factors.

The procedure that underlies the path integral depends on the fact that the multiplication of factors that are all very close to unity can be replaced by a summation.

The first sub-factor represents the jump from configuration space to momentum space. This sub-factor is given by the inner product of the Hilbert vector that represents the current location and the Hilbert vector that represents the momentum of the swarm. This second Hilbert vector is assumed to be constant during the generation of the location swarm.

The second sub-factor represents the effect of the hop in momentum space.

The third sub-factor represents the jump back from momentum space to configuration space.

In the sequence of factors the third sub-factor of the current term compensates the effect of the first sub-factor of next term. Their product equals unity.

What results is a sequence of factors that are very close to unity and that represent the effects of the hops in momentum space. Due to the fact that the momentum is considered to be constant, the logarithms of the terms can be taken and added in an overall sum. In this way, the multiplication is equal to the sum of the logarithms of the factors.

This summation approaches what is known as the "path integral". In our interpretation it is not an integral, but instead it is a finite summation. In more detail the procedure can be described as follows.

We suppose that momentum $\boldsymbol{p}_n$ is constant during the particle generation cycle in which the controlling mechanism produces the swarm $\{a_i\}$. Every hop gives a contribution to the path. These contributions can be divided into three steps per contributing hop:

1. Change to Fourier space. This involves as sub-factor the inner product $\langle a_i|p_n\rangle$.
2. Evolve during an infinitesimal progression step into the future.
    a. Multiply with the corresponding displacement generator $\boldsymbol{p}_n$.
    b. The generated step in configuration space is $(\boldsymbol{a}_{i+1} - \boldsymbol{a}_i)$.
    c. The action contribution factor in Fourier space is $\langle \boldsymbol{p}_n, \boldsymbol{a}_{i+1} - \boldsymbol{a}_i\rangle$.
3. Change back to configuration space. This involves as sub-factor the inner product $\langle p_n|a_{i+1}\rangle$
4. The combined term contributes a factor $\langle a_i|p_n\rangle\exp(\langle \boldsymbol{p}_n, \boldsymbol{a}_{i+1} - \boldsymbol{a}_i\rangle)\langle p_n|a_{i+1}\rangle$.
5. Two subsequent steps give:

$$\langle a_i|p_n\rangle\exp(\langle \boldsymbol{p}_n, \boldsymbol{a}_{i+1} - \boldsymbol{a}_i\rangle)\langle p_n|a_{i+1}\rangle\langle a_{i+1}|p_n\rangle\exp(\langle \boldsymbol{p}_n, \boldsymbol{a}_{i+1} - \boldsymbol{a}_i\rangle)\langle p_n|a_{i+2}\rangle \tag{1}$$

$$= \langle a_i|p_n\rangle\exp(\langle \boldsymbol{p}_n, \boldsymbol{a}_{i+2} - \boldsymbol{a}_i\rangle)\langle p_n|a_{i+2}\rangle$$

The red terms in the middle turn into unity. The other terms also join.

Over a full particle generation cycle with N steps this results in:

$$\prod_{i=1}^{N-1}\langle a_i|p_n\rangle\exp(\langle \boldsymbol{p}_n, \boldsymbol{a}_{i+1} - \boldsymbol{a}_i\rangle)\langle p_n|a_{i+1}\rangle \tag{2}$$

$$= \langle a_1|p_n\rangle\exp(\langle \boldsymbol{p}_n, \boldsymbol{a}_N - \boldsymbol{a}_1\rangle)\langle p_n|a_N\rangle = \langle a_1|p_n\rangle \exp\left(\sum_{i=2}^{N}\langle \boldsymbol{p}_n, \boldsymbol{a}_{i+1} - \boldsymbol{a}_i\rangle\right)\langle p_n|a_N\rangle$$

$$= \langle a_1|p_n\rangle \exp(L)\,\langle p_n|a_N\rangle$$

$$L\,d\tau = \sum_{i=2}^{N-1}\langle \boldsymbol{p}_n, \boldsymbol{a}_{i+1} - \boldsymbol{a}_i\rangle = \langle \boldsymbol{p}_n, d\boldsymbol{q}\rangle \tag{3}$$

$$L = \langle \boldsymbol{p}_n, \dot{\boldsymbol{q}}\rangle \tag{4}$$

L is known as the ***Lagrangian***.

Equation (4) holds for the special condition in which $\boldsymbol{p}_n$ is constant. If $\boldsymbol{p}_n$ is not constant, then the Hamiltonian H varies with location. In the next equations we ignore subscript $_n$.

$$\frac{\partial H}{\partial q_i} = -\dot{p}_i \tag{5}$$

$$\frac{\partial H}{\partial p_i} = \dot{q}_i \tag{6}$$

$$\frac{\partial L}{\partial q_i} = \dot{p} \tag{7}$$

$$\frac{\partial L}{\partial \dot{q}_i} = p_i \tag{8}$$

$$\frac{\partial H}{\partial \tau} = -\frac{\partial H}{\partial \tau} \tag{9}$$

$$\frac{d}{d\tau}\frac{\partial L}{\partial \dot{q}_i} = \frac{\partial L}{\partial q_i} \tag{10}$$

$$H + L = \sum_{i=1}^{3} \dot{q}_i p_i \tag{11}$$

Here we used proper time τ rather than coordinate time t.

The effect of the hopping path is that the geometric center of the symmetry center is moved over a small resulting distance $\boldsymbol{a}_N - \boldsymbol{a}_1$. Together with "charge" $(N \cdot Q_n)$ this move determines the next version of momentum $\boldsymbol{p}_n$.

The result is that both the symmetry related fields $\mathfrak{A}^x$ and the embedding field $\mathfrak{C}$ influence the location of the geometric center of the symmetry center $\mathfrak{S}_n^x$.

In this investigation we ignored the influence of the symmetry related field $\mathfrak{A}$. This field influences momentum $\boldsymbol{p}_n$ and the corresponding eigenvector $|p_n\rangle$. This means that the product of the red colored middle terms is no longer equal to unity. Instead the product differs slightly from unity and the effect can be included in the path integral. In this way a small slowly varying extra contribution is added to each subsequent term in the summation. This extra contribution is a smooth function of progression and thus, it is a smooth function of the index of the term.

17.1 Acceleration of the symmetry center

Due to their actions, the fields $\mathfrak{A}$ and $\mathfrak{C}$ may accelerate the location of the symmetry center on which an elementary object resides. This occurs via the interaction of these fields with the contributions that the symmetry center and the recurrently embedded elementary object add to the influences of these fields.

The symmetry center and with it the residing elementary object float over the background parameter space $\mathfrak{R}$. This means that these items also float over the fields $\mathfrak{A}$ and $\mathfrak{C}$.

17.1.1 The symmetry related field

The symmetry related charge Q_n^x of the symmetry center $\mathfrak{S}_n^x$ contributes the local scalar potential φ_{n_0} to the symmetry related field $\mathfrak{A}$.

$$\varphi_{n_0}(\boldsymbol{q}) = \frac{Q_n^x}{|\boldsymbol{q} - \boldsymbol{c}_n^x|} \tag{1}$$

On the other hand

$$\boldsymbol{E}_n(\boldsymbol{q}) = \boldsymbol{\nabla}\varphi_{n_0} = \frac{Q_n^x(\boldsymbol{q} - \boldsymbol{c}_n^x)}{|\boldsymbol{q} - \boldsymbol{c}_n^x|^3} \tag{2}$$

Another symmetry center $\mathfrak{S}_m^x$ contributes potential φ_{m_0} to the symmetry related field $\mathfrak{A}$. The force $\boldsymbol{F}_{nm}$ between the two symmetry centers equals:

$$\boldsymbol{F}_{nm} = \boldsymbol{E}_n Q_m^x = \frac{Q_n^x Q_m^x(\boldsymbol{c}_n^x - \boldsymbol{c}_m^x)}{|\boldsymbol{c}_n^x - \boldsymbol{c}_m^x|^3} = -\boldsymbol{F}_{mn} = -\boldsymbol{E}_m Q_n^x \tag{3}$$

This need not correspond to an actual acceleration. On the other hand, if relative to the parameter space $\mathfrak{R}$, the movement of the symmetry center $\mathfrak{S}_n^x$ is uniform with speed $\boldsymbol{v}_n$, then the scalar potential φ_{n_0} corresponds to a vector potential $\boldsymbol{\varphi}_n = \varphi_{n_0}\boldsymbol{v}_n$. If relative to the parameter space $\mathfrak{R}$, the symmetry center actually accelerates, then this goes together with an extra field $\boldsymbol{E}_n = \dot{\boldsymbol{\varphi}}_n = \dot{\varphi}_{n_0}\boldsymbol{v}_n$ that represents the corresponding change of field $\mathfrak{A}$. Thus. If the two forces $\boldsymbol{F}_{nm}$ and $\boldsymbol{F}_{mn}$ do not hold each other in equilibrium, then the field $\mathfrak{A}$ will change dynamically with this extra contribution.

17.1.2 The embedding field

The location swarms that are generated by dedicated controlling mechanisms produce a local potential that also can accelerate the symmetry center on which the location swarm resides relative to the parameter space $\mathfrak{R}$. We analyze the situation by assuming that the swarm is represented by a Gaussian location distribution. Thus, we use the corresponding artifact as a test particle. The corresponding local potential that contributes to field $\mathfrak{C}$ equals

$$\chi_n(r) = -\frac{Q_n}{4\pi}\frac{ERF\left(r/\sigma\sqrt{2}\right)}{r} \tag{1}$$

Here Q_n represents the strength of the local potential. At somewhat larger distances the potential behaves as a single "charge" potential.

$$\chi_n(\boldsymbol{q}) \approx \frac{-Q_n}{4\pi|\boldsymbol{q} - \boldsymbol{c}_n^x|} \tag{2}$$

This virtual "charge" is located at the center of the symmetry center $\mathfrak{S}_n^x$. The scalar potential $\chi_n(\boldsymbol{q})$ adds to the embedding field $\mathfrak{C}$. The result is that $\mathfrak{C}$ gets deformed.

The local scalar potential $\chi_n(\boldsymbol{q})$ corresponds to a derived field $\boldsymbol{\mathcal{E}}_n(\boldsymbol{q})$.

$$\boldsymbol{\mathcal{E}}_n(\boldsymbol{q}) = \boldsymbol{\nabla}\chi_n = -\frac{Q_n(\boldsymbol{q} - \boldsymbol{c}_n^x)}{|\boldsymbol{q} - \boldsymbol{c}_n^x|^3} \tag{3}$$

Another symmetry center $\mathfrak{S}_m^x$ contributes potential $\chi_m(\boldsymbol{q})$ to the embedding field $\mathfrak{C}$. The force $\boldsymbol{F}_{nm}$ between the two symmetry centers equals:

$$\boldsymbol{F}_{nm} = \boldsymbol{\mathcal{E}}_n Q_m = -\frac{Q_n Q_m(\boldsymbol{c}_n^x - \boldsymbol{c}_m^x)}{|\boldsymbol{c}_n^x - \boldsymbol{c}_m^x|^3} = -\boldsymbol{F}_{mn} = -\boldsymbol{\mathcal{E}}_m Q_n \tag{4}$$

This need not correspond to an actual acceleration.

If the platform $\mathfrak{S}_m^x$ on which the swarm resides moves with uniform speed $\boldsymbol{v}$, then the local potential corresponds to a local vector potential.

$$\boldsymbol{\chi}_n = \chi_n \boldsymbol{v} \tag{5}$$

If this platform accelerates, then this goes together with an extra contribution to field $\boldsymbol{\mathcal{E}}_n$ that counteracts the acceleration.

$$\boldsymbol{\mathcal{E}}_n = \dot{\boldsymbol{\chi}}_n = \chi_n \dot{\boldsymbol{v}} \tag{6}$$

This effect is known as ***inertia***.

17.2 Grouped artifacts

Next we consider grouped artifacts that cause discontinuities in the realm of a symmetry center. The concerned field is the embedding field. Since we do no longer focus on symmetry related charges, we will omit the superscript ^{x}.

We consider the case that the locations of the artifacts form a coherent swarm $\{\boldsymbol{c}_n\}$ that can be characterized by a continuous location density distribution $\rho(\boldsymbol{q})$.

$$\chi(\boldsymbol{q}) = \sum_{n=0}^{N} \iiint_V \rho(\boldsymbol{q})\, Q_n\, \delta(\boldsymbol{q} - \boldsymbol{c}_n) = -\frac{1}{4\pi} \sum_{n=0}^{N} \iiint_V \rho(\boldsymbol{q}) Q_n \left\langle \boldsymbol{\nabla}, \boldsymbol{\nabla} \frac{1}{|\boldsymbol{q} - \boldsymbol{c}|} \right\rangle \tag{1}$$

If we use the spherical symmetric ***Gaussian location distribution*** of artifacts $\rho(r)$ that was introduced earlier as ***test function***,

$$\rho(r) = \langle \boldsymbol{\nabla}, \boldsymbol{\nabla} \rangle \mathfrak{T}(r) = -\frac{Q}{\left(\sigma\sqrt{2\pi}\right)^3} \exp\left(-\frac{r^2}{2\sigma^2}\right) \tag{2}$$

then a potential in the form of

$$\mathfrak{T}(r) = -\frac{Q}{4\pi} \frac{ERF\left(r/_{\sigma\sqrt{2}}\right)}{r} \tag{3}$$

results.

At somewhat larger distances the potential behaves like a single charge potential.

$$\chi(r) \approx \frac{-Q}{4\pi r} \tag{4}$$

This gives an idea of what happens when a mechanism that acts within the realm of a symmetry center produces a coherent swarm of artifacts that will be embedded into a field that gets deformed by these artifacts.

Despite the fact that it is constituted from a myriad of singular contributions, the potential in equation (3) is a continuous function and its gradient at the center point equals zero! Thus the corresponding deformation has a “wide-spread” binding effect.

17.3 The smoothed embedding field

The embedding field $\mathfrak{C}$ is described by a mostly continuous function $\mathfrak{C}(q)$. The convolution of $\mathfrak{C}(q)$ with a blurring function transforms this function in an everywhere* continuous function $\mathfrak{U}(q)$. Space cavities exist where both $\mathfrak{C}(q)$ and $\mathfrak{U}(q)$ are not defined. The blurring function integrates over the regeneration cycle of elementary objects in the progression part of the domain. If in the spatial domain the test function $\mathfrak{T}(q)$ is used as the blurring function for isolated discontinuities and a Gaussian distribution is used for coherent swarms of discontinuities, then the function $\mathfrak{U}(q)$ defines the smoothed embedding field $\mathfrak{U}$. This field takes the role of a model-wide potential. In physics this is the role of the gravitation potential. In this model we consider $\mathfrak{U}$ to represent the equivalent of ***universe***, however it represents a blurred universe.

The local contribution to the embedding field $\mathfrak{C}$ by the elementary particle has a smoothed versions which is the equivalent of its individual potential. It contributes to field $\mathfrak{U}$.

17.4 Spurious artifacts

Due to their minor effect, spurious artifacts will be hidden for observers due to the blanket that is spread over the corresponding field by the smoothed version of this field that the observers will see. Only recurrent regeneration of the artifact can generate a reasonable detection probability.

18 Messengers

Messengers are configured by solutions of the quaternionic second order partial differential equation. For odd numbers of participating dimensions some of the solutions of the homogeneous second order partial differential equation are combinations of shape keeping fronts. In three dimensions the spherical shape keeping fronts diminish their amplitude as $1/r$ with distance r of the trigger point. One-dimensional wave fronts keep their amplitude. As a consequence these shape keeping fronts can travel huge distances through the field that supports them. Each shape keeping front can carry a bit of information and/or energy. In order to reach these distances the carrying field must exist long enough and it must reach far enough.

The symmetry related field $\mathfrak{A}$ does not fulfil the requirements for long distance travel. It depends on the nearby existence of symmetry related charges and its amplitude also diminishes as 1/r with distance from the charge.

The embedding field $\mathfrak{C}$ is a better candidate for long distance transfer of energy and information. $\mathfrak{C}$ exists always and everywhere. One-dimensional shape keeping fronts vibrate the $\mathfrak{C}$ field, but do not deform this field. They just follow existing deformations.

Creating a string of one-dimensional shape keeping fronts requires a recurrent shape keeping front generation process. Such processes do not underlay the generation of symmetry related charges that support the $\mathfrak{A}$ field. However, such processes exist during the recurrent embedding of artifacts that occurs in the $\mathfrak{C}$ field.

Recurrent generation of spherical shape keeping fronts is capable to deform the corresponding field. It has similar effects as a stationary deformation by a point-like artifact has.

18.1 Photons

The fixed speed of shape keeping fronts translates in the same fixed speed for the messengers. A string of one-dimensional shape keeping fronts can carry a quantized amount of energy. Photons appear to be the physical realizations of the messengers. The relation $E = h\,\nu$ and the fixed speed of photons indicate that at least at relative short range the string of shape keeping fronts takes a fixed amount of progression steps for its creation, for its passage and for its absorption.

However, observations of long range effects over cosmological distances reveal that these relations do not hold over huge distances. Red-shift of patterns of “old” photons that are emitted by atoms and arrive from distant galaxies indicate that the spatial part of field $\mathfrak{C}$ is extending as a function of progression.

With the interpretation of photons as strings of shape keeping fronts this means that the duration of emission and the duration of absorption are also functions of progression. As a consequence, some of the emitted wave fronts are “missed” at later absorption. The detected photon corresponds to a lower energy and a lower frequency than the emitted photon has. According to relation $E = h\,\nu$ that holds locally, the detected photon appears to be red-shifted. The energy of the “missed” shape keeping fronts is converted into other kinds of energy or the missed shape keeping fronts keep proceeding as lower energy photons. Spurious shape keeping fronts may stay undetected.

18.2 Consequences for our model

Thus, the quaternionic second order partial differential equation may be valid in the vicinity of the images of symmetry centers inside $\mathfrak{C}$, but does not properly describe the long range behavior of $\mathfrak{C}$. Due to its restricted range and the non-recurrent generation of its charges, the $\mathfrak{A}$ field does not show the equivalents of photons and red-shift phenomena.

The long range phenomena of photons indicate that the parameter space $\mathfrak{R}^{⓪}$ of $\mathfrak{C}$ may actually own an origin. For higher progression values and for most of the spatial reach of field $\mathfrak{C}$, that origin is located at huge distances. Information coming from low progression values arrives with photons that have travelled huge distances. They report about a situation in which symmetry centers were located on average at much smaller inter-distances.

Instead of photons the $\mathfrak{A}$ field may support waves, such as radio waves and microwaves. These waves are solutions of the wave equation, which is part of Maxwell based differential calculus.

On the other hand the wave equation also has shape keeping fronts as its solutions.

19 At the start of progression

At progression value $\tau = 0$, the mechanisms that generate the artifacts, which cause discontinuities in the embedding manifold $\mathfrak{C}$ have not yet done any work. It means that this manifold was flat and its defining function equaled its parameter space at instance $\tau = 0$.

The model offers the possibility that the domain Ω expands as a function of τ. In that case it is possible that domain Ω covers a growing amount of symmetry centers.

20 Discussion

This paper only considers the divergence based version of the generalized Stokes theorem. The consequences for the curl based version are not investigated in detail. From fluid dynamics it is known that artifacts that are embedded in a fluid may suffer from the vorticity of the embedding field [2].

This paper does not investigate the consequences of polar ordering. It probably relates to the spin properties of elementary objects. In that case the polar ordering of symmetry centers regulates the distinction between fermions and bosons. The half integer spin particles may use ordering of the azimuth, where the integer spin particles use the ordering of the polar angle. However, this does not explain the difference in behavior between these categories.

The concept of exterior derivative is carefully crafted by skillful mathematicians, such that it becomes independent of the selection of parameter spaces. However, in a situation like this in which several parameter spaces float on top of a background parameter space, the selection of the ordering of the parameter spaces does matter. The symmetry flavors of the coupled parameter spaces determine the values of the integrals that account for the contributions of the artifacts. It is represented by the symmetry related charges of these artifacts. These symmetry related charges are supposed to be located at the geometric centers of the symmetry centers.

As happens so often, physical reality reveals facts (such as the symmetry related charges) that cannot easily be discovered by skilled mathematicians. The standard model contains a short list of electric charges that correspond to the symmetry related charges. The standard model does not give an explanation for the existence of this short list. Here it becomes clear that the electric charge and the color charge are a properties of connected parameter spaces and not a property of the objects that use these parameter spaces. Instead, these objects inherit the charge properties from the platform on which they reside.

Both the symmetry related fields and the embedding continuum affect the geometric location of the symmetry center. They do that in different ways.

If electric charges are properties of the connection between spaces, then the fields to which these charges contribute implement the forces between these connections. No extra objects are needed to implement these forces!

It is sensible to expect that depending on the type of their "charges" all basic fields are capable of attracting or repelling the spaces on which these "charges" reside. This behavior is described by the differential and integral equations that are obeyed by the considered field.

This model is no more and no less than a mathematical test case. The paper does not pretend that physical reality behaves like this model. But the methods used and the results obtained in this paper might learn more about how physical reality can be structured and how it can behave.

21 References

[1] https://en.wikipedia.org/wiki/Mathematical_formulation_of_quantum_mechanics

[2] The lattices of quantum logic and classical logic are treated in detail in: http://vixra.org/abs/1411.0175 .

[3] Quantum logic was introduced by Garret Birkhoff and John von Neumann in their 1936 paper. G. Birkhoff and J. von Neumann, *The Logic of Quantum Mechanics*, Annals of Mathematics, Vol. 37, pp. 823–843

[4] The Hilbert space was discovered in the first decades of the 20-th century by David Hilbert and others. http://en.wikipedia.org/wiki/Hilbert_space.

[5] In the second half of the twentieth century Constantin Piron and Maria Pia Solèr proved that the number systems that a separable Hilbert space can use must be division rings. See: "Division algebras and quantum theory" by John Baez. http://arxiv.org/abs/1101.5690 and http://www.ams.org/journals/bull/1995-32-02/S0273-0979-1995-00593-8/ and http://arxiv.org/abs/quant-ph/0510095

[6] In 1843 quaternions were discovered by Rowan Hamilton. http://en.wikipedia.org/wiki/History_of_quaternions

[7] In the sixties Israel Gelfand and Georgyi Shilov introduced a way to model continuums via an extension of the separable Hilbert space into a so called Gelfand triple. The Gelfand triple often gets the name rigged Hilbert space. It is a non-separable Hilbert space. http://www.encyclopediaofmath.org/index.php?title=Rigged_Hilbert_space .

[8] Paul Dirac introduced the bra-ket notation, which popularized the usage of Hilbert spaces. Dirac also introduced its delta function, which is a generalized function. Spaces of generalized functions offered continuums before the Gelfand triple arrived.

Dirac, P.A.M. (1982) [1958]. Principles of Quantum Mechanics. International Series of Monographs on Physics (4th ed.). Oxford University Press. p. 255. ISBN 978-0-19-852011-5.

[9] https://en.wikipedia.org/wiki/Stokes%27_theorem#General_formulation.

[10] Justin Shaw, Invariant Vector Calculus. http://www.math.uwaterloo.ca/~j9shaw/Invariant%20Vector%20Calculus.pdf.

[11] Quaternionic function theory and quaternionic Hilbert spaces are treated in: http://vixra.org/abs/1411.0178 .

[12] Fermion Symmetry Flavors. http://vixra.org/abs/1512.0225

[12] https://en.wikipedia.org/wiki/Poisson%27s_equation#Potential_of_a_Gaussian_charge_density

[13] Foundation of a Mathematical Model of Physical Reality. http://vixra.org/abs/1511.0074

Appendix

1 Lattices

A lattice is a set of elements $a, b, c, \ldots$ that is closed for the connections ∩ and ∪. These connections obey:

- The set is ***partially ordered***.
  - This means that with each pair of elements a, b belongs an element c, such that $a \subset c$ and $b \subset c$.
- The set is a ∩ ***half lattice.***
  - This means that with each pair of elements a, b an element c exists, such that $c = a \cap b$.
- The set is a ∪ half lattice.
  - This means that with each pair of elements a, b an element c exists, such that $c = a \cup b$.
- The set is a lattice.
  - This means that the set is both a ∩ half lattice and a ∪ half lattice.

The following relations hold in a lattice:

$$a \cap b = b \cap a \tag{1}$$

$$(a \cap b) \cap c = a \cap (b \cap c) \tag{2}$$

$$a \cap (a \cup b) = a \tag{3}$$

$$a \cup b = b \cup a \tag{4}$$

$$(a \cup b) \cup c = a \cup (b \cup c) \tag{5}$$

$$a \cup (a \cap b) = a \tag{6}$$

The lattice has a ***partial order inclusion*** ⊂:

$$a \subset b \Leftrightarrow a \cap b = a \tag{7}$$

A ***complementary lattice*** contains two elements n and e with each element a a complementary element a' such that:

$$a \cap a' = n \tag{8}$$

$$a \cap n = n \tag{9}$$

$$a \cap e = a \tag{10}$$

$$a \cup a' = e \tag{11}$$

$$a \cup e = e \tag{12}$$

$$a \cup n = a \tag{13}$$

An ***orthocomplemented lattice*** contains two elements n and e and with each element a an element a'' such that:

$$a \cup a'' = e \tag{14}$$

$$a \cap a'' = n$$

$$(a'')'' = a \tag{15}$$

$$a \subset b \Leftrightarrow b'' \subset a'' \tag{16}$$

e is the ***unity element***; n is the ***null element*** of the lattice

A ***distributive lattice*** supports the distributive laws:

$$a \cap (b \cup c) = (a \cap b) \cup (a \cap c) \tag{17}$$

$$a \cup (b \cap c) = (a \cup b) \cap (a \cup c) \tag{18}$$

A ***modular lattice*** supports:

$$(a \cap b) \cup (a \cap c) = a \cap (b \cup (a \cap c)) \tag{19}$$

A ***weak modular lattice*** supports instead:

There exists an element d such that

$$a \subset c \Leftrightarrow (a \cup b) \cap c = a \cup (b \cap c) \cup (d \cap c) \tag{20}$$

where d obeys:

$$(a \cup b) \cap d = d \tag{21}$$

$$a \cap d = n \tag{22}$$

$$b \cap d = n \tag{23}$$

$$(a \subset g)\, and\, (b \subset g) \Leftrightarrow d \subset g \tag{24}$$

In an ***atomic lattice*** holds

$$\exists_{p \in L} \forall_{x \in L} \{x \subset p \Rightarrow x = n\} \tag{25}$$

$$\forall_{a \in L} \forall_{x \in L} \{(a < x < a \cap p) \Rightarrow (x = a\, or\, x = a \cap p)\} \tag{26}$$

p is an atom

2 Quaternionic and Maxwell field equations

In this section, we will compare two sets of differential equations. Both sets use pure space as part of the parameter space.

- Quaternionic differential equations
  - These equations use progression as one of its parameters.
- Maxwell based differential equations
  - These equations use quaternionic distance as one of its parameters.

In this chapter we will use a switch $\circledast = \pm 1$ that selects between two different sets of differential calculus. One set concerns low order quaternionic differential calculus. The other set concerns Maxwell based differential calculus. The switch will be used to highlight the great similarity and the significant differences between these sets.

By introducing new symbols $\mathfrak{E}$ and $\mathfrak{B}$ we will turn the quaternionic differential equations into Maxwell-like quaternionic differential equations. We introduced a simple switch $\circledast = \pm 1$ that apart from the difference between the parameter spaces, will turn one set of equations into the other set.

Maxwell based differential calculus splits quaternionic functions into a scalar function and a vector function. Instead of the quaternionic nabla $\nabla = \nabla_0 + \boldsymbol{\nabla}$ the Maxwell based equations use the scalar operator $\nabla_0 = \frac{\partial}{\partial t}$ and the vector nabla $\boldsymbol{\nabla}$ as separate operators. Maxwell equations use a switch α that controls the structure of a gauge equation.

$$\varkappa = \alpha \frac{\partial}{\partial t} \varphi_0 + \langle \boldsymbol{\nabla}, \boldsymbol{\varphi} \rangle \tag{1}$$

For Maxwell based differential calculus is $\alpha = +1$ and $\nabla_0 = \frac{\partial}{\partial t}$. The switch value is $\circledast -1$.

For quaternionic differential calculus is $\alpha = -1$ and $\nabla_0 = \frac{\partial}{\partial \tau}$. The switch value is $\circledast = +1$.

In the book EMFT the scalar field $\varkappa$ is taken as a gauge with

$\alpha = 1$; Lorentz gauge

$\alpha = 0$; Coulomb gauge

$\alpha = -1$; Kirchhoff gauge.

We will use the definition of a scalar field $\varkappa$:

$$\varkappa \stackrel{\text{def}}{=} \alpha \nabla_t \varphi_0 + \langle \boldsymbol{\nabla}, \boldsymbol{\varphi} \rangle \Leftrightarrow \phi_0 = \nabla_\tau \varphi_0 - \langle \boldsymbol{\nabla}, \boldsymbol{\varphi} \rangle \tag{2}$$

In Maxwell based differential calculus the scalar field $\varkappa$ is ignored or it is taken equal to zero. As will be shown, zeroing $\varkappa$ is not necessary for the derivation of the Maxwell based wave equation [13].

Maxwell equations split the considered functions in scalar functions and vector functions. The Maxwell differential operators are also split and as a consequence they cannot be treated as multiplying operators. We keep them together with curly brackets.

$$\phi = \{\phi_0, \boldsymbol{\phi}\} = \{\nabla_0, \boldsymbol{\nabla}\}\{\varphi_0, \boldsymbol{\varphi}\} \tag{3}$$

$$\phi_0 = \nabla_0\, \varphi_0 - \circledast\, \langle \boldsymbol{\nabla}, \boldsymbol{\varphi} \rangle \tag{4}$$

$$\boldsymbol{\phi} = \nabla_0 \boldsymbol{\varphi} + \boldsymbol{\nabla}\varphi_0 \pm \boldsymbol{\nabla} \times \boldsymbol{\varphi} \tag{5}$$

Equations (4) and (5) are not genuine Maxwell equations. We introduce them here as extra Maxwell equations. Choice $\circledast = -1$ conforms to the Lorenz gauge. We define extra symbols $\mathfrak{E}$ and $\mathfrak{B}$ for parts of the first order partial differential equation.

$$\mathfrak{E} \stackrel{\text{def}}{=} -\nabla_0 \boldsymbol{\varphi} - \boldsymbol{\nabla}\varphi_0 \tag{6}$$

$$\nabla_0 \mathfrak{E} = -\nabla_0 \nabla_0\, \boldsymbol{\varphi} - \nabla_0 \boldsymbol{\nabla}\varphi_0 \tag{7}$$

$$\langle \boldsymbol{\nabla}, \mathfrak{E} \rangle = -\nabla_0 \langle \boldsymbol{\nabla}, \boldsymbol{\varphi} \rangle - \langle \boldsymbol{\nabla}, \boldsymbol{\nabla} \rangle \varphi_0 \tag{8}$$

$$\mathfrak{B} \stackrel{\text{def}}{=} \boldsymbol{\nabla} \times \boldsymbol{\varphi} \tag{9}$$

These definitions imply:

$$\langle \mathfrak{E}, \mathfrak{B} \rangle = 0 \tag{10}$$

$$\nabla_0 \mathfrak{B} = -\boldsymbol{\nabla} \times \mathfrak{E} \tag{11}$$

$$\langle \boldsymbol{\nabla}, \mathfrak{B} \rangle = 0 \tag{12}$$

$$\boldsymbol{\nabla} \times \mathfrak{B} = \boldsymbol{\nabla} \langle \boldsymbol{\nabla}, \boldsymbol{\varphi} \rangle - \langle \boldsymbol{\nabla}, \boldsymbol{\nabla} \rangle \boldsymbol{\varphi} \tag{13}$$

Also the following two equations are not genuine Maxwell equations, but they relate to the gauge equation.

$$\nabla_0\phi_0 = \nabla_0\nabla_0\,\varphi_0 - \circledast\,\nabla_0\langle\boldsymbol{\nabla},\boldsymbol{\varphi}\rangle \tag{14}$$

$$\boldsymbol{\nabla}\phi_0 = \nabla_0\,\boldsymbol{\nabla}\varphi_0 - \circledast\,\boldsymbol{\nabla}\langle\boldsymbol{\nabla},\boldsymbol{\varphi}\rangle = \nabla_0\,\boldsymbol{\nabla}\varphi_0 - \circledast\,\boldsymbol{\nabla}\times\boldsymbol{\nabla}\times\,\boldsymbol{\varphi} - \circledast\,\langle\boldsymbol{\nabla},\boldsymbol{\nabla}\rangle\,\boldsymbol{\varphi} \tag{15}$$

$$\zeta = (\nabla_0 + \circledast\,\langle\boldsymbol{\nabla},\boldsymbol{\nabla}\rangle)\varphi = \zeta_0 + \boldsymbol{\zeta} \Leftrightarrow \{\zeta_0,\boldsymbol{\zeta}\} = \{\nabla_0,-\boldsymbol{\nabla}\}\{\phi_0,\phi\} \tag{16}$$

$$\zeta_0 = (\nabla_0\nabla_0 + \circledast\,\langle\boldsymbol{\nabla},\boldsymbol{\nabla}\rangle)\varphi_0 = \nabla_0\,\phi_0 - \circledast\,\langle\boldsymbol{\nabla},\mathfrak{E}\rangle \tag{17}$$

$$\boldsymbol{\zeta} = (\nabla_0\nabla_0 + \circledast\,\langle\boldsymbol{\nabla},\boldsymbol{\nabla}\rangle)\boldsymbol{\varphi} = -\boldsymbol{\nabla}\phi_0 - \nabla_0\mathfrak{E} - \circledast\,\boldsymbol{\nabla}\times\boldsymbol{\mathcal{B}} \tag{18}$$

More in detail the equations mean:

$$\begin{aligned}\zeta_0 &= \nabla_0\phi_0 + \circledast\,\langle\boldsymbol{\nabla},\boldsymbol{\phi}\rangle \\ &= \{\nabla_0\nabla_0\varphi_0 - \circledast\,\nabla_0\langle\boldsymbol{\nabla},\boldsymbol{\varphi}\rangle\} + \{\circledast\,\langle\boldsymbol{\nabla},\boldsymbol{\nabla}\rangle\varphi_0 + \circledast\,\nabla_0\langle\boldsymbol{\nabla},\boldsymbol{\varphi}\rangle \pm \circledast\,\langle\boldsymbol{\nabla},\boldsymbol{\nabla}\times\boldsymbol{\varphi}\rangle\} \\ &= (\nabla_0\nabla_0 + \circledast\,\langle\boldsymbol{\nabla},\boldsymbol{\nabla}\rangle)\varphi_0\end{aligned} \tag{19}$$

$$\begin{aligned}\zeta_0 &= \nabla_0\,\phi_0 - \circledast\,\langle\boldsymbol{\nabla},\mathfrak{E}\rangle \\ &= \{\nabla_0\nabla_0\,\varphi_0 - \circledast\,\nabla_0\langle\boldsymbol{\nabla},\boldsymbol{\varphi}\rangle\} + \{\circledast\,\nabla_0\langle\boldsymbol{\nabla},\boldsymbol{\varphi}\rangle + \circledast\,\langle\boldsymbol{\nabla},\boldsymbol{\nabla}\rangle\varphi_0\} \\ &= (\nabla_0\nabla_0 + \circledast\,\langle\boldsymbol{\nabla},\boldsymbol{\nabla}\rangle)\varphi_0\end{aligned} \tag{20}$$

$$\begin{aligned}\boldsymbol{\zeta} &= -\boldsymbol{\nabla}\phi_0 + \nabla_0\boldsymbol{\phi} \mp \boldsymbol{\nabla}\times\boldsymbol{\phi} \\ &= \{-\boldsymbol{\nabla}\nabla_0\varphi_0 + \circledast\,\boldsymbol{\nabla}\times\boldsymbol{\nabla}\times\boldsymbol{\varphi} + \circledast\,\langle\boldsymbol{\nabla},\boldsymbol{\nabla}\rangle\boldsymbol{\varphi}\} + \{\nabla_0\boldsymbol{\nabla}\varphi_0 + \nabla_0\nabla_0\boldsymbol{\varphi} \pm \nabla_0\boldsymbol{\nabla}\times\boldsymbol{\varphi}\} \\ &\qquad \{\mp\boldsymbol{\nabla}\times\boldsymbol{\nabla}\varphi_0 \mp \boldsymbol{\nabla}\times\nabla_0\boldsymbol{\varphi} - \boldsymbol{\nabla}\times\boldsymbol{\nabla}\times\boldsymbol{\varphi}\} \\ &= (\nabla_0\nabla_0 + \circledast\,\langle\boldsymbol{\nabla},\boldsymbol{\nabla}\rangle)\boldsymbol{\varphi} + \circledast\,\boldsymbol{\nabla}\times\boldsymbol{\nabla}\times\boldsymbol{\varphi} - \boldsymbol{\nabla}\times\boldsymbol{\nabla}\times\boldsymbol{\varphi}\end{aligned} \tag{21}$$

$$\begin{aligned}\boldsymbol{\zeta} &= -\boldsymbol{\nabla}\phi_0 - \nabla_0\mathfrak{E} - \circledast\,\boldsymbol{\nabla}\times\boldsymbol{\mathcal{B}} \\ &= \{-\boldsymbol{\nabla}\nabla_0\varphi_0 + \circledast\,\boldsymbol{\nabla}\times\boldsymbol{\nabla}\times\boldsymbol{\varphi} + \circledast\,\langle\boldsymbol{\nabla},\boldsymbol{\nabla}\rangle\boldsymbol{\varphi}\} + \{\nabla_0\nabla_0\,\boldsymbol{\varphi} + \nabla_0\boldsymbol{\nabla}\varphi_0\} - \circledast\,\boldsymbol{\nabla}\times\boldsymbol{\nabla}\times\boldsymbol{\varphi} \\ &= (\nabla_0\nabla_0 + \circledast\,\langle\boldsymbol{\nabla},\boldsymbol{\nabla}\rangle)\boldsymbol{\varphi}\end{aligned} \tag{22}$$

Equation (21) reveals why Maxwell based differential equations use the gauge $\varkappa$ rather than accept equation (4) as a genuine Maxwell equation.

$$\rho_0 = \circledast \langle \boldsymbol{\nabla}, \boldsymbol{\nabla} \rangle \varphi_0 = \zeta_0 - \nabla_0 \nabla_0 \varphi_0 \tag{23}$$

$$\boldsymbol{\rho} = \circledast \langle \boldsymbol{\nabla}, \boldsymbol{\nabla} \rangle \boldsymbol{\varphi} = \boldsymbol{\zeta} - \nabla_0 \boldsymbol{\nabla_0} \boldsymbol{\varphi} \tag{24}$$

Thus a simple change of a parameter and the control switch $\circledast$ turn quaternionic differential equations into equivalent Maxwell differential equations and vice versa. This makes clear that both sets represent two different views from the same subject, which is a field that can be stored in the eigenspace of an operator that resides in the Gelfand triple.

Still the comparison shows an anomaly in equation (21) that represents a significant difference between the two sets of differential equations that goes beyond the difference between the parameter spaces. A possible clue will be given in the section on the Dirac equation. This clue comes down to the conclusion that the Maxwell based equations do not lead via the coupling of two first order quaternionic partial differential equations to a regular second order partial quaternionic differential equation, but instead the wave equation represents a coupling between two solutions of different first order biquaternionic differential equations that use different parameter spaces. In the Dirac equation these solutions represent either particle behavior or antiparticle behavior.

3 Genuine Maxwell wave equations

The scalar part of the genuine Maxwell based differential equals zero. This is oppressed by the Lorenz gauge.

The genuine Maxwell differential equations deliver different inhomogeneous wave equations:

$$\mathfrak{E} \stackrel{\text{def}}{=} -\nabla_0 \varphi - \boldsymbol{\nabla}\varphi_0 \tag{1}$$

$$\mathfrak{B} \stackrel{\text{def}}{=} \boldsymbol{\nabla} \times \boldsymbol{\varphi} \tag{2}$$

The following definitions follow from the definitions of $\mathfrak{E}$ and $\mathfrak{B}$.

$$\nabla_0 \mathfrak{E} \stackrel{\text{def}}{=} -\nabla_0 \nabla_0 \, \boldsymbol{\varphi} - \nabla_0 \boldsymbol{\nabla}\varphi_0 \tag{3}$$

$$\langle \boldsymbol{\nabla}, \mathfrak{E} \rangle \stackrel{\text{def}}{=} -\nabla_0 \langle \boldsymbol{\nabla}, \boldsymbol{\varphi} \rangle - \langle \boldsymbol{\nabla}, \boldsymbol{\nabla} \rangle \varphi_0 \tag{4}$$

$$\nabla_0 \mathfrak{B} \stackrel{\text{def}}{=} -\boldsymbol{\nabla} \times \mathfrak{E} \tag{5}$$

$$\langle \boldsymbol{\nabla}, \mathfrak{B} \rangle \stackrel{\text{def}}{=} \mathbf{0} \tag{6}$$

$$\boldsymbol{\nabla} \times \mathfrak{B} \stackrel{\text{def}}{=} \boldsymbol{\nabla} \langle \boldsymbol{\nabla}, \boldsymbol{\varphi} \rangle - \langle \boldsymbol{\nabla}, \boldsymbol{\nabla} \rangle \boldsymbol{\varphi} \tag{7}$$

The Lorenz gauge means:

$$\nabla_0 \boldsymbol{\varphi_0} + \langle \boldsymbol{\nabla}, \boldsymbol{\varphi} \rangle = 0 \tag{8}$$

The genuine Maxwell based wave equations are:

$$(\nabla_0 \nabla_0 - \langle \boldsymbol{\nabla}, \boldsymbol{\nabla} \rangle) \varphi_0 = \rho_0 = \langle \boldsymbol{\nabla}, \mathfrak{E} \rangle \tag{9}$$

$$(\nabla_0 \nabla_0 - \langle \boldsymbol{\nabla}, \boldsymbol{\nabla} \rangle) \boldsymbol{\varphi} = J = \boldsymbol{\nabla} \times \mathfrak{B} - \nabla_0 \mathfrak{E} \tag{10}$$

4 Dirac equation

4.1 The Dirac equation in original format

In its original form the Dirac equation is a complex equation that uses spinors, matrices and partial derivatives [14].

Instead of the usual $\left\{\frac{\partial f}{\partial t}, \boldsymbol{i}\frac{\partial f}{\partial x}, \boldsymbol{j}\frac{\partial f}{\partial y}, \boldsymbol{k}\frac{\partial f}{\partial z}\right\}$ we want to use operators $\nabla = \{\nabla_0, \boldsymbol{\nabla}\}$

The subscript $_0$ indicates the scalar part. Bold face indicates the vector part.

The operator ∇ relates to the applied parameter space. This means that the parameter space is also configured of combinations $x = \{x_0, \boldsymbol{x}\}$ of a scalar x_0 and a vector $\boldsymbol{x}$. Also the functions $f = \{f_0, \boldsymbol{f}\}$ can be split in scalar functions f_0 and vector functions $\boldsymbol{f}$.

The local parameter $t = x_0$ represents the scalar part of the applied parameter space.

Dirac was searching for a split of the Klein-Gordon equation into two first order differential equations.

$$\frac{\partial^2 f}{\partial t^2} - \frac{\partial^2 f}{\partial x^2} - \frac{\partial^2 f}{\partial y^2} - \frac{\partial^2 f}{\partial z^2} = -m^2 f \tag{1}$$

$$(\nabla_0 \nabla_0 - \langle \boldsymbol{\nabla}, \boldsymbol{\nabla} \rangle) f = \Im f = -m^2 f \tag{2}$$

Here $\Im = \nabla_0 \nabla_0 - \langle \boldsymbol{\nabla}, \boldsymbol{\nabla} \rangle$ is the d'Alembert operator.

Dirac used a combination of matrices and spinors in order to reach this result. He applied the Pauli matrices in order to simulate the behavior of vector functions under differentiation.

The unity matrix I and the Pauli matrices $\sigma_1, \sigma_2, \sigma_3$ are given by [15]:

$$I = \begin{bmatrix} 1 & 0 \\ 0 & 1 \end{bmatrix}, \quad \sigma_1 = \begin{bmatrix} 0 & 1 \\ 1 & 0 \end{bmatrix}, \quad \sigma_2 = \begin{bmatrix} 0 & -\mathbb{i} \\ \mathbb{i} & 0 \end{bmatrix}, \quad \sigma_3 = \begin{bmatrix} 1 & 0 \\ 0 & -1 \end{bmatrix} \tag{3}$$

For one of the potential orderings of the quaternionic number system, the Pauli matrices together with the unity matrix I relate to the quaternionic base vectors 1, $\boldsymbol{i}$, $\boldsymbol{j}$ *and* $\boldsymbol{k}$

$$1 \mapsto I, \quad \boldsymbol{i} \mapsto \mathbb{i}\,\sigma_1, \quad \boldsymbol{j} \mapsto \mathbb{i}\,\sigma_2, \quad \boldsymbol{k} \mapsto \mathbb{i}\,\sigma_3 \tag{4}$$

$$\sigma_1\sigma_2 - \sigma_2\sigma_1 = 2\,\mathbb{i}\,\sigma_3;\ \sigma_2\sigma_3 - \sigma_3\sigma_2 = 2\,\mathbb{i}\,\sigma_1;\ \sigma_3\sigma_1 - \sigma_1\sigma_3 = 2\,\mathbb{i}\,\sigma_2 \tag{5}$$

$$\sigma_1\sigma_1 = \sigma_2\sigma_2 = \sigma_3\sigma_3 = I \tag{6}$$

The different ordering possibilities of the quaternionic number system correspond to different symmetry flavors. Half of these possibilities offer a right handed external vector product. The other half offer a left handed external vector product.

We will regularly use:

$$\langle \mathbb{i}\,\boldsymbol{\sigma}, \boldsymbol{\nabla}\rangle = \boldsymbol{\nabla}\,; \mathbb{i} = \sqrt{-1} \tag{7}$$

With

$$p_\mu = -\mathbb{i}\,\nabla_\mu \tag{8}$$

follow

$$p_\mu\sigma_\mu = -\mathbb{i}\,e_\mu\nabla_\mu \tag{9}$$

$$\langle \boldsymbol{\sigma}, \boldsymbol{p}\rangle \leftrightarrow \mathbb{i}\,\boldsymbol{\nabla} \tag{10}$$

4.2 Dirac's approach

The original Dirac equation uses 4x4 matrices $\boldsymbol{\alpha}$ and β. [6]:

$\boldsymbol{\alpha}$ and β *are* matrices that implement the quaternion arithmetic behavior including the possible symmetry flavors of quaternionic number systems and continuums.

$$\alpha_\mu = \begin{bmatrix} 0 & \sigma_\mu \\ \sigma_\mu & 0 \end{bmatrix} \tag{1}$$

$$\beta = \begin{bmatrix} 1 & 0 \\ 0 & -1 \end{bmatrix} \tag{2}$$

$$\beta\beta = I \tag{3}$$

The interpretation of the Pauli matrices as representation of a special kind of angular momentum has led to the half integer eigenvalue of the corresponding spin operator.

Dirac's selection leads to

$$\left(p_0 - \langle \boldsymbol{\alpha}, \boldsymbol{p} \rangle - \beta mc\right)\{\varphi\} = 0 \tag{4}$$

$\{\varphi\}$ is a four component spinor.

Which splits into

$$(p_0 - \langle \boldsymbol{\sigma}, \boldsymbol{p} \rangle - mc)\varphi_A = 0 \tag{5}$$

and

$$(p_0 - \langle \boldsymbol{\sigma}, \boldsymbol{p} \rangle + mc)\varphi_B = 0 \tag{6}$$

φ_A and φ_B are spinor components. Thus the original Dirac equation splits into:

$$(\nabla_0 - \boldsymbol{\nabla} - \mathbb{i}\, mc)\varphi_A = 0 \tag{7}$$

$$(\nabla_0 - \boldsymbol{\nabla} + \mathbb{i}\, mc)\varphi_B = 0 \tag{8}$$

This split does not lead easily to a second order partial differential equation that looks like the Klein Gordon equation.

4.3 Relativistic formulation

Instead of Dirac's original formulation, usually the relativistic formulation is used [16].

That formulation applies gamma matrices, instead of the alpha and beta matrices. This different choice influences the form of the equations that result for the two spinor components.

$$\gamma_\mu = \beta\, \alpha_\mu = \begin{bmatrix} 0 & \sigma_1 \\ -\sigma_\mu & 0 \end{bmatrix}; \mu = 1,2,3 \tag{1}$$

(2)

$$\gamma_0 = \beta = \begin{bmatrix} 1 & 0 \\ 0 & -1 \end{bmatrix}$$

$$\gamma_5 = i_0\gamma_0\gamma_1\gamma_2\gamma_3 = \begin{bmatrix} 0 & 1 \\ 1 & 0 \end{bmatrix} \tag{3}$$

The matrix γ_5 anti-commutes with all other gamma matrices.

Several different sets of gamma matrices are possible. The choice above leads to a "Dirac equation" of the form

$$\left(\mathbb{i}\,\gamma^\mu \nabla_\mu - mc\right)\varphi = 0 \tag{7}$$

More extended:

$$\left(\gamma_0 \frac{\partial}{\partial t} + \langle \boldsymbol{\gamma}, \boldsymbol{\nabla} \rangle - \frac{m}{\mathbb{i}\,\hbar}\right)\{\psi\} = 0 \tag{8}$$

$$\left(\begin{bmatrix} 1 & 0 \\ 0 & -1 \end{bmatrix}\frac{\partial}{\partial t} + \begin{bmatrix} 0 & \langle \boldsymbol{\sigma}, \boldsymbol{\nabla} \rangle \\ -\langle \boldsymbol{\sigma}, \boldsymbol{\nabla} \rangle & 0 \end{bmatrix} - \frac{m}{\mathbb{i}\,\hbar}\begin{bmatrix} 1 & 0 \\ 0 & 1 \end{bmatrix}\right)\begin{bmatrix} \varphi_A \\ \varphi_B \end{bmatrix} = 0 \tag{9}$$

$$\left(\mathbb{i}\begin{bmatrix} 1 & 0 \\ 0 & -1 \end{bmatrix}\frac{\partial}{\partial t} + \begin{bmatrix} 0 & \boldsymbol{\nabla} \\ -\boldsymbol{\nabla} & 0 \end{bmatrix} - \frac{m}{\hbar}\begin{bmatrix} 1 & 0 \\ 0 & 1 \end{bmatrix}\right)\begin{bmatrix} \varphi_A \\ \varphi_B \end{bmatrix} = 0 \tag{10}$$

$$\mathbb{i}\,\frac{\partial}{\partial t}\varphi_A + \boldsymbol{\nabla}\varphi_B - \frac{m}{\mathbb{i}\,\hbar}\varphi_A = 0 \tag{11}$$

$$-\mathbb{i}\,\frac{\partial}{\partial t}\varphi_B - \boldsymbol{\nabla}\varphi_A - \frac{m}{\mathbb{i}\,\hbar}\varphi_B = 0 \tag{12}$$

Also this split does not easily lead to a second order partial differential equation that looks like the Klein Gordon equation.

4.4 A better choice

Another interpretation of the Dirac approach replaces γ_0 with γ_5 [17]:

$$\left(\gamma_5 \frac{\partial}{\partial t} - \gamma_1 \frac{\partial}{\partial x} - \gamma_2 \frac{\partial}{\partial y} - \gamma_3 \frac{\partial}{\partial z} - \frac{m}{\mathbb{i}\,\hbar}\right)\{\psi\} = 0 \tag{1}$$

(2)

$$\left(\gamma_5 \frac{\partial}{\partial t} - \langle \boldsymbol{\gamma}, \boldsymbol{\nabla} \rangle - \frac{m}{\mathbb{i}\,\hbar}\right)\{\psi\} = 0$$

$$\left(\begin{bmatrix} 0 & 1 \\ 1 & 0 \end{bmatrix} \frac{\partial}{\partial t} - \begin{bmatrix} 0 & \langle \boldsymbol{\sigma}, \boldsymbol{\nabla} \rangle \\ -\langle \boldsymbol{\sigma}, \boldsymbol{\nabla} \rangle & 0 \end{bmatrix} - \frac{m}{\mathbb{i}\,\hbar} \begin{bmatrix} 1 & 0 \\ 0 & 1 \end{bmatrix}\right) \begin{bmatrix} \psi_A \\ \psi_B \end{bmatrix} = 0 \tag{3}$$

This invites splitting of the four component spinor equation into two equations for the two components ψ_A and ψ_B of the spinor:

$$\mathbb{i}\,\nabla_0 \psi_A + \mathbb{i}\,\langle \boldsymbol{\sigma}, \boldsymbol{\nabla} \rangle \psi_A = \frac{m}{\hbar}\,\psi_B \tag{4}$$

$$\mathbb{i}\,\nabla_0 \varphi_B - \mathbb{i}\,\langle \boldsymbol{\sigma}, \boldsymbol{\nabla} \rangle \psi_B = \frac{m}{\hbar}\,\psi_A \tag{5}$$

$$(\mathbb{i}\,\nabla_0 + \boldsymbol{\nabla})\psi_A = \frac{m}{\hbar}\,\psi_B \tag{6}$$

$$(\mathbb{i}\,\nabla_0 - \boldsymbol{\nabla})\psi_B = \frac{m}{\hbar}\,\psi_A \tag{7}$$

This looks far more promising. We can insert the right part of the first equation into the left part of the second equation.

$$(\mathbb{i}\,\nabla_0 - \boldsymbol{\nabla})(\mathbb{i}\,\nabla_0 + \boldsymbol{\nabla})\psi_A = (-\nabla_0\nabla_0 - \boldsymbol{\nabla}\boldsymbol{\nabla})\psi_A = (\langle \boldsymbol{\nabla}, \boldsymbol{\nabla} \rangle - \nabla_0\nabla_0)\psi_A \tag{8}$$

$$= \frac{m}{\hbar}(\mathbb{i}\,\nabla_0 - \boldsymbol{\nabla})\,\psi_B = \frac{m^2}{\hbar^2}\,\psi_A$$

$$(\langle \boldsymbol{\nabla}, \boldsymbol{\nabla} \rangle - \nabla_0\nabla_0)\psi_A = \frac{m^2}{\hbar^2}\,\psi_A \tag{9}$$

$$(\mathbb{i}\,\nabla_0 + \boldsymbol{\nabla})(\mathbb{i}\,\nabla_0 - \boldsymbol{\nabla})\psi_B = (-\nabla_0\nabla_0 - \boldsymbol{\nabla}\boldsymbol{\nabla})\psi_B = (\langle \boldsymbol{\nabla}, \boldsymbol{\nabla} \rangle - \nabla_0\nabla_0)\psi_B \tag{10}$$

$$= \frac{m}{\hbar}(\mathbb{i}\,\nabla_0 + \boldsymbol{\nabla})\,\psi_A = \frac{m^2}{\hbar^2}\,\psi_B$$

$$(\langle \boldsymbol{\nabla}, \boldsymbol{\nabla} \rangle - \nabla_0 \nabla_0)\psi_B = \frac{m^2}{\hbar^2}\,\psi_B \tag{11}$$

This is what Dirac wanted to achieve. The two first order differential equations couple into a second order differential equation that is equivalent to a Klein Gordon equation. The homogeneous version of this second order partial differential equation is a wave equation and offers solutions that are waves.

The nabla operator acts differently onto the two component spinors ψ_A and ψ_B.

4.5 The quaternionic nabla and the Dirac nabla

The modified Pauli matrices together with a 2×2 identity matrix implement the equivalent of a quaternionic number system with a selected symmetry flavor.

$$I = \begin{bmatrix} 1 & 0 \\ 0 & 1 \end{bmatrix};\ \mathbb{i}\,\sigma_1 = \begin{bmatrix} 0 & \mathbb{i} \\ \mathbb{i} & 0 \end{bmatrix};\ \mathbb{i}\,\sigma_2 = \begin{bmatrix} 0 & 1 \\ -1 & 0 \end{bmatrix};\ \mathbb{i}\,\sigma_3 = \begin{bmatrix} \mathbb{i} & 0 \\ 0 & -\mathbb{i} \end{bmatrix} \tag{1}$$

The modified Pauli matrices together with the I_0 matrix implements another structure, which is not a version of a quaternionic number system.

$$I_0 = \begin{bmatrix} \mathbb{i} & 0 \\ 0 & \mathbb{i} \end{bmatrix};\ \mathbb{i}\,\sigma_1 = \begin{bmatrix} 0 & \mathbb{i} \\ \mathbb{i} & 0 \end{bmatrix};\ \mathbb{i}\,\sigma_2 = \begin{bmatrix} 0 & 1 \\ -1 & 0 \end{bmatrix};\ \mathbb{i}\,\sigma_3 = \begin{bmatrix} \mathbb{i} & 0 \\ 0 & -\mathbb{i} \end{bmatrix} \tag{2}$$

Both the quaternionic nabla and the Dirac nabla implement a way to let these differential operators act as multipliers.

The quaternionic nabla is defined as

$$\nabla = \nabla_0 + \boldsymbol{\nabla} = e^{\mu}\nabla_{\mu} = \nabla_0 + \mathbb{i}\,\langle \boldsymbol{\sigma}, \boldsymbol{\nabla} \rangle \tag{3}$$

$$\nabla^* = \nabla_0 - \boldsymbol{\nabla} \tag{4}$$

For scalar functions and for vector functions hold:

$$\nabla^*\nabla = \nabla\nabla^* = \nabla_0\nabla_0 + \langle \boldsymbol{\nabla}, \boldsymbol{\nabla} \rangle \tag{5}$$

The Dirac nabla is defined as

$$\mathcal{D} = \mathbb{i}\,\nabla_0 + \boldsymbol{\nabla} = \mathbb{i}\,\nabla_0 + \mathbb{i}\,\langle \boldsymbol{\sigma}, \boldsymbol{\nabla} \rangle \tag{6}$$

$$\mathcal{D}^* = \mathbb{i}\,\nabla_0 - \boldsymbol{\nabla} \tag{7}$$

$$\mathcal{D}^*\mathcal{D} \;= \mathcal{D}\,\mathcal{D}^* = \; -\nabla_0\nabla_0 + \langle \boldsymbol{\nabla}, \boldsymbol{\nabla} \rangle \tag{8}$$

4.5.1 Prove

We use

$$\nabla_0 \boldsymbol{\nabla} f_0 = \boldsymbol{\nabla}\nabla_0 f_0 \tag{1}$$

$$\nabla_0 \boldsymbol{\nabla} \boldsymbol{f} = \boldsymbol{\nabla}\nabla_0 \boldsymbol{f} = -\nabla_0 \langle \boldsymbol{\nabla}, \boldsymbol{f} \rangle + \nabla_0 \boldsymbol{\nabla} \times \boldsymbol{f} \tag{2}$$

$$\boldsymbol{\nabla}\boldsymbol{\nabla} f_0 = -\langle \boldsymbol{\nabla}, \boldsymbol{\nabla} \rangle f_0 + \boldsymbol{\nabla} \times \boldsymbol{\nabla} f_0 = -\langle \boldsymbol{\nabla}, \boldsymbol{\nabla} \rangle f_0 \tag{3}$$

$$\boldsymbol{\nabla}(\boldsymbol{\nabla} \boldsymbol{f}) = -\boldsymbol{\nabla}\langle \boldsymbol{\nabla}, \boldsymbol{f} \rangle + \boldsymbol{\nabla} \times \boldsymbol{\nabla} \times \boldsymbol{f} = -\langle \boldsymbol{\nabla}, \boldsymbol{\nabla} \rangle \boldsymbol{f} = (\boldsymbol{\nabla}\boldsymbol{\nabla})\boldsymbol{f} \tag{4}$$

$$\boldsymbol{\nabla} \times \boldsymbol{\nabla} \times \boldsymbol{f} = \boldsymbol{\nabla}\langle \boldsymbol{\nabla}, \boldsymbol{f} \rangle - \langle \boldsymbol{\nabla}, \boldsymbol{\nabla} \rangle \boldsymbol{f} \tag{5}$$

$$\langle \boldsymbol{\nabla}, \boldsymbol{\nabla} \times \boldsymbol{f} \rangle = 0 \tag{6}$$

$$\boldsymbol{\nabla} \times \boldsymbol{\nabla}\, f_0 = \boldsymbol{0} \tag{7}$$

This results in

$$(\alpha\nabla_0 + \boldsymbol{\nabla}) f_0 = \alpha\nabla_0 f_0 + \boldsymbol{\nabla} f_0 \tag{8}$$

$$(\alpha\nabla_0 - \boldsymbol{\nabla})(\alpha\nabla_0 + \boldsymbol{\nabla}) f_0 \tag{9}$$

$$= \alpha^2 \nabla_0\nabla_0 + \alpha\nabla_0 \boldsymbol{\nabla} f_0 - \alpha \boldsymbol{\nabla}\nabla_0 f_0 + \langle \boldsymbol{\nabla}, \boldsymbol{\nabla} \rangle f_0 - \boldsymbol{\nabla} \times \boldsymbol{\nabla} f_0$$

$$= \alpha^2 \nabla_0\nabla_0 + \langle \boldsymbol{\nabla}, \boldsymbol{\nabla} \rangle f_0$$

$$(\alpha\nabla_0 + \boldsymbol{\nabla})\boldsymbol{f} = \alpha\nabla_0\boldsymbol{f} - \langle\boldsymbol{\nabla},\boldsymbol{f}\rangle + \boldsymbol{\nabla}\times\boldsymbol{f} \tag{10}$$

$$(\alpha\nabla_0 - \alpha\nabla_0\boldsymbol{f} - \langle\boldsymbol{\nabla},\boldsymbol{f}\rangle + \boldsymbol{\nabla}\times\boldsymbol{f})(\alpha\nabla_0 + \boldsymbol{\nabla})\boldsymbol{f}$$

$$(\alpha\nabla_0 - \boldsymbol{\nabla})(\alpha\nabla_0 + \boldsymbol{\nabla})f_0 \tag{11}$$

$$= \alpha^2\nabla_0\nabla_0\boldsymbol{f} - \alpha\nabla_0\langle\boldsymbol{\nabla},\boldsymbol{f}\rangle + \alpha\nabla_0\boldsymbol{\nabla}\times\boldsymbol{f} + \alpha\nabla_0\langle\boldsymbol{\nabla},\boldsymbol{f}\rangle$$

$$-\alpha\nabla_0\boldsymbol{\nabla}\times\boldsymbol{f} + \boldsymbol{\nabla}\langle\boldsymbol{\nabla},\boldsymbol{f}\rangle + \langle\boldsymbol{\nabla},\boldsymbol{\nabla}\times\boldsymbol{f}\rangle - \boldsymbol{\nabla}\times\boldsymbol{\nabla}\times\boldsymbol{f}$$

$$= \alpha^2\nabla_0\nabla_0\boldsymbol{f} + \langle\boldsymbol{\nabla},\boldsymbol{\nabla}\rangle\boldsymbol{f}$$

4.5.2 Discussion

For $\alpha = 1$ the equations

$$(\nabla^*\nabla\, f_0 = \nabla\nabla^*\, f_0 = \nabla_0\nabla_0 + \langle\boldsymbol{\nabla},\boldsymbol{\nabla}\rangle)\, f_0 \tag{1}$$

$$(\nabla^*\nabla\, \boldsymbol{f} = \nabla\nabla^*\, \boldsymbol{f} = \nabla_0\nabla_0 + \langle\boldsymbol{\nabla},\boldsymbol{\nabla}\rangle)\, \boldsymbol{f} \tag{2}$$

work for both parts of a quaternionic function $f = f_0 + \boldsymbol{f}$.

For $\alpha = \mathbb{i}$ the equations

$$(\mathcal{D}^*\mathcal{D}\, f_0 = \mathcal{D}\mathcal{D}^*\, f_0 = -\nabla_0\nabla_0 + \langle\boldsymbol{\nabla},\boldsymbol{\nabla}\rangle)\, f_0 \tag{3}$$

$$(\mathcal{D}^*\mathcal{D}\, \boldsymbol{f} = \mathcal{D}\mathcal{D}^*\boldsymbol{f} = -\nabla_0\nabla_0 + \langle\boldsymbol{\nabla},\boldsymbol{\nabla}\rangle)\, \boldsymbol{f} \tag{4}$$

work separately for scalar function f_0.and vector function $\boldsymbol{f}$. The right sides of the equations work for quaternionic functions. Thus

$$(g = \mathfrak{D}f = -\nabla_0\nabla_0 + \langle\boldsymbol{\nabla},\boldsymbol{\nabla}\rangle)\, f \tag{5}$$

is a valid equation for quaternionic functions f and g.

Thus the d'Alembert operator $\Im = -\nabla_0\nabla_0 + \langle \boldsymbol{\nabla}, \boldsymbol{\nabla} \rangle$ is a valid quaternionic operator.

The nabla operators reflects the structure of the parameter space of the functions on which they work. Thus the quaternionic nabla operator reflects a quaternionic number system. The Dirac nabla operator reflects the structure of the parameters of the two component spinors that figure in the modified Dirac equation.

Between the two spinor components ψ_A and ψ_B, the scalar part of the parameter space appears to change sign with respect to the vector part.

Applied to a quaternionic function, the quaternionic nabla results again in a ***quaternionic*** function.

$$\phi = \phi_0 + \boldsymbol{\phi} = (\nabla_0 + \boldsymbol{\nabla})(f_0 + \boldsymbol{f}) = \nabla_0 f_0 - \langle \boldsymbol{\nabla}, \boldsymbol{f} \rangle + \boldsymbol{\nabla} f_0 + \nabla_0 \boldsymbol{f} + \boldsymbol{\nabla} \times \boldsymbol{f} \tag{6}$$

Applied to a quaternionic function, the Dirac nabla results in a ***biquaternionic*** function.

$$(\mathbb{i}\,\nabla_0 + \boldsymbol{\nabla})(f_0 + \boldsymbol{f}) = \nabla_0\,\mathbb{i}\,f_0 - \langle \boldsymbol{\nabla}, \boldsymbol{f} \rangle + \boldsymbol{\nabla} f_0 + \mathbb{i}\,\nabla_0 \boldsymbol{f} + \boldsymbol{\nabla} \times \boldsymbol{f} \tag{7}$$

Neither the Dirac nabla $\mathcal{D}$ nor its conjugate $\mathcal{D}^*$ delivers quaternionic functions from quaternionic functions. They are not proper quaternionic operators.

Thus, the d'Alembert operator cannot be split into two operators that map quaternionic functions onto quaternionic functions.

In contrast the operators $\nabla^*\nabla$, ∇ and ∇^* are all three proper quaternionic operators.

4.6 Quaternionic format of Dirac equation

The initial goal of Dirac was to split the Klein Gordon equation into two first order differential equations. He tried to achieve this via the combination of matrices and spinors. This leads to a result that does not lead to an actual second order differential equation, but instead it leads to two different first order differential equations for two different spinors that can be coupled into a second order partial differential equation that looks like a Klein Gordon equation. The homogeneous version of the Klein Gordon equation is a wave equation. However, that equation misses an essential right part of the Klein-Gordon equation.

Quaternionic differential calculus supports first order differential equations that in a natural way lead to a second order partial differential equation that differs significantly from a wave equation.

The closest quaternionic equivalents of the first order Dirac equations for the electron and the positron are:

$$\nabla\psi = (\nabla_0 + \boldsymbol{\nabla})(\psi_0 + \boldsymbol{\psi}) = m\varphi \tag{1}$$

$$\nabla^*\varphi = (\nabla_0 - \boldsymbol{\nabla})(\varphi_0 + \boldsymbol{\varphi}) = m\psi \tag{2}$$

$$\nabla^*\nabla\psi = (\nabla_0 - \boldsymbol{\nabla})(\nabla_0 + \boldsymbol{\nabla})(\psi_0 + \boldsymbol{\psi}) = m^2\psi \tag{3}$$

$$\nabla^*\nabla\psi = \nabla^*\nabla\psi = (\nabla_0\nabla_0 + \langle\boldsymbol{\nabla},\boldsymbol{\nabla}\rangle)\,\psi = m^2\psi \tag{4}$$

$$\nabla\nabla^*\varphi = \nabla^*\nabla\varphi = (\nabla_0\nabla_0 + \langle\boldsymbol{\nabla},\boldsymbol{\nabla}\rangle)\,\varphi = m^2\varphi \tag{5}$$

A similar equation exists for spherical coordinates.

These second order equations are not wave equations. Their set of solutions does not include waves.

4.7 Interpretation of the Dirac equation

The original Dirac equation can be split into two equations. One of them describes the behavior of the electron. The other equation describes the behavior of the positron.

The positron is the anti-particle of the electron. These particles feature the same rest mass, but other characteristics such as their electric charge differ in sign. The positron can be interpreted as an electron that moves back in time. Sometimes the electron is interpreted as a hole in a sea of positrons. These interpretations indicate that the functions that describe these particles feature different parameter spaces that differ in the sign of the scalar part.

4.7.1 Particle fields

The fields that characterize different types of particles can be related to parameter spaces that belong to different versions of the quaternionic number system. These fields are coupled to an embedding field on which the particles and their private parameter spaces float.

The reverse bra-ket method shows how fields can on the one hand be coupled to eigenspaces and eigenvectors of operators which reside in quaternionic non-separable Hilbert spaces and on the other hand can be coupled to pairs of parameter spaces and quaternionic functions. Quaternionic functions can be split into scalar functions and vector functions. In a quaternionic Hilbert space several different natural parameter spaces can coexist. Natural parameter spaces are formed by versions of the quaternionic number system. These versions differ in the way that these number systems are ordered.

The original Dirac equations might represent this coupling between the particle field and the embedding field.

4.8 Alternatives

4.8.1 Minkowski parameter space

In quaternionic differential calculus the local quaternionic distance can represent a scalar that is independent of the direction of progression. It corresponds to the notion of coordinate time t. This means that a small coordinate time step Δt equals the sum of a small proper time step $\Delta\tau$ and a small pure space step $\Delta\boldsymbol{x}$. In quaternionic format the step $\Delta\tau$ is a real number. The space step $\Delta\boldsymbol{x}$ is an imaginary quaternionic number. The original Dirac equation does not pay attention to the difference between coordinate time and proper time, but the quaternionic presentation of these equations show that a progression independent scalar can be useful as the scalar part of the parameter space. This holds especially for solutions of the homogeneous wave equation.

In this way coordinate time is a function of proper time τ and distance in pure space $|\Delta\boldsymbol{x}|$.

$$|\Delta t|^2 = |\Delta\tau|^2 + |\Delta\boldsymbol{x}|^2$$

Together t and $\boldsymbol{x}$ deliver a spacetime model that has a Minkowski signature.

$$|\Delta\tau|^2 = |\Delta t|^2 - |\Delta\boldsymbol{x}|^2$$

4.8.2 Other natural parameter spaces

The Dirac equation in quaternionic format treats a coupling of parameter spaces that are each other's quaternionic conjugate. The β matrix implements isotropic conjugation. An adapted conjugation matrix can apply anisotropic conjugation. This concerns conjugations in which only one or two dimensions get a reverse ordering. In that case the equations handle the dynamic behavior of anisotropic particles such as quarks. Quarks correspond to solutions that have anisotropic parameter spaces. Also for these quarks exist advanced particle solutions and retarded antiparticle solutions.

5 Tensor differential calculus

We restrict to 3+1 D parameter spaces.

Parameter spaces can differ in the way they are ordered and in the way the scalar part relates to the spatial part.

Fields are functions that have values, which are independent of the selected parameter space. Fields exist in scalar fields, vector fields and combined scalar and vector fields.

Combined fields exist as continuum eigenspaces of normal operators that reside in quaternionic non-separable Hilbert spaces. These combined fields can be represented by quaternionic functions of quaternionic parameter spaces. However, the same field can also be interpreted as the eigenspaces of the Hermitian and anti-Hermitian parts of the normal operator. The quaternionic parameter space can be represented by a normal quaternionic reference operator that features a flat continuum eigenspace. This reference operator can be split in a Hermitian and an anti-Hermitian part.

The eigenspace of a normal quaternionic number system corresponds to a quaternionic number system. Due to the four dimensions of quaternions, the quaternionic number systems exist in 16 versions that differ in their Cartesian ordering. If spherical ordering is pursued, then for each Cartesian start orderings two extra orderings are possible. All these choices correspond to different parameter spaces.

Further it is possible to select a scalar part of the parameter space that is a scalar function of the quaternionic scalar part and the quaternionic vector part. For example it is possible to use quaternionic distance as the scalar part of the new parameter space.

Tensor differential calculus relates components of differentials with corresponding parameter spaces.

Components of differentials are terms of the corresponding differential equation. These terms can be split in scalar functions and in vector functions. Tensor differential calculus treats scalar functions different from vector functions.

Quaternionic fields are special because the differential operators of their defining functions can be treated as multipliers.

5.1 The metric tensor

The metric tensor determines the local “distance”.

$$g_{\mu\nu} = \begin{bmatrix} g_{00} & g_{01} & g_{02} & g_{03} \\ g_{10} & g_{11} & g_{12} & g_{13} \\ g_{20} & g_{21} & g_{22} & g_{23} \\ g_{30} & g_{31} & g_{32} & g_{33} \end{bmatrix} \quad (1)$$

The consequences of coordinate transformations $dx^\nu \Rightarrow dX^\nu$ define the elements $g_{\mu\nu}$ as

$$g_{\mu\nu} = \frac{dX^\mu}{dx^\nu} \quad (2)$$

5.2 Geodesic equation

The geodesic equation describes the situation of a non-accelerated object. In terms of proper time this means:

(1)

$$\frac{\partial^2 x^\mu}{\partial \tau^2} = -\Gamma^\mu_{\alpha\beta}\frac{dx^\alpha}{d\tau}\frac{dx^\beta}{d\tau}$$

In terms of coordinate time this means:

$$\frac{\partial^2 x^\mu}{\partial t^2} = -\Gamma^\mu_{\alpha\beta}\frac{dx^\alpha}{dt}\frac{dx^\beta}{dt} + \Gamma^0_{\alpha\beta}\frac{dx^\alpha}{dt}\frac{dx^\beta}{dt}\frac{dx^\mu}{dt} \tag{2}$$

5.2.1 Derivation:

We start with the double differential. Let us investigate a function X that has a parameter space existing of scalar τ and a three dimensional vector $\boldsymbol{x} = \{x^1, x^2, x^3\}$. The function X represents three dimensional curved space. The geodesic conditions are:

$$\frac{\partial^2 X^\lambda}{\partial \tau^2} = 0\ ;\ \lambda = 1,2,3 \tag{1}$$

First we derive the first order differential.

$$dX^\lambda = \sum_{\beta=1}^{3}\frac{\partial X^\lambda}{\partial x^\beta}dx^\beta \tag{2}$$

We can use the summation convention for subscripts and superscripts. This avoids the requirement for summation symbols.

$$\frac{dX^\lambda}{d\tau} = \frac{\partial X^\lambda}{\partial x^\beta}\frac{dx^\beta}{d\tau} \tag{3}$$

$$d^2X^\lambda = \sum_{\beta=1}^{3}\left(\frac{\partial X^\lambda}{\partial x^\beta}d^2x^\beta + dx^\beta\sum_{\alpha=1}^{3}\frac{\partial^2 X^\lambda}{\partial x^\beta \partial x^\alpha}dx^\alpha\right) \tag{4}$$

Now we obtained the double differential equation.

$$\frac{d^2X^\lambda}{d\tau^2} = \frac{\partial X^\lambda}{\partial x^\beta}\frac{d^2x^\beta}{d\tau^2} + \frac{\partial^2 X^\lambda}{\partial x^\beta \partial x^\alpha}\frac{dx^\alpha}{d\tau}\frac{dx^\beta}{d\tau} = 0 \tag{5}$$

The geodesic requirement results in:

$$\frac{\partial X^\lambda}{\partial x^\beta}\frac{d^2x^\beta}{d\tau^2} = -\frac{\partial^2 X^\lambda}{\partial x^\beta \partial x^\alpha}\frac{dx^\alpha}{d\tau}\frac{dx^\beta}{d\tau} \tag{6}$$

If we use summation signs:

$$\sum_{\beta=1}^{3}\frac{\partial X^\lambda}{\partial x^\beta}d^2x^\beta = -\sum_{\beta=1}^{3}\left(dx^\beta\sum_{\alpha=1}^{3}\left(\frac{\partial^2 X^\lambda}{\partial x^\beta \partial x^\alpha}dx^\alpha\right)\right) \tag{7}$$

Next we multiply both sides with $\frac{\partial X^\lambda}{\partial x^\beta}$ and sum again:

$$\sum_{\lambda=1}^{3}\left(\frac{\partial x^\lambda}{\partial X^\mu}\left(\sum_{\beta=1}^{3}\frac{\partial X^\lambda}{\partial x^\beta}d^2x^\beta\right)\right) = -\sum_{\lambda=1}^{3}\left(\frac{\partial x^\lambda}{\partial X^\mu}\sum_{\beta=1}^{3}\left(dx^\beta\sum_{\alpha=1}^{3}\left(\frac{\partial^2 X^\lambda}{\partial x^\beta \partial x^\alpha}dx^\alpha\right)\right)\right) \tag{8}$$

We apply the fact:

$$\sum_{\lambda=1}^{3}\left(\frac{\partial x^{\lambda}}{\partial X^{\mu}}\frac{\partial X^{\lambda}}{\partial x^{\beta}}\right)=\delta_{\beta}^{\mu} \tag{9}$$

This results into:

$$d^2x^{\mu}=\sum_{\lambda=1}^{3}\left(\frac{\partial x^{\lambda}}{\partial X^{\mu}}\sum_{\beta=1}^{3}\left(dx^{\beta}\sum_{\alpha=1}^{3}\left(\frac{\partial^2 X^{\lambda}}{\partial x^{\beta}\partial x^{\alpha}}dx^{\alpha}\right)\right)\right)=\Gamma_{\alpha\beta}^{\mu}dx^{\alpha}dx^{\beta} \tag{10}$$

Without summation signs:

$$\Gamma_{\alpha\beta}^{\mu}dx^{\alpha}dx^{\beta}\overset{\text{def}}{=}\left(\frac{\partial x^{\mu}}{\partial X^{\lambda}}\frac{\partial^2 X^{\lambda}}{\partial x^{\alpha}\partial x^{\beta}}\right)dx^{\alpha}dx^{\beta} \tag{11}$$

$$\frac{d^2x^{\mu}}{d\tau^2}=-\Gamma_{\alpha\beta}^{\mu}\frac{dx^{\beta}}{d\tau}\frac{dx^{\alpha}}{d\tau} \tag{12}$$

$$\frac{d^2x^{\mu}}{d\tau^2}=-\left(\frac{\partial x^{\mu}}{\partial X^{\lambda}}\frac{\partial^2 X^{\lambda}}{\partial x^{\alpha}\partial x^{\beta}}\right)\frac{dx^{\beta}}{d\tau}\frac{dx^{\alpha}}{d\tau} \tag{13}$$

$$\frac{d^2x^{\mu}}{dt^2}=-\left(\frac{\partial x^{\mu}}{\partial X^{\lambda}}\frac{\partial^2 X^{\lambda}}{\partial x^{\alpha}\partial x^{\beta}}\right)\frac{dx^{\beta}}{dt}\frac{dx^{\alpha}}{dt}+\left(\frac{\partial x^{0}}{\partial X^{\lambda}}\frac{\partial^2 X^{\lambda}}{\partial x^{\alpha}\partial x^{\beta}}\right)\frac{dx^{\beta}}{dt}\frac{dx^{\alpha}}{dt}\frac{dx^{\mu}}{dt} \tag{14}$$

5.3 Toolbox

Coordinate transformations:

$$S_{\nu'\rho'}^{\mu'}=\frac{\partial x^{\mu'}}{\partial x^{\mu}}\frac{\partial x^{\nu}}{\partial x^{\nu'}}\frac{\partial x^{\rho}}{\partial x^{\rho'}}S_{\nu\rho}^{\mu} \tag{1}$$

The Christoffel symbol plays an important role:

$$2\,g_{\alpha\delta}\,\Gamma_{\beta\alpha}^{\delta}=\frac{\partial g_{\alpha\beta}}{\partial x^{\gamma}}+\frac{\partial g_{\alpha\gamma}}{\partial x^{\beta}}+\frac{\partial g_{\beta\gamma}}{\partial x^{\alpha}} \tag{2}$$

$$\Gamma_{\alpha\beta}^{\mu}\overset{\text{def}}{=}\frac{\partial x^{\mu}}{\partial X^{\lambda}}\frac{\partial^2 X^{\lambda}}{\partial x^{\alpha}\partial x^{\beta}} \tag{3}$$

$$\Gamma_{\beta\alpha}^{\delta}=\Gamma_{\alpha\beta}^{\delta} \tag{4}$$

Covariant derivative $\nabla_{\mu}\alpha$ and partial derivative $\partial_{\mu}\alpha$ of scalars

$$\partial_{\mu'}\alpha=\frac{\partial x^{\mu'}}{\partial x^{\mu}}\partial_{\mu}\alpha \tag{5}$$

Covariant derivative $\nabla_{\mu}V^{\nu}$ and partial derivative $\partial_{\mu}V^{\nu}$ of vectors

$$\nabla_{\mu}V^{\nu}=\partial_{\mu}V^{\nu}+\Gamma_{\mu\lambda}^{\nu}V^{\lambda} \tag{6}$$

$$\nabla_{\mu}\varphi_{\nu}=\partial_{\mu}\varphi_{\nu}-\Gamma_{\mu\nu}^{\lambda}\varphi_{\lambda} \tag{7}$$

$$\nabla_{\mu}g_{\alpha\beta}=0 \tag{8}$$

$$\nabla_\mu g^{\alpha\beta} = 0 \tag{9}$$

$$g^{\nu\mu} g_{\nu\mu} = \delta^\mu_\nu \tag{10}$$

$$g = \det(g_{\nu\mu}) \tag{11}$$

$$g' = \left(\det\left(\frac{\partial x^{\mu'}}{\partial x^\mu}\right)\right)^{-2} g \tag{12}$$

$\det\left(\frac{\partial x^{\mu'}}{\partial x^\mu}\right)$ is Jacobian (13)

$$d^4x \stackrel{\text{def}}{=} dx^0 dx^1 dx^2 dx^3 \tag{14}$$

$$d^4x' = \det\left(\frac{\partial x^{\mu'}}{\partial x^\mu}\right) d^4x \tag{15}$$